

Department of Chemical Engineering

**High Energy Density Fuels Derived from Mallee Biomass:
Fuel Properties and Implications**

Hanisom binti Abdullah


**This thesis is presented for the Degree of
Doctor of Philosophy
of
Curtin University**

November 2010

Declaration

To the best of my knowledge and belief this thesis contains no material previously published by any other person except where due acknowledgement has been made.

This thesis contains no material which has been accepted for the award of any other degree or diploma in any university.

Signature:.....

Date:..... 12/7/2011

To my beloved family

“And We have enjoined upon man, to his parents, good treatment. His mother carried him with hardship and gave birth to him with hardship, and his gestation and weaning[period]is thirty months.[He grows] until, when he reaches maturity and reaches[the age of] forty years, he says, “ My lord, enable me to be grateful for Your favour which You have bestowed upon me and upon my parents and to work righteousness of which You will approve and make righteous for me my offspring.

Indeed, I have repented to You, and indeed, I am of the Muslims.”

(Surah Al-‘Ahqaf, 46:15-The Holy Qur’an)

ABSTRACT

Mallee biomass is considered to be a second-generation renewable feedstock in Australia and will play an important role in bioenergy development in Australia. Its production is of large-scale, low cost, small carbon footprint and high energy efficiency. However, biomass as a direct fuel is widely dispersed, bulky, fibrous and of high moisture content and low energy density. High logistic cost, poor grindability and mismatch of fuel property with coal are some of the key issues that impede biomass utilisation for power generation. Therefore, innovations are in urgent need to improve biomass volumetric energy densification, grindability and good fuel matching if co-fired with coal. Biomass pyrolysis is a flexible and low-cost approach that can be deployed for this purpose. Via pyrolysis, the bulky biomass can be converted to biomass-derived high-energy-density fuels such as biochar and/or bio-oil. So far there has been a lack of fundamental understanding of mallee biomass pyrolysis and properties of the fuel products.

The series of study in this PhD thesis aims to investigate the production of such high-energy-density fuels obtained from mallee pyrolysis and to obtain some new knowledge on properties of the resultant fuels and their implications to practical applications. Particularly, the research has been designed and carried out to use pyrolysis as a pretreatment technology for the production of biochar, bio-oil and bioslurry fuels. The main outcomes of this study are summarised as follows.

Firstly, biochars were produced from the pyrolysis of centimetre-sized particles of mallee wood at 300-500°C using a fixed-bed reactor under slow-heating conditions. The data show that at pyrolysis temperatures $> 320^{\circ}\text{C}$, biochar as a fuel has similar fuel H/C and O/C ratios compared to Collie coal which is the only coal being mined in WA. Converting biomass to biochar leads to a substantial increase in fuel mass energy density from ~ 10 GJ/tonne of green biomass to ~ 28 GJ/tonne of biochars prepared from pyrolysis at 320°C , in comparison to 26 GJ/tonne for Collie coal. However, there is little improvement in fuel volumetric energy density, which is still

around 7-9 GJ/m³ in comparison to 17 GJ/m³ of Collie coal. Biochars are still bulky and grinding is required for volumetric energy densification. Biochar grindability experiments have shown that the fuel grindability increases drastically even at pyrolysis temperature as low as 300°C. Further increase in pyrolysis temperature to 500°C leads to only small increase in biochar grindability. Under the grinding conditions, a significant size reduction (34-66 % cumulative volumetric size <75 µm) of biochars can be achieved within 4 minutes grinding (in comparison to only 19% for biomass after 15 minutes grinding), leading to a significant increase in volumetric energy density (e.g. from ~8 to ~19 GJ/m³ for biochar prepared from pyrolysis at 400°C). Whereas grinding raw biomass typically result in large and fibrous particles, grinding biochar produce short and round particles highly favourable for fuel applications.

Secondly, it is found that the pyrolysis of different biomass components produced biochars with distinct characteristics, largely because of the differences in the biological structure of these components. Leaf biochars showed the poorest grindability due to the presence of abundant tough oil glands in leaf. Even for the biochar prepared from the pyrolysis of leaf at 800°C, the oil gland enclosures remained largely intact after grinding. Biochars produced from leaf, bark and wood components also have significant differences in ash properties. Even with low ash content, wood biochars have low Si/K and Ca/K ratios, suggesting these biochars may have a high slagging propensity in comparison to bark and leaf biochars.

Thirdly, bio-oil and biochar were also produced from pyrolysis of micron-size wood particle using a fluidised-bed reactor system under fast-heating conditions. The excellent grindability of biochar had enabled desirable particle size reduction of biochar into fine particles which can be suspended into bio-oil for the preparation of bioslurry fuels. The data have demonstrated that bioslurry fuels have desired fuel and rheological characteristics that met the requirements for combustion and gasification applications. Depending on biochar loading, the volumetric energy density of bioslurry is up to 23.2 GJ/m³, achieving a significant energy densification (by a factor > 4) in comparison to green wood chips. Bioslurry fuels with high biochar

concentrations (11-20 wt%) showed non-Newtonian characteristics with pseudoplastic behaviour. The flow behaviour index, n decreases with the increasing of biochar concentration. Bioslurry with higher biochar concentrations has also demonstrated thixotropic behaviour. The bioslurry fuels also have low viscosity (<453 mPa.s) and are pumpable at both room and elevated temperatures. The concentrations of Ca, K, N and S in bioslurry are below the limits of slurry fuel guidelines.

Fourthly, bio-oil is extracted using biodiesel to produce two fractions, a biodiesel-rich fraction (also referred as bio-oil/biodiesel blend) and a bio-oil rich fraction. The results has shown that the compounds (mainly phenolic) extracted from bio-oil into the biodiesel-rich fraction reduces the surface tension of the resulted biodiesel/bio-oil blends that are known as potential liquid transport fuels. The bio-oil rich fraction is mixed with ground biochar to produce a bioslurry fuel. It is found that bioslurry fuels with 10% and 20% biochar loading prepared from the bio-oil rich fraction of biodiesel extraction at a biodiesel to bio-oil blend ratio 0.67 have similar fuel properties (e.g. density, surface tension, volumetric energy density and stability) in comparison to those prepared using the original whole bio-oil. The slurry fuels have exhibited non-Newtonian with pseudoplastic characteristics and good pumpability desirable for fuel handling. The viscoelastic behaviour of the slurry fuels also has shown dominantly fluid-like behaviour in the linear viscoelastic region therefore favourable for atomization in practical applications. This study proposes a new bio-oil utilisation strategy via coproduction of a biodiesel/bio-oil blend and a bioslurry fuel. The biodiesel/bio-oil blend utilises a proportion of bio-oil compounds (relatively high value small volume) as a liquid transportation fuel. The bioslurry fuel is prepared by mixing the rest low-quality bio-oil rich fractions (relatively low value and high volume) with ground biochar, suitable for stationary applications such as combustion and gasification.

Overall, the present research has generated valuable data, knowledge and fundamental understanding on advanced fuels from mallee biomass using pyrolysis as a pre-treatment step. The flexibility of pyrolysis process enables conversion of

bulky, low fuel quality mallee biomass to biofuels of high volumetric energy density favourable to reduce logistic cost associated with direct use of biomass. The significance structural, fuel and ash properties differences among various mallee biomass components were also revealed. The production of bioslurry fuels as a mixture of bio-oil and biochar is not only to further enhance the transportability/handling of mallee biomass but most importantly the slurry quality highly matched requirements in stationary applications such as combustion and gasification. The co-production of bioslurry with bio-oil/biodiesel extraction was firstly reported in this field. Such a new strategy, which uses high-quality extractable bio-oil compounds into bio-oil/biodiesel blend as a liquid transportation fuel and utilises the low-quality bio-oil rich fraction left after extraction for bioslurry preparation, offers significant benefits for optimised use of bio-oil.

ACKNOWLEDGEMENTS

All Praise to Allah, God of the Worlds.

I gratefully acknowledge the Ministry of Higher Education Malaysia and my employer, Sultan Idris University of Education in Malaysia for financial support through the SLAB sponsorship to cover my tuition fee and living allowance during my PhD study.

I also greatly acknowledge the financial support for my PhD research received from the Australia's Department of Innovation Industry, Science and Research through the Australia-China Special Fund for S&T Cooperation under the International Science Linkage scheme (Project No: CH070008), and also partially from the Australian Commonwealth Government as part of the Asia-Pacific Partnership on Clean Development and Climate.

I am especially indebted to my supervisor, Professor Hongwei Wu, for providing me the opportunity to join his research group, for his utmost guidance, advice, support and patience throughout the course of this study. I am sincerely grateful for all his time, commitments and inspirations which I learn as invaluable lessons in life. Without him, my PhD research would not be possible.

I would also like to acknowledge Mr. John Bartle from the industry and Professor Moses Tadé for assistance and help as thesis committee members.

I would like to express my deepest gratitude to my parents and family, for their moral support, encouragement and understanding during my life in overseas. Most importantly, I would like to express my greatest appreciation to my husband, Zaidi for his love, support and understanding. His invaluable sacrifice, patience and help are things that I hold dearly in my heart. I thank God everyday for our two beautiful sons Syakir and Izat.

Special thanks go to Gull Petroleum in providing biodiesel, Professor Chun-Zhu Li and Dr. Daniel Mourant for supplying fast pyrolysis bio-oil and biochar, Ms. Kun Aussieanita Mediaswanti for help in part of experiments in Chapter 5, Dr. Charlie Kong for assistance in SEM specimen preparation. Thanks also go to Drs. Caroline Lievens, Richard Gunawan and Monica Gumulya for their advice to some of the analytical analysis.

I would like to express my appreciation to Ms. Karen Haynes, Ms. Ann Carroll, Ms. Angelina Rossiter, Mr. Zeno Zhang and Mr. Jason Wright for their laboratory assistance. Thanks also go to the staff from Chemical Engineering Department for their assistance and the staff from Applied Physics Department for help in SEM analysis.

Last but not the least, Dr. Fujun Tian, Dr. Kongvui Yip, Dr. Yun Yu, Mr. Qiang Fu, Mr. Xiangpeng Gao, Ms. Yi Li, Ms. Yanwu Yang, Ms. Zhaoying Kong, Mr. Alan Burton, Mr. William Hendrawinata, Mr. Vlad Curteanu in our research group, my friends Ms. Monita Olivia, Mr. Gunawan Wibisono, Mr. Chao Li, Ms. Le Ngoc Thu, Mr. He Min and Ms. Yenny Gonzalez as well as all my other colleagues in Department of Chemical Engineering are thanked for their help in various ways.

LIST OF PUBLICATIONS

Journal Papers

- [1] **Hanisom Abdullah**, Hongwei Wu. Biochar as a Fuel: 1. Properties and Grindability of Biochars Produced from the Pyrolysis of Mallee Wood under Slow-Heating Conditions, *Energy & Fuels* **2009**, 23: 4174-4181.
- [2] **Hanisom Abdullah**, Kun Aussieanita Mediaswanti, Hongwei Wu. Biochar as a Fuel: 2. Significant Differences in Fuel Quality and Ash Properties of Biochars from Various Biomass Components of Mallee Trees, *Energy & Fuels* **2010**, 24: 1972-1979.
- [3] **Hanisom Abdullah**, Daniel Mourant, Chun-Zhu Li, Hongwei Wu. Bioslurry as a Fuel. 3. Fuel and Rheological Properties of Bioslurry Prepared from the Bio-oil and Biochar of Mallee Biomass Fast Pyrolysis, *Energy & Fuels* **2010**, 24: 5669-5676.
- [4] **Hanisom Abdullah**, Hongwei Wu. Bioslurry as a Fuel: 4. Preparation of Bioslurry Fuels from Biochar and the Bio-oil Rich Fractions after Bio-oil/Biodiesel Extraction, *Energy & Fuels*, **2011**, 25:1759-1771.

Submitted Conference Papers

- [1] **Hanisom Abdullah**, Hongwei Wu. Direct Utilisation of Biomass for Bioenergy Generation: Key Technical Challenges and Pre-treatment Technology, Universiti Malaysia Terengganu 10th International Annual Symposium (UMTAS 2011) to be held from 11th until 13th July 2011 in Kuala Terengganu, Malaysia. Accepted for oral presentation and proceeding publication.

TABLE OF CONTENTS

Declaration	I
Dedication	II
ABSTRACT	III
ACKNOWLEDGEMENTS	VII
LIST OF PUBLICATIONS	IX
TABLE OF CONTENTS	X
LIST OF FIGURES	XV
LIST OF TABLES	XXI
CHAPTER 1 INTRODUCTION	1
1.1 Background and Motive	1
1.2 Scope and Objectives	5
1.3 Thesis Outline	5
CHAPTER 2 LITERATURE REVIEW	8
2.1 Introduction	8
2.2 Biomass and Classification	9
2.3 Significance of Mallee Biomass in Australia	10
2.4 Technical Challenges in Biomass Utilisation	14
2.4.1 Biomass Fuel Chemistry and Implications	15
2.4.2 Inorganic Species in Biomass Fuels and Ash-related Problems during Biomass Utilisation	17
2.4.3 Biomass Fuel Grindability	18
2.4.4 Biomass Fuel Bulk and Energy Densities	19
2.4.5 Heterogeneities among Different Biomass Components and Biomass Materials	20
2.4.6 Summary	21
2.5 Biomass Pre-treatment Technologies	22
2.5.1 Drying	23
2.5.2 Pulverisation	24
2.5.3 Washing/leaching	25

2.5.4 Baling, Briquetting and Pelletizing	26
2.5.5 Torrefaction and Torrefaction combined with Pelletizing (TOP)	28
2.5.6 Pyrolysis	30
2.6 Slurry Fuel Technologies	32
2.7 Conclusions and Research Gaps	35
2.8 Research Objectives of the Present Study	37
CHAPTER 3 METHODOLOGY AND ANALYTICAL TECHNIQUES	38
3.1 Introduction	38
3.2 Methodology	38
3.2.1 Properties and Grindability of Biochars Produced from Pyrolysis of Mallee Wood under Slow-Heating Condition	39
3.2.2 Differences in Fuel Quality and Ash Properties of Biochars from Various Biomass Components of Mallee Trees	41
3.2.3 Bioslurry Production from Mallee Wood Biomass Fast Pyrolysis Oil and Biochar	41
3.2.4 Bioslurry Production from Biochar and the Bio-oil Rich Fraction after Bio-oil/Biodiesel Extraction	42
3.3 Experimental	45
3.3.1 Biomass and Fuel Preparation	45
3.3.2 Reactor Systems for Pyrolysis Experiment	46
3.4 Instruments and Analytical Techniques	47
3.4.1 Proximate, Ultimate and Calorific Value Analysis	47
3.4.2 Grindability of Solid Fuels	48
3.4.3 Bulk Density	48
3.4.4 Particle Size Analysis	49
3.4.5 Scanning Electron Microscope	49
3.4.6 Particle Shape Analysis	49
3.4.7 Quantification of Ash-forming Species in Solid and Liquid/Slurry Fuels	50
3.4.8 Biochar Surface Area, Porosity and Soakability	50

3.4.9 Preparation of Bioslurry	51
3.4.10 Extraction of Bio-oil/Biodiesel	51
3.4.11 Optical Microscope	51
3.4.12 Density and Surface Tension	51
3.4.13 Static Stability	52
3.4.14 Gas Chromatography-Mass Spectroscopy (GC-MS)	52
3.4.15 Rheological Study	52
3.5 Summary	53
CHAPTER 4 PROPERTIES AND GRINDABILITY OF BIOCHAR PRODUCED FROM THE PYROLYSIS OF MALLEE WOOD BIOMASS UNDER SLOW-HEATING CONDITIONS	54
4.1 Introduction	54
4.2 Methodology	55
4.3 Results and Discussion	55
4.3.1 Biochar Yield and Properties of Biochar as a Fuel	55
4.3.2 Grindability of Biochar	59
4.3.3 Particle Shape	64
4.4 Conclusions	67
CHAPTER 5 SIGNIFICANT DIFFERENCES IN FUEL QUALITY AND ASH PROPERTIES OF BIOCHARS FROM VARIOUS BIOMASS COMPONENTS OF MALLEE TREES	68
5.1 Introduction	68
5.2 Methodology	69
5.3. Results and Discussion	69
5.3.1 Partition and Compositions of Mallee Biomass Components	69
5.3.2 Differences in Biochar Yield and Fuel Chemistry	70
5.3.3 Significant Differences in Biochar Grindability	72
5.3.4 SEM Imaging	74
5.3.5 Differences in Biochar Energy Densities	76
5.3.6 Differences in Biochar Ash Properties	79

5.4. Conclusions	82
CHAPTER 6 FUEL AND RHEOLOGICAL PROPERTIES OF BIOSLURRY PREPARED FROM THE BIO OIL AND BIOCHAR OF MALLEE BIOMASS FAST PYROLYSIS	
6.1 Introduction	84
6.2 Methodology	87
6.2.1 Preparation of Bioslurry	87
6.3 Results and Discussion	87
6.3.1 Properties of Ground Biochar for the Preparation of Bioslurry Fuels	88
6.3.2 Fuel Properties and Significant Energy Densification via the Preparation of Bioslurry	90
6.3.3 Inorganic Species in Bioslurry Fuels	92
6.3.4 Bioslurry Static Stability	94
6.3.5 Rheological Property of Bioslurry	95
6.3.6 Benchmarking of Bioslurry against Other Slurry Fuels and Implications	98
6.4 Conclusions	99
CHAPTER 7 PREPARATION OF BIOSLURRY FUELS FROM BIOCHAR AND THE BIO-OIL RICH FRACTIONS AFTER BIO-OIL/BIODIESEL EXTRACTION	100
7.1 Introduction	100
7.2 Methodology	101
7.3 Results and Discussion	103
7.3.1 Fuel Chemistry	103
7.3.2 Solubility of Bio-oil in Biodiesel	105
7.3.3 Fuels Density, Surface Tension and GC-MS	108
7.3.4 Fuel Volumetric Energy Density and Stability	113
7.3.5 Rheology of Bioslurry Fuels Prepared from the Bio-oil Rich Fractions after Biodiesel Extraction	114
7.4 Implications	123
7.5 Conclusions	124

CHAPTER 8 CONCLUSIONS AND RECOMMENDATIONS	126
8.1 Introduction	126
8.2 Conclusions	127
8.2.1 Properties and Grindability of Biochar Produced from the Pyrolysis of Mallee Wood Biomass under Slow-heating Conditions	127
8.2.2 Significant Differences in Fuel Quality and Ash Properties of Biochars from Various Biomass Components of Mallee Trees	128
8.2.3 Fuel and Rheological Properties of Bioslurry Prepared from the Bio-oil and Biochar of Mallee Biomass Fast Pyrolysis	129
8.2.4 Preparation of Bioslurry Fuels from Biochar and the Bio- oil Rich Fractions after Bio-oil/Biodiesel Extraction	130
8.3 Recommendations	132
REFERENCES	134

LIST OF FIGURES

Figure 1-1 Thesis map	7
Figure 2-1 Alley farming of mallee in agricultural land under the threat of dryland salinity at Kalannie, WA. (courtesy from the Oil Mallee Association) ⁶² Mallee trees are grown sustainably in the form of long narrow lines and conventional annual crops are planted between the mallee lines.	13
Figure 2-2 Mallee production system for biomass production ¹³	14
Figure 2-3 van Krevelen diagram for various solid fuels ⁴⁵	15
Figure 2-4 Moisture content of fuels (Data taken from reference ⁷)	16
Figure 2-5 Main components of mallee biomass	21
Figure 2-6 Green house residue pellets before (left) and after screw feeding (right) ⁶	27
Figure 2-7 Products from various densification processes	29
Figure 2-8 Volumetric energy density of various solid fuel (SB- straw bales, TB-torrefied biomass, GTLR-ground torrefied logging residue, W-wood, GTPC-ground torrefied pine chip, WP-wood pellets, CSBr-corn stover briquettes, TOP- Torrefaction in combination with pelletizing, Coal-typical black coal)	29
Figure 3-1 Research Methodology	40
Figure 3-2 Biomass and Collie coal samples	45

Figure 3-3 A schematic diagram of fixed-bed pyrolysis reactor	46
Figure 3-4 A schematic diagram of the fluidised-bed pyrolyser used in this study ⁹⁹	47
Figure 3-3 Haake Mars II rheometer and Z20 sensor system	53
Figure 4-1 Biochar yield of mallee wood pyrolysis in a fixed-bed reactor at various temperatures	56
Figure 4-2 Relationship between fuel H/C and O/C ratios for various solid fuels. Legends: DWB, dried wood biomass; WCxxx, biochar prepared from the pyrolysis of the dried wood biomass at xxx°C; Collie, Collie coal	57
Figure 4-3 Mass energy density (A), bulk density (B), and volumetric energy density (C) of various fuels. GWB, green wood biomass; DWB, dried wood biomass; WCxxx, biochar prepared from the pyrolysis of the dried wood biomass at xxx°C; Collie, Collie coal	58
Figure 4-4 Particle size distributions of selected ground fuels. DWB, dried wood biomass; WCxxx, biochar prepared from the pyrolysis of the dried wood at xxx°C; Collie, Collie coal	60
Figure 4-5 Particle size distributions of selected ground fuels at 4 min grinding time. DWB, dried wood biomass; WCxxx, biochar prepared from the pyrolysis of the dried wood at xxx°C; Collie, Collie coal	61
Figure 4-6 Bulk energy density (A) and volumetric energy density (B) of various fuels as a function of grinding time. DWB, dried wood	63

biomass; WCxxx, biochar prepared from the pyrolysis of the dried wood biomass at xxx°C; Collie, Collie coal	
Figure 4-7 Images of ground fuel samples. (Legends: DWB, dried wood biomass; WCxxx, biochar prepared from the pyrolysis of the dried wood biomass at xxx°C; Collie, Collie coal)	65
Figure 4-8 Major/minor axis length ratio and roundness of fuel particles after grinding for 1 min (A and B) and 4 mins (C and D). DWB, dried wood biomass; WCxxx, biochar prepared from the pyrolysis of the dried wood biomass at xxx°C; Collie, Collie coal	67
Figure 5-1 Biochar yield of mallee partitions in a fixed-bed reactor at various temperatures. (Legends: LC, biochar prepared from leaf component; BC, biochar prepared from bark component; WC, biochar prepared from wood component)	71
Figure 5-2 Particle size distributions (PSDs) of selected ground biochars. (Legends: LC, biochar prepared from leaf component; BC, biochar prepared from bark component; WC, biochar prepared from wood component)	73
Figure 5-3 Images of unground and ground fuel samples. (Legends: LC, biochar prepared from leaf component; BC, biochar prepared from bark component; WC, biochar prepared from wood component)	75
Figure 5-4 Bulk density and volumetric energy density of various fuels. (Legend: DB, dried biomass, and Cxxx, biochar prepared at xxx°C)	77
Figure 5-5 Retention of AAEM species in (○) leaf biochar, (□) wood biochar, and (▽) bark biochar as a function of pyrolysis temperature	80

Figure 5-6 Relationship between fuel Si/K and Ca/K ratios. LCxxx-biochar prepared from dried leaf biomass at xxx °C; BCxxx-biochar prepared from dried bark biomass at xxx °C; WCxxx-biochar prepared from dried leaf biomass at xxx °C. DLB-dried leaf biomass; DBB- dried bark biomass; DWB- dried wood biomass	82
Figure 6-1 Particle size distributions of ground biochar at various grinding time	88
Figure 6-2 Particle size distributions of ground biochar at 8 mins grinding time	89
Figure 6-3 Mass energy, bulk and volumetric energy densities of fuels. BM- biomass	91
Figure 6-4 Static stability of fuels	94
Figure 6-5 Shear stress and apparent viscosity of fuels as a function of shear rate	95
Figure 6-6 Apparent viscosity of fuels at shear rate 100s^{-1} . Guideline limit: 1000 mPa.s in boilers, 700 mPa.s in pressurised gasifier	97
Figure 6-7 Thixotropic behaviour of fuels	98
Figure 7-1 van Krevelen diagram showing relationship of fuel H/C ratio to O/C ratio. BOR x.xx – bio-oil rich fraction obtained from biodiesel extraction at a biodiesel to bio-oil ratio of x.xx, BDR x.xx – biodiesel rich fraction obtained from biodiesel extraction at a biodiesel to bio-oil ratio of x.xx	105

Figure 7-2 Extraction curve of biodiesel/mallee bio-oil blends	106
Figure 7-3 Photomicroscopy of fuels. BOR x.xx – bio-oil rich fraction obtained from biodiesel extraction at a biodiesel to bio-oil ratio of x.xx	108
Figure 7-4 Surface tension of various fuels. BOR x.xx – bio-oil rich fraction obtained from biodiesel extraction at a biodiesel to bio-oil ratio of x.xx; BDR x.xx – biodiesel rich fraction obtained from biodiesel extraction at a biodiesel to bio-oil ratio of x.xx	110
Figure 7-5 GC-MS of selected compounds in bio-oil, biodiesel and resulted fractions. BDR 0.67 – biodiesel rich fraction obtained from biodiesel extraction at a biodiesel to bio-oil ratio of 0.67; BOR 0.67 – bio-oil rich fraction obtained from biodiesel extraction at a biodiesel to bio-oil ratio of 0.67	111
Figure 7-6 Volumetric energy density of various fuels. GB – green biomass; WP – wood pellets; TOP – torrefaction in combination with pelletizing; BOR x.xx – bio-oil rich fraction obtained from biodiesel extraction at a biodiesel to bio-oil ratio of x.xx; BDR x.xx – biodiesel rich fraction obtained from biodiesel extraction at a biodiesel to bio-oil ratio of x.xx; BO-10% and BO-20% – bioslurry fuels prepared from the whole bio-oil with 10 wt% and 20 wt% biochar loading, respectively; BOR 0.67-10% and BOR 0.67-20% – bioslurry fuels prepared from bio-oil rich fraction after biodiesel extraction (at a biodiesel to bio-oil ratio of 0.67) with 10 wt% and 20 wt% biochar loading, respectively	113
Figure7-7 Apparent viscosity of various fuels as a function of shear rate. BOR x.xx – bio-oil rich fraction obtained from biodiesel extraction at a biodiesel to bio-oil ratio of x.xx; BO-10% and BO-	115

20% – bioslurry fuels prepared from the whole bio-oil with 10 wt% and 20 wt% biochar loading, respectively; BOR 0.67-10% and BOR 0.67-20% – bioslurry fuels prepared from bio-oil rich fraction after biodiesel extraction (at a biodiesel to bio-oil ratio of 0.67) with 10 wt % and 20 wt% biochar loading, respectively

Figure 7-8 Storage (G') and loss (G'') moduli of fuels as a function of stress. BO-10% and BO-20% – bioslurry fuels prepared from the whole bio-oil with 10 wt% and 20 wt% biochar loading, respectively; BOR 0.67-10% and BOR 0.67-20% – bioslurry fuels prepared from bio-oil rich fraction after biodiesel extraction (at a biodiesel to bio-oil ratio of 0.67) with 10 wt% and 20 wt% biochar loading, respectively 120

Figure 7-9 Storage (G') and loss (G'') moduli of fuels as a function of frequency. BO-10% and BO-20% – bioslurry fuels prepared from the whole bio-oil with 10 wt% and 20 wt% biochar loading, respectively; BOR 0.67-10% and BOR 0.67-20% – bioslurry fuels prepared from bio-oil rich fraction after biodiesel extraction (at a biodiesel to bio-oil ratio of 0.67) with 10 wt% and 20 wt% biochar loading, respectively 121

Figure 7-10 Value of fuels $\tan \delta$ as a function of frequency. BO-10% – bioslurry fuels prepared from the whole bio-oil with 10 wt% biochar loading; BOR 0.67-10% – bioslurry fuels prepared from bio-oil rich fraction after biodiesel extraction (at a biodiesel to bio-oil ratio of 0.67) with 10 wt % biochar loading 122

Figure 7-11 A proposed strategy for the coproduction of biodiesel/bio-oil blend (as a liquid transport fuel) and bioslurry fuel (as a high-energy-density fuel for combustion and gasification applications) from bio-oil and biochar products of biomass fast pyrolysis 124

LIST OF TABLES

Table 2-1 Classification of biomass as solid fuels resources ⁵³	10
Table 2-2 A scheme for assessing feedstocks for biofuels and bioenergy in Australia based on current and future production bases, and first and second generation processing technologies ¹⁴	12
Table 2-3 Milling test experience using ball mill systems	19
Table 2-4 Key biomass properties and its associated technical challenges	22
Table 2-5 Role and limitation of various pre-treatment methods	30
Table 2-6 Slurry fuel requirements in combustion system and significant impact ^{51,109-126}	33
Table 3-1 Summary of methodology	43
Table 4-1 Proximate and ultimate analysis of various fuels	57
Table 5-1 Proximate and ultimate analysis of biomass	69
Table 5-2 Proximate and ultimate analysis of biochars	71
Table 5-3 Contents (wt% db) of inorganic species, including AAEM species in fuel samples	79
Table 5-4 Indices in applications of biomass for fuel generation	81

Table 6-1 Summary of reviews in recent developments of biomass-derived slurry fuels	85
Table 6-2 Ultimate and proximate analysis of biomass, biochar and bio-oil	90
Table 6-3 Elemental analysis of fuels	93
Table 6-4 Flow behaviour index, n of bioslurry (25°C)	96
Table 6-5 Benchmarking of bioslurry against fuel requirements ^{51,109-116,118-121,123-126,170,171} in combustion/gasification	99
Table 7-1 Fuel properties and heating values. BOR x.xx – bio-oil rich fraction obtained from biodiesel extraction at a biodiesel to bio-oil ratio of x.xx; BDR x.xx – biodiesel rich fraction obtained from biodiesel extraction at a biodiesel to bio-oil ratio of x.xx	103
Table 7-2 Fuel density and equilibrium surface tension. BOR x.xx – bio-oil rich fraction obtained from biodiesel extraction at a biodiesel to bio-oil ratio of x.xx; BDR x.xx – biodiesel rich fraction obtained from biodiesel extraction at a biodiesel to bio-oil ratio of x.xx; BO-10% and BO-20% – bioslurry fuels prepared from the whole bio-oil with 10 wt% and 20 wt% biochar loading, respectively; BOR 0.67-10% and BOR 0.67-20% – bioslurry fuels prepared from bio-oil rich fraction after biodiesel extraction (at a biodiesel to bio-oil ratio of 0.67) with 10 wt% and 20 wt% biochar loading, respectively	109

Table 7-3 Estimation of Ohnesorge number based on fuel properties at 40°C. BOR x.xx – bio-oil rich fraction obtained from biodiesel extraction at a biodiesel to bio-oil ratio of x.xx; BDR x.xx – biodiesel rich fraction obtained from biodiesel extraction at a biodiesel to bio-oil ratio of x.xx; BO-10% and BO-20% – bioslurry fuels prepared from the whole bio-oil with 10 wt% and 20 wt% biochar loading, respectively; BOR 0.67-10% and BOR 0.67-20% – bioslurry fuels prepared from bio-oil rich fraction after biodiesel extraction (at a biodiesel to bio-oil ratio of 0.67) with 10 wt% and 20 wt% biochar loading, respectively	117
Table 7-4 Flow behaviour index, n of various fuels. BO-10% and BO-20% – bioslurry fuels prepared from the whole bio-oil with 10 wt% and 20 wt% biochar loading, respectively; BOR 0.67-10% and BOR 0.67-20% – bioslurry fuels prepared from bio-oil rich fraction after biodiesel extraction (at a biodiesel to bio-oil ratio of 0.67) with 10 wt% and 20 wt% biochar loading, respectively	117
Table 7-5 Summary of bioslurry fuels prepared using bio-oil rich fractions, benchmarking against those prepared using the whole bio-oil	123

CHAPTER 1

INTRODUCTION

1.1 Background and Motive

Coal is responsible for the majority of electricity generation in Australia and will continue to provide cheap and secure energy for powering the Australian economy in the foreseeable future.¹ However, the use of fossil fuels (particularly stationary coal-fired power generation) is known as one of the biggest contributors to green house gases emissions, leading to global warming and the problems related to climate change.² Global fossil fuel used in the Reference Scenario increases energy-related CO₂ emissions from ~29Gt in 2007 to >40Gt in 2030.³ In the transition to future sustainable development, renewable energy sources are becoming increasingly important in the global energy supply mix. The International Energy Agency (IEA) predicts that renewable energy will increase to 16% of the global energy supply by 2030, of which biomass will be the single most important renewable energy source,³ accounting for ~ 73% of the total renewable energy supply. For world primary energy demand from year 2007-2030, biomass and wastes are expected to have an average 1.4% annual growth.³

There are significant advantages of biomass utilisation for power generation. If produced in sustainable manner, biomass delivers many environmental benefits such as mitigation of green house gases emissions and soil improvement.⁴ Biomass can be closed to carbon neutral, depending on their production processes.⁵ Biomass can also be coprocessed with coal, such as co-firing, to achieve significant emission reductions.^{6,7} Therefore, development of a biomass-based bioenergy system can both reduces our reliance on fossil fuels and promotes sustainable rural and regional development.

Australia is projected for significant expansion of a biomass-based power generation industry especially from short rotation crops of mallee eucalyptus.⁸⁻¹² Mallee is typically grown in conventional agricultural land in the form of alley farming i.e. narrow belts occupying <10% of the land. Alley farming promotes yield through better water capture.^{8,13} In comparison to other dedicated energy crops, mallee biomass has many unique advantages:

- *A true second generation biomass feedstock.* As dual purpose crop to manage the serious dryland salinity in the premium agricultural lands of Australia and producing biomass as a byproduct, mallee biomass does not compete with, rather on the contrary enhances food production.⁸
- *Large-scale biomass production.* Mallee biomass is produced from relatively small area agricultural land offering significant contribution to a streamline bioenergy supply chain.⁸ In Western Australia (WA) alone, the annual production of mallee biomass can be up to ~10 million dry tonnes per annum.^{9,10}
- *Efficient bioenergy production for CO₂ mitigation with high energy productivity in Australia.* Recent life cycle analysis has demonstrated that mallee biomass production is close to carbon neutral⁵ and achieves an energy ratio of 41.7 and an energy productivity of 206.3 GJ/ (ha year), far exceeding the performance of other annual crops such as canola which has energy ratio below 7.0 and energy productivity below 40.0GJ/ (ha year).¹³
- *Significant contribution to local energy security and sustainable development in rural and regional Australia.* Apart from bioenergy as key products, new industries/markets can be established for various co-products from mallee biomass eg. solid wood products for timber and furniture, wood composite, activated carbon, essential oil, tannins and biopolymers.¹⁴

In summary, mallee biomass is a key second generation biomass feedstock in Australia. It can play a significant and positive role in Australia's future bioenergy industry and economy.

However, biomass as a fuel suffers from several undesired characteristics which limit its utilisation. These undesired characteristics are listed below:

- *Bulky, high moisture and low energy density.* In the case of mallee, the green chipped mallee biomass (~10 cm length dimensions) typically contains 45% moisture and has a volumetric energy density ~18% that of typical black coals (Chapter 6).
- *Poor grindability.* Due to its fibrous nature, biomass size reduction is problematic with conventional grinders that use compressive force originally designed to mill a more brittle coal.
- *Mismatch of biomass fuel properties with those of coal.* For example in co-firing, biomass combustion generates huge quantity of flue gas¹⁵ which influences combustion stability, reduces coal residence time leading to loss of plant efficiency.^{16,4}
- *Ash related issues.* Biomass often contains high alkali leading to various ash related problems i.e deposition, corrosion, fouling and sintering.¹⁶⁻¹⁸
- *Heterogenous nature.* Biomass feedstock often contains various components which have very different characteristics. The highly heterogenous feedstock further complicated the coal vs. biomass fuel mismatch effects.¹⁹

Fuel supply chain plays a significant role in biomass utilisation. As a result of low energy density, long distance transportation of mallee biomass is not economic and the capacity of dedicated bioenergy plants utilising mallee biomass as feedstock is constrained.²⁰ Logistics cost can be > 50% of total bioenergy production cost.^{20,21} Poor grindability further increase grinding energy, fuel handling cost and overall plant investment cost.¹⁹ Additionally, while poor grindability determines that feasible biomass utilisation must deal with large particles, unfortunately large biomass particles are undesirable for efficient combustion and limits fuel feeding.¹⁶ These key issues significantly impedes the development of downstream applications such as biomass co-firing, which is known to be a main strategy to increase biomass feedstock in the vast existing coal-based power station infrastructure.⁴ As results of biomass-related problems, the uptake of biomass for co-firing in coal-fired power stations is limited²² and the average cost of power generation is also increased.^{19,23}

Several approaches have been made to address the problems associated with the direct use of biomass as a fuel. This includes upstream measures to pre-treat biomass such as:

- Drying technology for moisture reduction and improve biomass heating value.^{19,24,25}
- Washing/leaching to remove problematic ash forming species.^{19,26,27}
- Installation of independent biomass grinders in conventional coal stations to address poor grindability issue and increase biomass uptake >5%.²⁸
- Compaction/densification methods such as baling,^{4,19} briquetting,^{6,29} and pelletizing^{6,19,30-32} to increase bulk and energy density of biomass.
- Light thermal pre-treatment method (torrefaction)³³⁻³⁶ to partially decompose biomass, improving its grindability and heating value.
- Combination of torrefaction and pelletizing (TOP) to increase biomass volumetric energy density.^{19,37}

These methods were able to solve the biomass problem to a certain extent. The volumetric energy density accomplished is moderate. Regardless to particle fineness achieved, some techniques such as pulverisation technology, briquetting and pelletizing are expensive and require high grinding energy. Product durability and applicability of these methods to existing coal-fired power plant is still an issue. Therefore, further innovation is required to:

- Drastically increasing volumetric energy density of the fuel;
- Significant improvement in fuel grindability; and
- Satisfactorily addressing fuel mismatching in co-firing applications.

An alternative pre-treatment method is pyrolysis, through which the bulky green biomass can be converted to biofuels such as biochar and/or bio-oil. Pyrolysis is a flexible low-cost technology which is capable of processing a wide variety of feedstocks.^{38-41,42} Pyrolysis of mallee biomass for the production of biochar and bio-oil is one of the possible routes targeted to establish a high- energy-density biofuels industry in WA.

1.2 Scope and Objectives

This study aims to fundamentally investigate the production and properties of high-energy-density fuels derived from mallee biomass. It addresses the key issues associated with the direct use of biomass as a fuel, using pyrolysis as a biomass pre-treatment method. The detailed objectives of the present study are:

- (1) To explain the fuel properties and grindability of wood biochar benchmarked to a local coal;
- (2) To understand the differences of fuel and ash properties of biochar produced from mallee leaf, bark and wood components and implications of individual components/whole mallee tree as fuel feedstock;
- (3) To investigate the production, fuel and rheological properties of bioslurry from bio-oil/biochar blend; and
- (4) To study the properties of bioslurry and fuel derivatives produced from bio-oil rich fraction after extraction of bio-oil/biodiesel.

1.3 Thesis Outline

There are a total of 8 chapters in this thesis. Each chapter is organized as follows, and the thesis structure is schematically outlined in the thesis map (Figure 1-1):

Chapter 1 introduces the background and aims of the current research;

Chapter 2 summarizes literature survey for significance of mallee biomass, technical challenges associate with direct utilisation of biomass and current technologies deployed to treat biomass to achieve fuel densification finally leading to the identification of gaps and specific objectives for the current study;

Chapter 3 presents the methodology employed to achieve the research objectives, along with detailed explanation of the experimental equipments and materials used;

Chapter 4 discusses the fuel properties/compositions, grindability, energy densification and particle size/shape of biochar produced from slow pyrolysis of mallee wood at various temperatures, and the data is benchmarked against Collie coal;

Chapter 5 understands the significant differences in the fuel and ash properties between biochars derived from various components of mallee trees i.e leaf, bark and wood using slow pyrolysis;

Chapter 6 examines fuel properties, steady fluid rheology and densification of bioslurry produced from mixtures of fast pyrolysis bio-oil and biochar of mallee wood matching the bioslurry properties with fuel demands in various combustion applications;

Chapter 7 develops a method for the production of bioslurry from bio-oil rich fraction after extraction of bio-oil/biodiesel, and investigates the fuels compositions, chemical compounds, surface tension and slurry rheology; and

Chapter 8 concludes the present study and recommends several areas for future research.

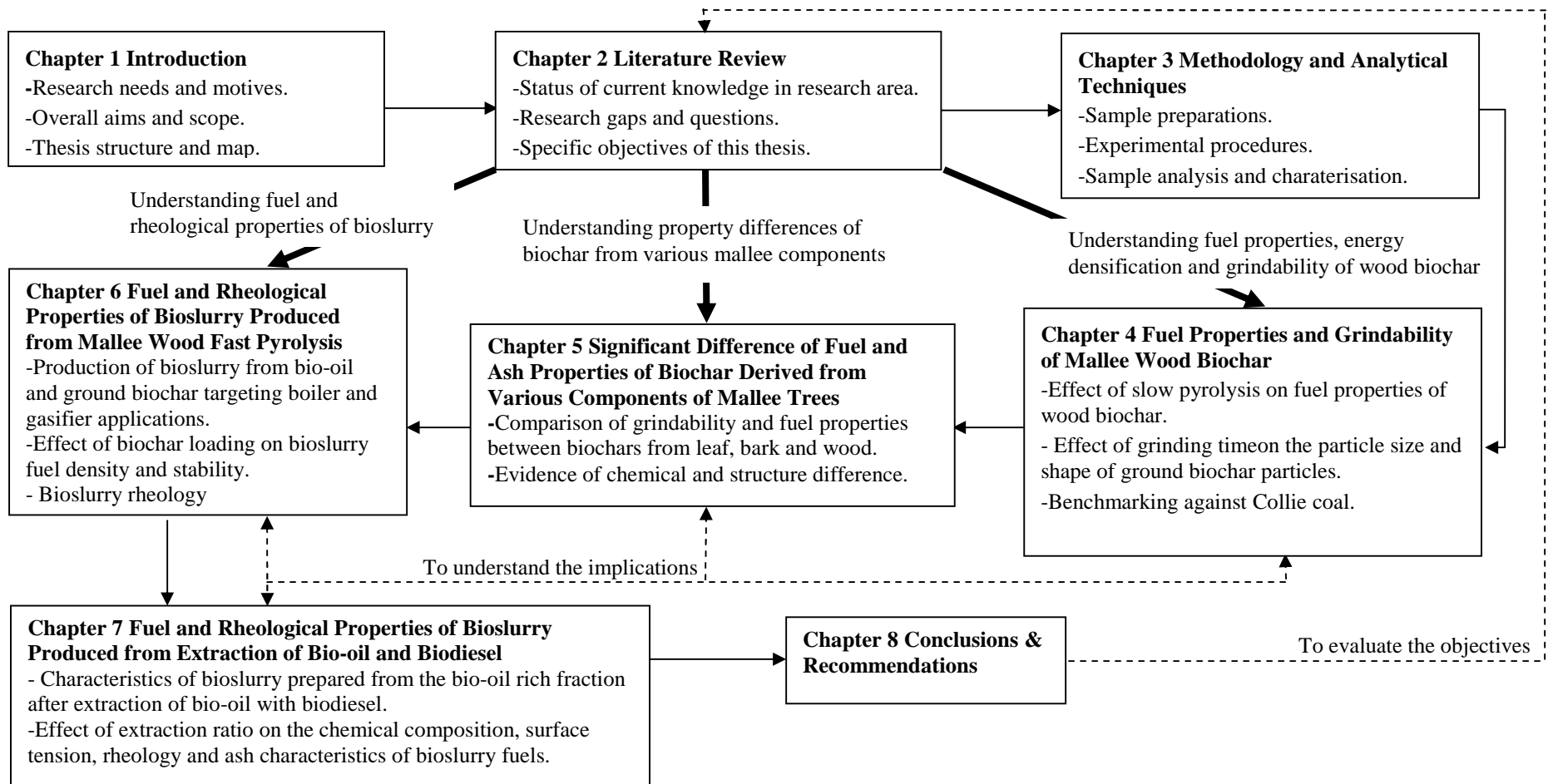


Figure 1-1 Thesis map

CHAPTER 2

LITERATURE REVIEW

2.1 Introduction

In the past twenty years, significant research and development have been carried out to address the undesirable issues of biomass for power generation.^{16,17,34,41,43-51,6,52} The previous studies were focused on various solutions for the problems associated with biomass utilisation, including upstream pre-treatment technologies¹⁹ to tailor the source of problems (biomass properties) and downstream solutions for addressing unwanted consequences of biomass applications (change of corroded equipment, cleaning of deposits, soot blowing, chemical addition etc). The objectives of this chapter are to review the up-to-date research progress on upstream biomass pre-treatment methods and to evaluate its potential applications, particularly on biomass energy densification and fuel matching technology.

This review firstly gives a brief introduction on biomass and the important roles of mallee biomass as a bioenergy resource in Australia. A discussion on biomass properties with key technical challenges associated with direct utilisation of biomass then follows. The chapter then reviews biomass pre-treatment methods deployed to solve these problems including drying, pulverisation technology, washing/leaching, baling, pelletizing, briquetting, torrefaction and pyrolysis. The typical operation conditions, products properties, application potentials and limitation of these technologies are then summarised. This chapter concludes with several research gaps identified on production of high-energy-density fuels from biomass and the scope of study defined in this PhD thesis.

2.2 Biomass and Classification

Biomass is a complex biogenic organic-inorganic solid material produced by natural and technogenic processes. It includes natural constituents produced from growing land- and water-based vegetation via photosynthesis process or generated via animal and human food digestion. Any products derived from technical processing of these natural constituents are also biomass.⁵³ Biomass composes of polymers that have extensive chains of carbon atoms linked into macromolecules. There are three major types of carbohydrate polymers in biomass, i.e. cellulose, hemicelluloses and lignin. Other biomass compounds are lipids, proteins, simple sugars, water and inorganic species.⁵⁴

With regards to biomass usage as solid fuel resources worldwide, biomass can be classified into several groups according to their biological diversity, source and origin (Table 2-1). While the combustion of biomass itself does produce CO₂, biomass utilisation is carbon neutral or close to carbon neutrals, depending on biomass production process. If biomass is produced in a sustainable manner, its application for energy production offers significant advantages. This is due to the fact that plant growth for the production of biomass feedstock consumes atmospheric CO₂ thus offsets the CO₂ emission from biomass fuel combustion. Therefore, sustainable use of biomass energy could be among the ways for nations to meet the Kyoto agreement and decrease their reliance on foreign petroleum.⁵⁵

Table 2-1 Classification of biomass as solid fuels resources⁵³

Biomass groups	Biomass sub-groups, varieties and species
1. Wood and woody biomass	Coniferous or deciduous; angiospermous or gymnospermous; soft or hard; stem, branches, foliage, bark, chips, lumps, pellets, briquettes, sawdust, sawmill and others from various wood species.
2. Herbaceous and agricultural biomass	Annual or perennial and field-based or processed-based such as: <ol style="list-style-type: none"> a. Grasses and flowers (alfalfa, arundo, bamboo, bana, brassica, cane, cynara, miscanthus, switchgrass, timothy, other) b. Straws (barley, bean, flax, corn, mint, oat, rape, rice, rye, sesame, sunflower, wheat, others) c. Other residues (fruits, shells, husks, hulls, pits, pips, grains, seeds, coir, stalks, cobs, kernels, bagasse, food, fodder, pulps, cakes, others)
3. Aquatic biomass	Marine or freshwater algae; macroalgae (blue, green, blue-green, brown, red) or microalgae; seaweed, kelp, lake weed, water hyacinth, others.
4. Animal and human biomass wastes	Bones, meat-bone meal, chicken litter, various manures, others.
5. Contaminated biomass and industrial biomass wastes (semi biomass)	Municipal solid waste, demolition wood, refuse-derived fuel, sewage sludge, hospital waste, paper-pulp sludge, waste papers, paperboard waste, chipboard, fibreboard, plywood, wood pallets and boxes, railway sleepers, tannery waste, others.
6. Biomass mixtures	Blends from the above varieties

2.3 Significance of Mallee Biomass in Australia

In Australia, black coal remains the largest contributor to the nation's total energy production. For example, in the year of 2006-07, energy supply from black coal is ~44% in Australia's national energy mix. However, the supplies of renewable energy products have been increased steadily from 2001-02 and 2006-07. For example, biomass wood/bagasse grew by 10% and biofuel (liquid or gas) increased by 30%, although biomass wood/bagasse and biofuels made up of only ~1% and 0.06% of the total energy consumption in 2006-2007,⁵⁶ indicating substantial room for future growth. At present, biofuel productions are developed based on various dedicated energy crops containing sugar/starch/oil such as sugar cane, wheat and canola (Table 2-2). For these first generation biofuels produced from food crops, conversion

technologies and markets are well established for relatively easy market penetration.⁵⁷ However, it is known that utilisation of large quantities of first generation biofuels is of low energy efficiency and high carbon footprint and will lead to serious competition with food production.^{58,59} Therefore, second generation feedstock such as lignocellulosic materials are becoming more viable and significant. Available as primary source (in the field), secondary (residue from forest/agroindustry) or tertiary waste (from urban/industrial activity),⁸ second generation biofuels are abundant, of low cost and have high ratio of energy output to input.

Woody perennial species from the genus *Eucalypts* or mallee are widely recognized as key second generation bioenergy feedstock at present and in the future (shown as dotted lines in Table 2-2). In Western Australia (WA), the development of mallee plantation in alleys between wheat crops began since 1990s with 12 000 ha of mallee have been collectively planted so far.⁸ The key objective is to manage the serious dryland salinity problems which impact the sustainability of wheat production in the “wheatbelt agricultural area”.^{10,60} Mallees has outstanding coppice ability i.e new vegetation can resprout from rootstocks after harvest. During 3-6 years harvest cycle, only above-ground biomass is coppiced leaving the root systems intact. New shoots grow rapidly from the root system and as the root system matures with age, more robust vegetation is produced. Once planted, the life duration of mallee tree can be well over 100 years.⁶¹ It was estimated that a total carbon sequestration of ~90 million tonnes in the form of living biomass can be generated for every 3 million hectares of mallee farm.⁶¹ With the assumptions of 30 tonnes mean carbon dioxide increment per year, the rate of sequestration would be 90 million tonnes/yr therefore over a thirty year period a carbon sink of 2.7 billion tonnes would be created.

Table 2-2 A scheme for assessing feedstocks for biofuels and bioenergy in Australia based on current and future production bases, and first and second generation processing technologies¹⁴

	1st generation biofuels	2nd generation biofuels
Current production base	Box 1 Ethanol and biodiesel: Ethanol <ul style="list-style-type: none"> • Sugar, C-molasses • Wheat • Barley • Oats • Sorghum • Maize • Sweet sorghum • Sugar beet Biodiesel <ul style="list-style-type: none"> • Used cooking oil • Tallow • Canola • Mustard 	Box 2 Lignocellulosic for ethanol, butanol, methanol, biogas or electricity , as well as Box 1 crops in biorefining to produce multiple co-products including biofuels: Crops residues <ul style="list-style-type: none"> • Sugar bagasse and cane trash • Cereal stubble Grasses <ul style="list-style-type: none"> • Annual and perennial grasses Farm forestry crops <ul style="list-style-type: none"> • Oil mallee • Short rotation coppicing trees Forestry <ul style="list-style-type: none"> • Wood harvested for sawlogs and pulpwood • Firewood • Residue currently left in native forests • Residue currently left in plantations • Increased forest thinnings Waste streams <ul style="list-style-type: none"> • Waste from wood processing facilities • Urban wood waste • Black liquor (byproduct of pulping) • Residues from food processing • Municipal Solid Waste
Future production base	Box 3 Ethanol and biodiesel: <ul style="list-style-type: none"> • Expanded production of Box 1 crops • GM crops • Tree crops with high production potential, largely untested in Australia eg <i>Jatropha</i>, <i>Pongamia</i>, <i>Moringa</i>, <i>Hura crepitans</i>. • Algae 	Box 4 Biorefineries for range of high value biobased products, with energy co-products: Forestry or farm forestry <ul style="list-style-type: none"> • Expansion of current hardwood or softwood plantation forestry • Expansion of oil mallee industry • 'FloraSearch' type farm forestry-high value new wood products with energy as coproduct Grasses <ul style="list-style-type: none"> • Expansion of new grasses eg Switchgrass Algae GM crops, grasses, trees Other unidentified 'biorefinery' initiatives

In reality, the target is not far to be achieved. In WA alone, the potential annual production of mallee biomass can be ~10 million dry tones per annum.^{9,10} As a byproduct rather than a dedicated energy crop, mallee biomass complements conventional agriculture by delivering environmental services to lowering the salty water table at the same time producing feedstock for bioenergy industry⁸ (Figure 2-1). Competition with commercial crops is minimal as mallee biomass only occupies <10 % of agricultural land.⁸

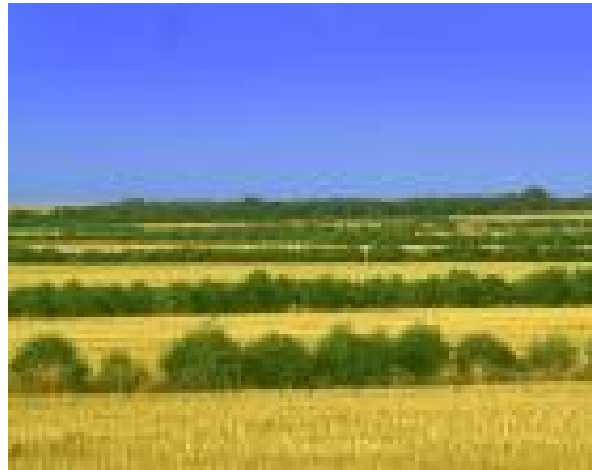


Figure 2-1 Alley farming of mallee in agricultural land affected by dryland salinity at Kalannie, WA. (courtesy from the Oil Mallee Association) ⁶² Mallee trees are grown sustainably in the form of long narrow lines and conventional annual crops are planted in between the mallee lines.

Wu et al.¹³ assessed the overall energy balance during mallee biomass growth, harvest, transport and delivery to a central processor over a production period of 50 years, considering all direct and indirect energy inputs associated with all activities eg heat, electricity, fertilizers etc. (Figure 2-2). The energy consumption associated with each input was converted to the equivalent non-renewable primary energy required to the production, supply and use of the energy. The energy output is the primary energy contained in all mallee biomass components. It is estimated that the ratio of energy output in biomass to non-renewable energy inputs during the whole process (i.e. energy ratio) for mallee is over 40, in comparison to other annual dedicated crops grown in the same region, such as canola that has much lower energy ratio < 7.0 . Overall, the results have indicated that mallee could be the largest and cheapest source of secondary generation biomass fuel in WA.

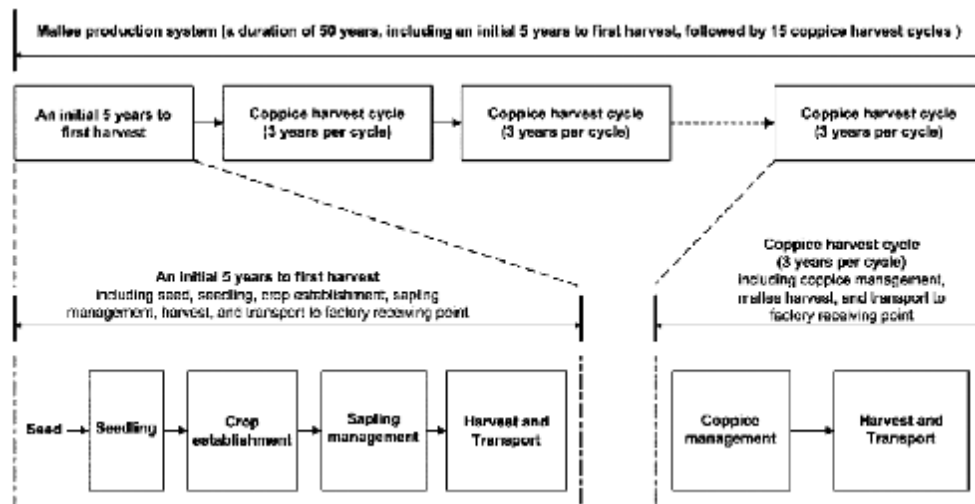


Figure 2-2 Mallee production system for biomass production¹³

2.4 Technical Challenges in Biomass Utilisation

Despite the advantages of biomass as a renewable bioenergy resource, biomass utilisation is often limited to ~10% in practical application. While biomass is often considered as a relatively cheap resource as some biomass are available as waste, fuel handling cost for biomass can be very high due to several constraints.⁶³ Compared to coal, biomass also has considerably different organic and inorganic compositions as well as physical properties. For example, biomass contains much less carbon, more oxygen and moisture leading to lower heating value than coal. While biomass has advantages in terms of higher volatility and reactivity in both biomass fuel and char. Biomass also has high moisture content. Such characteristics dictated that biomass combustion has low process efficiency. Due to its high alkali contents, ash-related issues such as fouling, deposition and corrosion are also important consideration during biomass combustion.⁶⁴

Biomass has poor grindability as a result of its bulky and fibrous nature. Therefore, such a feature significantly impacts plant milling cost, feeding/fluidisation processes and handling operations.¹⁹ Poor grindability of biomass also typically leads to the production of large biomass fuel particles with a low packing/bulk density and volumetric energy density.⁶ A low volumetric energy density leads to high fuel transportation and storage costs, making it uneconomic for long-distance

transportation.²¹ Lastly, the heterogeneous nature and the broad diversity of biomass fuels (Table 2-1), requires the knowledge on each individual fuel component in order to develop a process which can flexibly handle these fuels. The following sections give more details on these biomass constraints.

2.4.1 Biomass Fuel Chemistry and Implications

The technology chosen for a combustion process is often largely based on fuel properties.⁶ Due to its complex carbohydrate polymers (Section 2.2), biomass is highly oxygenated.⁶⁵ On a dry mass basis, the typical percentages for C, H and O are 30-60%, 5-6% and 30-45% respectively.⁶ The contents of C, H, O can vary significantly for different types of biomass.⁶⁶ Fuel properties can be illustrated as a correlation between the O:C and H:C ratios of the fuel, i.e. the so-called van Krevelen diagram as shown in Figure 2-3. It can be seen in Figure 2-3 that biomass has higher contents of O and H and a lower C content than fossil fuels. This leads to significantly lower energy content in biomass because in theoretically, C-O and C-H bonds have lower energy than C-C bonds.⁴⁵

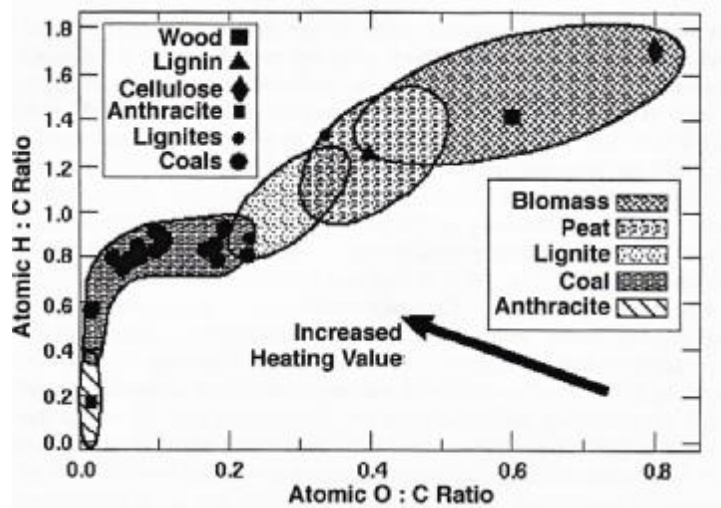


Figure 2-3 van Krevelen diagram for various solid fuels⁴⁵

Another important factor that influences fuel heating value is the fuel's moisture content. Figure 2-4 presents the moisture contents of some solid fuels used as blends in co-combustion facilities, as reported in a previous study.⁷ The solid fuels are

Bellambi coal, Federal coal, wheat straw, wood, the woody matter of pressed olive stone (WPOS) and sewage sludge (SS). Figure 2-4 clearly shows the significant differences in the fuel moisture contents not only between coal and biomass, but also among various types of biomass fuels. A recent review of 86 varieties of biomass has reported a range of moisture contents 3-63 %.⁵³ It is also noted that the specific moisture requirement is ~15-30 wt% for syngas production and below 10 wt% for pyrolysis.²⁴ Higher biomass moisture content can impose significant adverse impacts on the overall energy balance and the volume of flue gas produced per unit of energy therefore dewatering of the fuels will be required. High moisture content can also cause fuel ignition issues and reduce the combustion temperature, which in turn hinders the efficiency, stability and quality of fuel combustion.⁶⁷

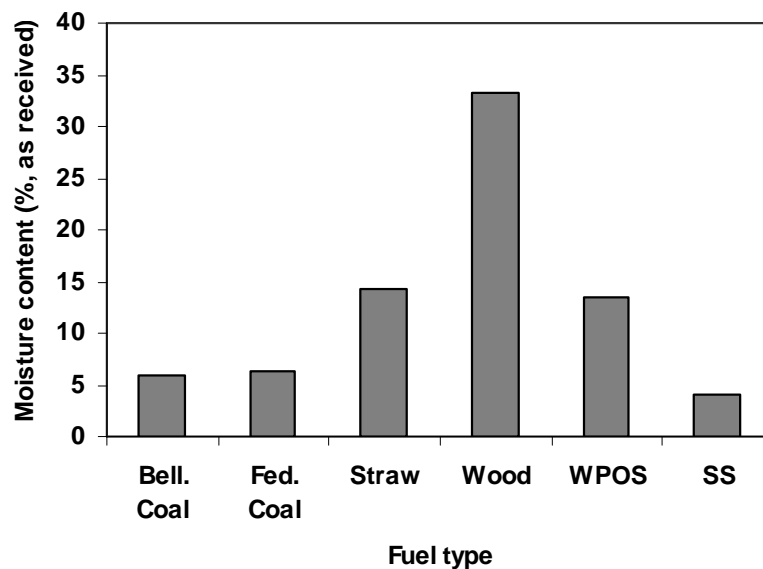


Figure 2-4 Moisture content of fuels (Data taken from reference ⁷)

Biomass usually consists of 70–80% volatile matter (VM) in comparison to 10 – 50% of coal.²² A high volatile content affects the combustion system in various ways. The fuel is easier to ignite and gives a rapid combustion. As a result, the conversion of biomass is dominantly in the gaseous phase and can lose up to 90% of biomass mass during the initial pyrolysis stage in comparison to <10% for anthracite and 20 - 30% for bituminous coal. The combustion of such quickly-released of volatiles produces a large volume of flue gas which requires a bigger reactor volume to accommodate in order to achieve complete combustion at a high efficiency and to

ensure low pollutant emissions (e.g. CO and PAH, unburned pollutants or products of incomplete combustion).⁶

2.4.2 Inorganic Species in Biomass Fuels and Ash-related Problems during Biomass Utilisation

As a result of nutrients uptake during biomass growth, biomass also contains abundant inorganic species, which are ash-forming precursors during biomass combustion. The major inherent ash-forming species in biomass include alkali and alkaline metallic (AAEM) species, i.e. mainly Ca, Mg, Na, K, and S, P, Si, Cl, Al, Ti and Fe. The ash content in biomass fuels vary from biomass to biomass, ranging from typically <1% for wood to 30-40% for green house residue.⁶ The ash content together with other fuel properties of biomass can sometime dictate the specific biomass utilisation technology to be deployed. For example herbaceous biomass like straw contains high alkali causing deposition and corrosion problem. Whereas wood biomass is more preferred feedstock as it typically has less ash and alkali problem. As straw and wood have different combustion behavior, blends of straw-wood cannot be combusted together in grate furnaces.^{19,68}

The ash content of biomass can also influence fuel handling/ processing costs and the cost of biomass-based energy production.⁶⁶ High ash fuels require efficient dust removal systems to handle particulate emissions and have low heating values.⁶ The release of inorganic species during solid fuel combustion is influenced both by its inherent volatility and organic matter reactions. Inorganic species that are inherently volatile at combustion temperatures include derivatives of some AAEM species (AAEM) especially K and Na. Other non-volatile material (Ca, Mg etc) can also be possibly released by convective transport during rapid pyrolysis.⁶⁵

Ash slagging, fouling and corrosion in combustors depend strongly on the volatilisation of ash species.⁴⁵ These are key issues associated with the usage of biomass as a fuel in combustion applications. It is known that the key ash-forming species responsible for ash sintering, agglomeration, deposition, erosion and corrosion during biomass combustion are the AAEM species which can form alkali silicates, chlorides and sulphates.⁴⁵ The alkali silicates and sulphates have lower

melting points (below 700°C) and form deposits on the heat transfer walls of a boiler, or on the particles bed in a fluidised-bed combustion and causes bed sintering and defluidisation.^{27,69} Chlorine enhances mobility of the AAEM species, especially potassium. Potassium chloride is one of the most stable high-temperature ash forming species in gas-phase leading to slagging and fouling problems in biomass combustors.⁶⁵ Moreover, in downstream syngas utilisation such as gas turbines, the alkali in syngas can cause deleterious problems like deposition, erosion and corrosion on the turbine parts.⁷⁰

2.4.3 Biomass Fuel Grindability

Naturally, biomass has fibrous structure and is difficult to fracture by applying compressive forces in conventional coal mills, leading to significant costs for size reduction of biomass materials as well as other operating and maintenance costs. Poor grindability of biomass is a key factor limiting the uptake of biomass as a fuel for co-firing applications in conventional coal-based power plants. For example, the common mill systems used for coal includes Vertical Spindle, Ball and Cutting/Knife mill.⁷¹ It is found that during the co-milling of coal and biomass in pilot scale vertical spindle mill, the vertical spindle mill uptake was limited only up to 5 wt% of biomass blend.⁷¹ Ball mill is less suitable to grind biomass for its gravity impacts and tumbling actions only flattened biomass fibre rather than cutting. Previous trials⁷¹⁻⁷⁴ of biomass grinding in ball mill systems and combination of ball-race and ball-bowl systems were unsuccessful, as summarised in Table 2-3.

The poor grindability of biomass leads to various technical problems in biomass utilisation. Coarse biomass particles have slow devolatilisation rate, decreased burning rate and lowered ignition front speed compared to small biomass particles.⁷⁵ Therefore, such biomass particles result in longer residence time required for complete combustion, incomplete burn out, blockage/bridging to feeding system, sedimentation and mixing problem causing high level of CO emission.¹⁶ Therefore, there is stringent requirement on the size of fuel particles, e.g. the guidelines requires that the pulverised coal particles injected into boiler to have 80% of fuel particles to be <74-75µm in pulverised coal-fired power stations.¹⁶

Table 2-3 Milling test experience using ball mill systems

Plant	Biomass type	Biomass blend ratio (wt %)	Summary
Macquarie Generation, Australia ⁷¹	woodchips	5	Ball mill. Unsuccessful, fibrous biomass flattened but particle size remains large. Difference densities contribute to biomass build up problem on coal and ball charge bed.
Shawville Generating Station, USA ⁷²	sawdust, tree trimming, hybrid poplar	3	Ball-race mill and bowl mill. Grindability index reduced by 6 points. Feeder limitation causes 8-10 MW loss of boiler capacity, milling power increase 4-5%, mill outlet temperature increase.
Plant Hammond, USA ⁷³	wood	9.7-13.5	Ball-race mill. Larger particle size, mill power increase, unburned combustibles higher compared to firing coal although associated boiler operates at full capacity.
Georgia Power Company, USA ⁷⁴	bark	5-20	Ball-Race mill. Unsuccessful, fibrous bark material formed "bird nests", blockage of fuel flow.

Apart from the requirement of fuel particle size, the desired particle shape for fuel handling is those close to spherical with a major axis to minor axis length ratio (aspect ratio) of ~ 1 . In practice, due to the poor grindability and fibrous nature of biomass, many demonstration plants for biomass/coal co-firing use ground biomass particles with sizes of ~ 3 mm⁶⁴ and aspect ratios of 3-7 or even higher.⁶ These large and irregular biomass particle lead to reduced biomass conversion efficiency and more difficult fuel fluidisation or even fuel blockage.^{6,34}

2.4.4 Biomass Fuel Bulk and Energy Densities

Most biomasses have low bulk densities. For example chopped straw and rice husks have bulk densities around 50-120 and 100-125 kg/m³ respectively much less than brown coal (560-600 kg/m³) and bituminous coal (800-900 kg/m³).⁶ The low bulk densities of these fuels significantly increase milling, storage, handling and transportation costs.¹⁹ Fuels with a low bulk density also has a low volumetric energy density causing process and feeding control difficulties, and requires large storage

and expensive transportation. Due to its high moisture, low calorific value and low bulk density, biomass volumetric energy density is around 10% of coal.⁴⁴ As a consequence, in practical applications such as biomass co-firing in coal-fired power stations, the volume requirements of coal and biomass at only 10% of coal heat input rate is similar.¹⁹ This translates to a disproportionately high biomass operating cost for relatively small proportion of heat contribution from biomass.

In addition, biomass bulk density also impacts the requirement of fuel storage, sizing of the material handling system and the subsequent fuel thermo-chemical conversion process.⁶⁶ For example in continuous biomass supply chain, it is known that transportation cost accounting for >50% of the total delivered biomass-fuel cost largely relates to the low volumetric energy density of the biomass.^{20,21}

2.4.5 Heterogeneities among Different Biomass Components and Biomass Materials

It is known that fuel characteristics are broadly diverse among various biomass materials or biomass components.^{76,77} The broad spectrums signify biomass distinct characteristics compared to fossil fuel and raise key factors limiting biomass uptake as fuels. Previous reviews^{68,53} compared the compositions and characteristics of various biomass fuels. Those studies concluded that biomass fuels are very heterogeneous and have significant different characteristics in comparison to coal. Specifically for the genus eucalyptus, the variations in fuel chemical compositions and heating value are evidenced in not only different species and tree age but also different components such as leaf and bark of the same trees.^{76,78} Similar results have also been reported for other biomass components such as leaf, stems and reproductive parts of *Cyanara*, fibre and sweet *Sorghum* and *Miscanthus* which suggested biomass quality may be drastically altered with biomass partition.⁷⁹



Figure 2-5 Main components of mallee biomass

For mallee in Western Australia, the whole mallee trees are harvested from the field and the total biomass consists of mainly wood, leaf, and bark (Figure 2-5). A practical supply chain of mallee biomass to a bioenergy plant will need to consider the utilisation of the whole mallee trees.^{13,20} There are various possible scenarios for the utilisation of the whole biomass. For example, a typical scenario is to separate leaf component from the whole biomass for the production of eucalyptus oil which is a value-added product. This was part of the integrated wood processing concept⁸⁰ which produces multiple products including eucalyptus oil, electricity and activated carbon. In other cases, the total biomass may also be used without separation, which is more likely in future large-scale application of mallee biomass based on a continuous supply chain.²⁰ Unfortunately, little information is currently available on the fuel properties of various mallee components hence a systematic fundamental understanding on these aspects is needed.

2.4.6 Summary

Based on the discussion in previous sub sections, the major biomass properties which may lead to key issues in biomass utilisation, along with the associated technical challenges are summarised in Table 2-4. Obviously, the abundant supply/varieties of biomass cannot be fully utilised for bioenergy and biofuels production due to these constraints. The wide varieties in biomass fuels also require innovations in order to improve or upgrade the quality of the raw biomass to meet the requirements of conventional feeding systems and conversion process considered. Therefore, technological innovations are required to develop an efficient biomass pre-treatment technology to substantially increase biomass volumetric energy density (therefore

reduce the logistics cost), the fuel's grindability and the fuel's feeding/handling properties. Such a method must be effective to lower the fuel's moisture content, H:C/O:C ratio and to increase the fuel's heating value, therefore to synergise volumetric energy increase with bulk density improvement. It is also clear that the characteristics of ash-forming species inherent in biomass fuels must be well understood and if economically possible be reduced within the guideline limits. The next sections review the current progress on various biomass pre-treatment technologies, understand the properties of resulted fuels and evaluates the limitations and potential applications of these technologies.

Table 2-4 Key biomass properties and its associated technical challenges

Biomass properties	Technical challenges
differences in fuel chemistry compared to coal (higher oxygen, moisture and volatiles, low carbon) ash related problem	low calorific value, combustion efficiency and combustion behavior. slagging, deposition, fouling, sintering, agglomeration, fly ash logistics, pollutants, emissions.
poor grindability	size reduction problem, low bulk density, low volumetric energy density, incomplete burnout, expensive storage and handling/transportation, segregation/entrainment, longer residence time, feeding problem, emission problem
low bulk and (volumetric) energy densities	high transport cost, difficulties in process control and feeding control, requirement of large storage, limitation on suitable available technology.
heterogeneity among different biomass and biomass components	requirements of process flexibility, fuel components partitions, fuel feeding problems.

2.5 Biomass Pre-treatment Technologies

So far, the technology deployed to pre-treat biomass into a fuel of improved quality can be divided into a) physical/mechanical process i.e drying, washing/leaching, pulverisation technology, baling, briquetting and pelletizing ; b) thermochemical process i.e torrefaction and pyrolysis or c) a combination of thermal and physical/mechanical treatment i.e torrefaction combined with pelletizing (TOP).

2.5.1 Drying

Drying is a major step in the pre-treatment of biomass. Raw biomass feedstock usually need to be dried to bring down the moisture from 30-60 wt% to 10-15 wt% prior to the conversion process.²⁴ Usually, biomass drying is carried out mainly to both increase biomass energy input and minimize the risk of microbial decomposition and self ignition.¹⁹

The most common dryer used in a bio-energy plant is rotary dryer. Other dryer systems employed including the band dryer, steam rotary dryer, pressurized fluid-bed dryer and pneumatic steam dryer.²⁴ Apart from dedicated dryers, natural drying is also commonly applied in the field although this method has disadvantage of unforeseeable weather conditions.¹⁹ Upon drying, the biomass material can achieve a bulk density in the range 50-400 kg/m³ depending on biomass type and moisture content.²⁴ However, drying in dryers generally requires size reduction of biomass particles. For example, at the point of delivery, large biomass particles are delivered in the form of chips and chunks with a size dimension of 1-8 cm. Rotary dryers can accept various particle sizes but flash and belt dryers usually require crushing of fuel particles of sizes < 1 cm. Therefore, the drying process sometimes can be problematic due to sizing specifications and poor biomass grindability.¹⁹

Wang et al.(2008)²⁵ studied the influence of microwave drying on biomass (pine wood sawdust, peanut shell and maize stalk) pyrolysis. A microwave oven (MO) was used to dry the biomass using four power levels i.e. 200, 400, 600 and 800 W. It was found that the moisture removal property was highly depended on the power capacity. Under optimised condition, a much shorter dehydration time was achieved with microwave oven (6 mins at 600 W) compared to electrical oven (EO) drying (~40 mins). The BET surface areas of the MO-dried samples were also increased compared to those obtained with EO-dried. Fast pyrolysis experiment was conducted on the MO-dried biomass using a fluidised-bed reactor (500°C). An increase of solid char and bio-oil were observed in this study. The bio-oil produced has less water content with increased heating value and viscosity due to the fact that secondary reaction of volatiles was suppressed in pyrolysis of MO-dried biomass.

2.5.2 Pulverisation

A number of pulverisation technologies were developed to mechanically assist the grinding of biomass in coal plant. One option is to install separate biomass grinders when the amount of biomass processed is higher than 5% of the total fuel flow in coal power plants. Esteban and Carrasco (2006)²⁸ evaluated the pulverisation of various forest biomass (poplar chips, pine chips and pine bark) using a series of hammermill system. Satisfactory biomass particle sizes (95 wt% pass 1000 μ m mesh, 12 wt% pass 125 μ M mesh) were obtained from grinding the biomass fuels in a primary grinder (single bearing horizontal axis hammermill) with different screen pore sizes, followed by classification in a dynamic separator and grinding of the separator reject in a secondary grinder (double bearing horizontal axis hammermill) with 1.5 mm screen pore size. These three types of biomass materials required different amount of milling energy to achieve the specified sizes. For an outdoor use, the mean energy consumption for poplar chips, pine chip and pine bark were 85.4, 118.5 and 19.7 kWh/t respectively. Only the electricity used for bark milling reported in this work is comparable to the electricity consumed to pulverize anthracite coal (20 kWh/t).²⁸ However, the density data of resulted ground biomass from this work is not reported.

Mani et al. (2006)⁸¹ reported the grinding and properties of wheat straw, barley straw, corn stover and switchgrass after grinding using a hammermill. The energy requirement are 43.56, 27.09, 19.84 and 58.57 kWh/ t for wheat straw, barley straw, corn stover and switch grass, respectively. Ground switchgrass from a hammermill with a screen size of 0.8mm had the highest bulk density (181.56 kg/m³). In other study, the performance of vibration and cutter mill for grinding wood biomass was assessed.⁸² It was found that 80% the pulverized particles by vibration mill have aspect ratios < 2.0 compared to those particles ground using a cutter mill (80% having aspect ratios of 2.0-12.0). Total energy consumption of a scaled-up vibration mill for pulverising wood chip with a starting size of 22 mm down to wood powders (~150 μ m) was 800 kWh/t. The fine wood powders were successfully gasified with little tar generation in an entrained flow gasifier at 1027°C. Generally, the installation of new milling systems (rather than co-milling biomass in existing coal mills) can solve some of the problems arose from the poor grindability of biomass,

mainly in terms of reduction in size and aspect ratio. However, substantially more grinding energy is generally required for biomass than coal. Although grinding does assist the packing of the biomass, the bulk density of ground biomass ($\sim 226\text{-}329\text{ kg/m}^3$) is still much less than that of coal ($\sim 600\text{-}900\text{ kg/m}^3$).⁶ It is generally accepted that the extra investment required for installing new grinding systems for biomass is not a cost-effective option.¹⁹

2.5.3 Washing/leaching

Attempts were also made to utilise biomass washing and leaching to remove the notorious inherent alkali elements and chlorine from biomass.^{26,83-85} Such a pre-treatment was generally done by either simple washing with water or a more thorough leaching by a suitable acid solution or hot water.^{26,27,49} It was found that potassium, sodium and chlorine were easily removed from rice straw and wheat straw by water washing.⁸³ Alkali released from untreated, washed and acid leached biomass i.e wheat straw, wood waste and cellulose was studied during pyrolysis at $200\text{-}500^\circ\text{C}$ and $> 600^\circ\text{C}$.²⁶ It was found that, washing with water has reduced the alkali emission from wood waste and wheat straw by 5-30% while acid leaching effectively reduced the emission to $\sim 70\%$ during pyrolysis. The washing procedure were sufficient to reduce the alkali release at $>600^\circ\text{C}$ more than 90%. However, experiments with pure cellulose of very low ash content (0.07%) indicated water washing is ineffective in removing alkali which is bound to the organic structure of cellulose.

Jensen et al.(2001)⁸⁶ studied the removal of potassium by water washing of straw char at temperature $25\text{-}80^\circ\text{C}$ and with the addition of KCl in the washing water. In this study, at 25°C , about 35-58% of the char potassium dissolved within a few minutes. After that, slow release of potassium occurred when smaller particles used and the washing temperature rose from 25°C to 80°C . The residual 5-10% of the char potassium remains in the char and is very hard to be washed. Another study⁸⁴ reported that fine milling and multi-step dewatering on banagrass biomass resulted in substantial reductions in ash content (by 45%), or element-wise K (by 90%), Cl (by 98%), S (by 55%), Na (by 68%), P (by 72%) and Mg (by 68%). However, washing is not always effective for all biomass materials. For example, washing is effective to

significantly improve ash thermal behaviour of olive residues but is ineffective to prevent the formation of ash deposits/agglomerates in fluidised combustion test of straw samples.²⁷ It is also found that after washing, the moisture content of washed biomass may increase.¹⁹

2.5.4 Baling, Briquetting and Pelletizing

Densification is a process utilised to overcome the low bulk density of biomass. There are 3 major mechanical densification techniques commonly used in the practice, i.e. baling, briquetting and pelletizing, in an increasing order of equipment complexity, energy requirement, and costs.⁶

For example, pressing of straw to bales can increase the fuel's bulk density to almost twice than that of chopped straw⁶ giving an increase volumetric energy density from 0.7 GJ/m^3 in chopped straw to $\sim 1.3 \text{ GJ/m}^3$ in straw bales. It was also claimed that baling can significantly reduce forest biomass transportation cost up to 50%.⁴ Briquettes can be produced from biomass or coal-biomass blends.^{29,87,88} Biomass is dried and milled before pressed in mould.⁸⁹ A previous study²⁹ has produced corn stover briquettes with an average size of 32 mm in diameter and 20–25 mm long. In comparison to loose corn stover that has a bulk density of merely 42 kg/m^3 (volumetric energy density $\sim 0.8 \text{ GJ/m}^3$), the corn stover briquettes have a considerably higher bulk density ($600 - 950 \text{ kg/m}^3$) resulted in an increase of volumetric energy density to $\sim 17 \text{ GJ/m}^3$. In another study, hazel nut shell briquettes were produced at various percentages of binder and pressures led to briquettes with a bulk density of $370\text{-}770 \text{ kg/m}^3$,⁹⁰ achieving volumetric energy density of $\sim 8\text{-}16 \text{ GJ/m}^3$.

The overall pelletizing process involves drying, milling, conditioning, actual pelletizing and cooling processes which ultimately compacting biomass into a homogenous fuel in cylindrical shapes with 6 – 8 mm in diameter.⁴ Pellets are a refined and dry product which permits good fuel handling and feeding. The energy density achieved through the pelletizing ranges from 8 to 11 GJ/m^3 for wood pellets of various biomass origin.¹⁹ In another study,⁹¹ the pelletizing of reed canary grass only achieved a moderate increase in bulk density from 150 kg/m^3 of the raw

biomass to 270 kg/m^3 of the pellets indicating an increase of volumetric energy density from $\sim 2 \text{ GJ/m}^3$ to $\sim 4 \text{ GJ/m}^3$ respectively.

Both briquetting and pelletizing may use suitable binders to glue biomass particles together during compaction. Among these processes, pelletizing offers several advantages including higher press output and acceptance of materials with a wider range of moisture contents. However, pelletizing requires the starting samples to have a narrower size range. The design of a briquetting machine is also simpler.⁶ Although various densification methods address the problems associated with the low bulk and energy density of biomass, these densification processes typically add significant energy costs in the fuel production. For example, in pelletizing, the whole compaction process of wood chips including drying and crushing would make up to 35% of the energy content of the pellet.¹⁹ There are several additional drawbacks. Firstly, the biomass drying that depends dominantly on the moisture content of raw material plays a crucial role in pellet quality such as bulk density and durability.⁹¹ Secondly, the particle size/shape of the raw biomass has a huge influence on the feeding process and the durability of the pellet products. Biomass with smaller particle sizes generally leads to pellets with better durability.⁹² Lastly, pellets may disintegrate during screw feeding and induce hair-like structures that block the feeder as experienced during the production of greenhouse residue pellets (Figure 2-6). Decreasing feed particle size or using a strong binder or a different feeding system are among potential solutions for solving this problem.⁶

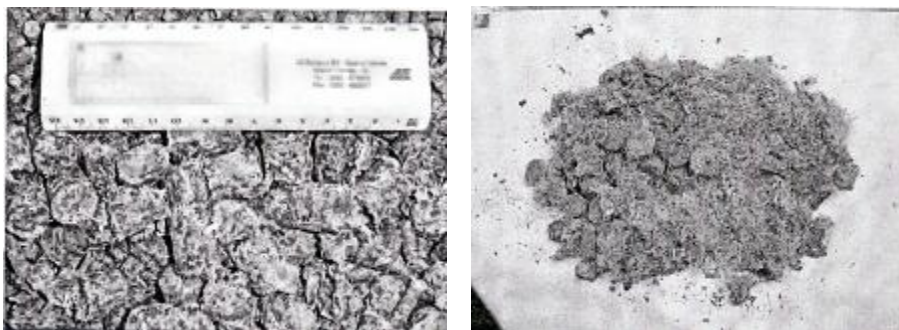


Figure 2-6 Greenhouse residue pellets before (left) and after screw feeding (right)⁶

2.5.5 Torrefaction and Torrefaction combined with Pelletizing (TOP)

Torrefaction is a light thermochemical process which is carried out at 200-300°C in the absence of oxygen.³⁴ During torrefaction, biomass is partially decomposed giving the remaining solid or char as a final product. Via torrefaction, the fuel quality can be improved in terms of increasing heating value, being more hydrophobic, enhanced grindability, better uniformity and improved durability.^{34,36,43,93,94} Grindability of torrefied wood was found to increase significantly after treatment at 275-300°C. In comparison to the untreated biomass, torrefaction at 300°C reduced the energy consumption during grinding using a knife mill by 10 times for pine chips and 6 times for logging residues.³⁵ However, other grinding experiments on torrefied wood using ball-mill systems did not produce ground fuels that met the coal particle size criterion although in overall, the fuel grindability was improved with the increasing of torrefaction temperature.⁹³

An extension of the torrefaction is a process which combines torrefaction with pelletizing, i.e. the so-called TOP (torrefaction in combination with pelletizing) process.⁵¹ As described previously, pellets do offer several advantages over untreated biomass but suffers from several issues regarding moisture uptake, particle size/shape and durability. Torrefaction can be a solution to solve some of these issues by improving fuel grindability, reducing fuel H:C/ O:C ratio and decreasing fuel hydroscopicity. Additionally, the energy density of torrefied biomass is still low, around ~5 GJ/m³¹⁹ since torrefaction has little effect on the fuel's bulk density. Therefore, torrefaction and pelletizing are two complementing processes, overcoming each other's limitation.

Figure 2-7 has illustrated some examples of the finished products via biomass baling, briquetting, pelletizing, torrefaction and TOP. Volumetric energy densities of coal and various fuels from biomass pre-treatment are presented in Figure 2-8, summarised from data in the literature.^{6,19,29,35} It is also noted that there is little work done on mallee biomass in Australia hence Figure 2-8 only includes available data reported in the literature.

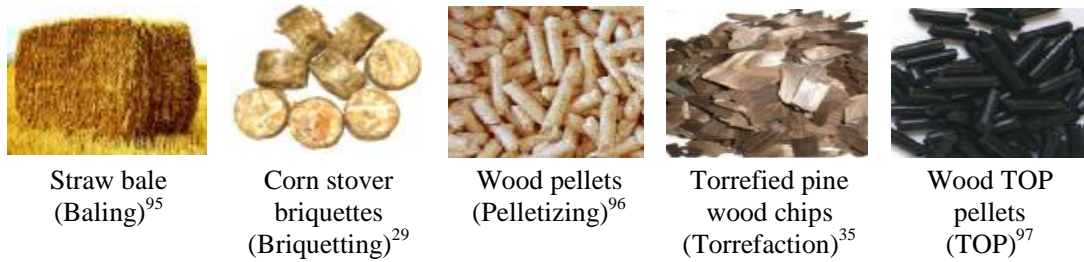


Figure 2-7 Products from various biomass densification processes

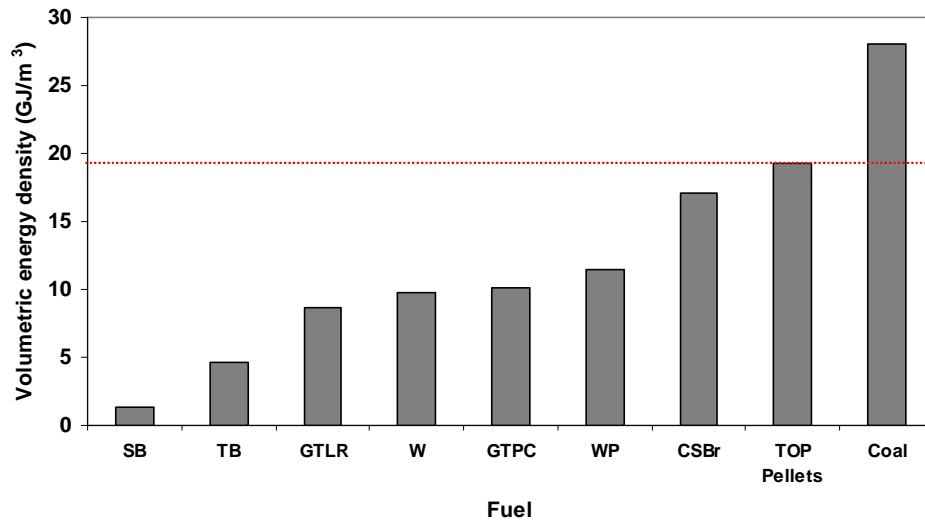


Figure 2-8 Volumetric energy density of various solid fuel (SB- straw bales, TB-torrefied biomass, GTLR-ground torrefied logging residue, W-wood, GTPC-ground torrefied pine chip, WP-wood pellets, CSBr- corn stover briquettes, TOP- Torrefaction in combination with pelletizing, Coal-typical black coal)

The data in Figure 2-8 suggested that through densification, fuel energy density can be increased significantly, achieving a moderate ~69% of that of a typical black coal. Among the densification processes reviewed, TOP achieved the highest energy density of ~19 GJ/m³ while baling achieved the lowest (~1 GJ/m³). The positive roles and limitations of various pre-treatment methods discussed in Sections 2.5.1-2.5.5 are summarised in Table 2-5.

Table 2-5 Role and limitation of various pre-treatment methods

Process	Positive roles	Limitations
drying	reduce biomass moisture content to suit application guidelines.	challenges in size reduction as some dryers require size-specific biomass, none of ash-related problems being addressed.
installation of separate biomass milling system	reduce biomass size and particle aspect ratio, improve feeding.	high grinding energy, high cost, little improvements in fuel heating value and volumetric energy density, none of ash-related problems being addressed.
washing/leaching	reduce biomass ash-related problems.	only effective to some biomass materials, an ultimate proportion (5-10 %) of alkali being not washable, potentially increasing fuel moisture content after washing, none of grindability issues being addressed.
baling	increase fuel bulk density, reduce transport/ storage costs.	low energy density, none of ash-related problems being addressed.
briquetting	increase fuel bulk and energy density, produce more homogenized biofuel, reduce transport/storage costs.	high production cost, production quality being sensitive to the moisture content of starting materials, prone to mechanical damaging, size reduction problems of the starting materials, none of ash-related problems being addressed.
pelletizing	high fuel bulk and energy density, produce homogenized products, enable automatic feeding, reduce transport/storage cost.	high production cost, prone to mechanical damaging, moisture absorbance leading to disintegration that causes feeder blockage, size reduction and particle shape problem, none of ash-related problems being addressed.
torrefaction	improve fuel grindability low moisture, safe storage, increase fuel heating value and uniformity.	low energy density, none of ash-related problems addressed, size reduction limit with ball-mill system.
torrefaction in combination with pelletising (TOP)	higher energy density, homogenized products enabling automatic feeding, low moisture, reduce transport/ storage costs.	none of ash-related problems being addressed.

2.5.6 Pyrolysis

Pyrolysis is the process of the decomposition of organic components in biomass in the absence of oxygen at various temperatures. Technically, pyrolysis is similar to torrefaction but pyrolysis is conducted at a wide range of temperatures from 300°C to 800°C, resulting in more severe biomass decomposition. During pyrolysis, a series of processes take place: (1) heat is transferred from a heat source to the biomass particle, resulting an increase in the temperature inside the biomass, followed by (2) the initiation of primary pyrolysis reactions at the pyrolysis temperature, releasing volatiles and forming char; (3) continuous proceeding of the biomass pyrolysis

reactions; (4) secondary reactions of the primary volatile product; (5) autocatalytic secondary pyrolysis reactions proceed in parallel with the simultaneous primary pyrolytic reactions (item 2); and in combination with (6) other thermal decomposition reactions including reforming, water gas shift reactions, radicals recombination, and dehydrations.^{55,98}

Via pyrolysis,^{41,99,100} biomass can be converted to biochar and bio-oil while light gases can be used to supply the energy requirement of pyrolyser operations. The yield and composition of pyrolysis products might vary depending on feedstock,⁴⁷ reactor configurations and pyrolysis conditions.¹⁰¹⁻¹⁰⁴ Key pyrolysis parameters including residence time, heating rate and temperature.⁵² A low temperature and long vapour residence time favour the production of biochar. A high temperature and long residence time increase the cracking of volatiles hence gas yield while a moderate temperature and a short vapour residence time are optimum for producing bio-oil.⁴¹ In addition, the inorganic species in biomass also have important effect on pyrolysis, for example, it is known that alkali salts has a great influence on pyrolysis reactions.⁵² In fast pyrolysis, the inherent AAEM species, especially potassium and calcium, catalyse biomass decomposition and char-forming reactions. The alkali metals retained in bio-oil makes it problematic for bio-oil combustion in engines.¹⁰⁵ Therefore, it is crucial to understand the roles of these ash-forming species in biomass during pyrolysis and to understand the ash properties of these pyrolysis products.

Pyrolysis is one of the most thermal efficient pre-treatment processes to obtain liquid fuels from biomass.¹⁰⁶ Bio-oil is a biofuel of the lowest cost, produced from lignocellulosic materials.⁴⁷ Bio-oil production converts up to 50-90% of biomass energy into the liquid.⁵² The process thermal efficiency (PTE) of bio-oil production by fast pyrolysis ranges from 0.61 to 0.68.⁵² For applications as renewable energy, biochar, bio-oil and pyrolytic syngas can be used as alternative fuels in boiler and turbine/engines to produce electricity/heat.^{41,107} An analysis⁴⁷ shows that bio-oil co-fired in large power stations and turbine plants is technically most advanced.

Pyrolysis is an interesting option to solve the constraints experienced in other pre-treatment method discussed previously (Section 2.5.1-2.5.5 and Table 2-5). Biochar may be a good alternative solid fuel for bioenergy production. Therefore, using biochar as a fuel may provide the opportunities to address the key issues associated with the use of bulky biomass as a direct fuel, including high moisture content, low energy density and poor grindability. However, fine char particles may be dusty and prone to ignition during transportation.¹⁵ On the other hand, bio-oil is favourable for fuel handling and transportation. The volumetric energy content of bio-oil is $\sim 19 \text{ GJ/m}^3$ which is similar to TOP pellets (see Figure 2-7).

2.6 Slurry Fuel Technologies

Suspension of fine ground char into bio-oil results in a slurry fuel. Recent techno-economic assessments show that bioslurry supply chain can be an attractive option for co-firing application in coal-fired power stations.^{15,108} Slurry fuels technologies are developed mainly to improve fuel transportability and increase volumetric energy density. Liquid/slurry fuels are more favourable for fuel handling/fluidisation as it enables pumping and atomisation.

Typical slurry fuel production involves preparation, storage, transportation and end-use applications. A review of some previous studies was carried out on the use of coal-oil mixture (COM),¹⁰⁹⁻¹¹¹ coal-water mixture (CWS),¹¹²⁻¹¹⁶ peat-oil mixture,¹¹⁷ bio-oil^{51,118-124} and bioslurry.^{125,126} The most adopted systems for these fuels are boilers, gasifiers and stationary engines. Some of the basic fuel requirements for these applications are briefly outlined in Table 2-6.

Table 2-6: Slurry fuel requirements in combustion system and significant impact^{51,109-126}

Aspects	Parameters ^{51,109-126}	Applications	Significant Impact
fuel chemistry	<i>fuel compositions</i> <ul style="list-style-type: none"> • low moisture, low ash, low H and O to C ratio/high heat value • water $\leq 32\%$ • low N $< 0.6\text{ wt\% (db)}$ • low S $< 0.1\text{ wt\% (db)}$ limit for corrosion, $< 0.2\text{ wt\% (db)}$ limit for Sox emissions • ash $< 0.01\text{ wt\% (db)}$ 	boiler, gasifier diesel engine boiler boiler diesel engine (No. 2 diesel fuel)	heating value, vapour formation. ash related problems, emissions.
Fuel physical and handling property	<i>bulk density</i> <ul style="list-style-type: none"> • similar to coal $\sim 0.6\text{-}0.9\text{ Tonne/m}^3$ or higher <i>particle size</i> <ul style="list-style-type: none"> • PSD of $80\% < 74\text{-}75\mu\text{m}$ • PSD of $< 150\mu\text{m}$ <i>Rheological properties</i> <ul style="list-style-type: none"> • viscosity $\leq 1000\text{ mPa}\cdot\text{s}$ at shear rate 100s^{-1} at 25°C is desirable for fuel handling. • viscosity $100\text{-}1000\text{ mPa}\cdot\text{s}$ for heavy fuel oil at 50°C • fuel exhibit non-Newtonian pseudoplastic is preferable <i>good sedimentative/static stability</i>	boiler and gasifier boiler (coal, COM, CWS) entrained flow gasifier boiler boiler boiler, entrained flow gasifier, diesel engine.	transportation, storage, volumetric energy density, fuel feeding combustion efficiency, viscosity, sedimentation stability, additives/stabilizer requirement, spray atomisation quality. pumpability, piping, burner requirements, spray atomisation quality
		boiler (COM,CWS)	degree of which coal/solid particles remain suspended in liquid phase, storage and transportation

It is known that co-firing bio-oil with coal has the potential to substitute a much higher energy ratio of coal.¹²¹ A previous investigation showed the application of biomass-diesel-kerosene slurry fuels in stationary engines.¹²⁷ Therefore, bio-oil/biochar slurry (bioslurry) fuels may also be suitable for co-firing with coal in coal-fired power plant and combustion in stationary engines apart from gasification applications.¹⁵ To extend mallee bioslurry fuels in these applications, bioslurry must be developed to match existing guidelines in Table 2-6.

Bio-oil properties differ significantly from fossil fuel oil. Bio-oil is a polar, viscous and highly oxygenated (50 wt%) liquid which has a multiphase nature, high water content and low pH.^{41,55,104,120,128-130} Bio-oil experiences aging when heated (especially in air), becoming unstable and more viscous.¹³¹ Stabilisation and upgrading of bio-oil are some of the key targets in bio-oil commercialisation. So far, various upgrading technologies have been developed for bio-oil utilisation, including (1) addition of polar solvent^{101,119,132} (2) hydrodeoxygenation¹²⁹ (3) zeolite upgrading/catalytic cracking of pyrolysis vapors¹²⁹ (4) emulsification with diesel^{123,133} or biodiesel^{134,135} with the aid of a surfactant and (5) converting bio-oils and chars into H₂ or syngas by steam reforming.⁵²

Bio-oil may be further upgraded and refined for the production of liquid transport fuels.^{52,55,106} Garcia-Perez et al.(2007)¹⁰⁶ reported a viable method to extract some of the best fuel fractions of bio-oil by blending it with biodiesel. Monolignols, furans, sugars, extractive-derived compounds and a small fraction of oligomers were the main bio-oil compounds extracted in biodiesel. The addition of bio-oils to biodiesel did not seem to greatly influence the calorific value of resulting bio-oil/biodiesel blend. Further extraction with sodium bicarbonate increased the pH of the biodiesel blend to near neutral. However, in these studies the fuel properties or applications of bio-oil left over after extraction were not emphasized. At present, apart from using the whole bio-oil; the application of residue bio-oil after bio-oil/biodiesel is another interesting option for producing bioslurry fuels from mallee pyrolysis. While the biodiesel/bio-oil blends may be used as a liquid transport fuel, the bio-oil fractions after bio-oil/biodiesel extraction can be used to prepare a bioslurry fuel that is suitable for stationary applications such as combustion and gasification.

2.7 Conclusions and Research Gaps

Through literature review, it can be seen that mallee biomass is a key second-generation feedstock for CO₂ mitigation and biofuels production in WA. The main challenge is to develop a viable pre-treatment technology which can address the major issues associated with the unique and undesired characteristics of biomass i.e bulky, high moisture content, poor grindability, low bulk/energy density and mismatch in fuel quality if co-processed with coal.

The pre-treatment methods developed so far have various limitations so that R&D is still required to develop innovative method to transform raw biomass into a more suitable form for used in the conventional milling and feeding facilities. While there have been research activities on the biomass pyrolysis, little work has been done so far on the grindability of biochars and the development of densified fuels from the pyrolysis products. For bioslurry fuels, although such fuels were attempted by commercial developments(e.g. “BioOil Plus” from Dynamotive¹²⁶ and “Bioliq” from Karlsruhe,¹²⁵ there are few technical data available on bioslurry fuels in the open literature. At present, little investigation has been conducted on the production and properties of bioslurry from mallee biomass in WA. Based on the requirements of slurry fuels (Tables 2-6), developments of bioslurry fuels from mallee bio-oil/char components will be more likely targeted for boilers and gasifiers systems. Since mallee biomass has various components, the fuel properties of each component need also to be well understood. Therefore, further R&D is needed to improve the applications of mallee biomass using pyrolysis technology including:

- (1) Using biochar as a fuel. This requires understanding the biochar compositions obtained under various pyrolysis conditions and its fuel quality. Particularly, research is required to assess biochar chemistry, grindability, particle shapes and energy densification achieved.
- (2) Differences in biochars produced from various mallee components. Such knowledge is required for developing a flexible technology to deal with the whole biomass. Key fuel properties (size reduction, energy densification achieved, ash forming species) and possible limitations of each biochars components to various applications have to be identified.

- (3) Bioslurry production from bio-oil and biochar from mallee. It is particularly important to study bioslurry' fuel properties, energy densification, fuel stability and fluid behaviour. The outcomes are important to evaluate if it is feasible to apply bioslurry fuels in combustion and gasification applications.
- (4) Smart use of bio-oil for biofuels production. Utilisation of the whole bio-oil for bioslurry product may not be the best solution. It is plausible to use biodiesel to extract the high-quality components as a liquid transport fuels (i.e. biodiesel/bio-oil blends) and to use the residual low-quality components for bioslurry production. The key is to understand bioslurry compositions and fuel properties, benchmarking against those prepared from the whole bio-oil. Such data are important to achieve the co-production of biodiesel/bio-oil as a liquid transportation fuel and bioslurry fuels for combustion and gasification applications.
- (5) Bioslurry production from the bio-oil/biochar from the whole and different components of mallee biomass. Such data are important to assess the viability in using the whole mallee biomass for bioslurry production.
- (6) Roles of inorganic species in biomass. Particularly, a systematic study on the washing/leaching of biomass on the reduction of ash forming species and its significant effect on ash-related aspects for biomass utilisation, particularly ash fouling, corrosion, deposition and sintering in combustion applications.
- (7) Aging of bioslurry fuels. This aspect is important to improve bioslurry storage properties, fluidisation and process efficiency. The key is to gain a fundamental understanding on how aging progresses and developing new method in using additives/chemicals to stabilize and prolong the shelf life of bioslurry.
- (8) Combustion/gasification of biochar and bioslurry. As fuels for end use, it is important to understand the behaviour of biochar and bioslurry combustion/gasification, on both organic and inorganic matter reactions.

2. 8 Research Objectives of the Present Study

The above review has identified a series of gaps in the field. However, within a 3.5-years of PhD study, it is impossible to conduct research to fill all of the research gaps. Therefore this thesis focuses on a systematic investigation on the production of high-energy-density fuels from pyrolysis of mallee biomass under various conditions:

The main objectives of this thesis are listed as follows:

- (1) To investigate the production of biochar from mallee wood using slow pyrolysis process at various temperatures and understand fuel chemistry, quality, grindability and other properties of biochar as well as the implications of using biochar as a fuel to transport/fuel handling, benchmarking against Collie coal.
- (2) To examine differences in fuel properties of biochars produced from the slow pyrolysis of different mallee components (wood, leaf and bark) and further identify the potential advantages and/or limitations of using biochars produced from individual biomass components as fuels in power generation facilities.
- (3) To develop a method for bioslurry production from biochar and bio-oil of mallee wood fast pyrolysis, particularly to assess the fuel properties, energy density, stability, rheology and fluid behaviour of bioslurry fuels prepared.
- (4) To investigate the feasibility of bioslurry fuels preparation from biochar and the low-quality bio-oil rich fractions after bio-oil/biodiesel extraction, particularly to gain a good understanding on the resultant bioslurry fuel properties and fluid behaviour, benchmarking against bioslurry fuels prepared from the whole bio-oil.

CHAPTER 3

METHODOLOGY AND ANALYTICAL TECHNIQUES

3.1 Introduction

This chapter explains the overall research methodology employed in this PhD study to achieve the thesis objectives outlined in Chapter 2. The detailed experimental and analytical techniques are described accordingly in each following chapter.

3.2 Methodology

Biomass samples were prepared from mallee trees via components separation, drying and cutting. Coal samples were prepared from Collie coal (the only coal being mined in Western Australia) by cutting and drying. Preparation of biochar and/or bio-oil samples was conducted using a fixed-bed reactor system and a fluidised-bed reactor system. Char samples produced from the slow pyrolysis of biomass and Collie coal samples were ground using a ball-mill system to assess the grindability of these chars. All fuels were also subjected to compositional/elemental analysis, particle size analysis, image analysis and scanning electron microscopic (SEM) analysis.

Bio-oil and biochar samples were prepared from the fast pyrolysis of mallee wood using a fluidised-bed reactor system at 500°C. The biochar is then ground and mixed into the fast pyrolysis bio-oil to prepare bioslurry fuels. Further experiments were also designed and carried out to extract bio-oil with biodiesel to prepare two fractions. The biodiesel-rich fraction has the potential to be used as a liquid transport fuel while the bio-oil rich fraction is mixed with the ground biochar to produce bioslurry fuels.

An array of advanced analytical instruments such as rheometer, inductively coupled plasma atomic emission spectroscopy (ICP-AES), gas chromatography-mass

spectrometry (GC-MS), optical microscope and surface tensiometer etc were employed to characterise the liquid and slurry products. In this research, experiments or analytical analysis were replicated to ensure reproducibility of results.

The overall methodology to achieve the objectives in Chapter 2 is shown in Figure 3-1 with further explanations in the following sections.

3.2.1 Properties and Grindability of Biochars Produced from Pyrolysis of Mallee Wood under Slow-Heating Condition

In this study, the wood component of mallee biomass (see sample preparation in Section 3.3.1-a) was pyrolysed under slow heating conditions at moderate temperatures to produce biochars using method explained in Section 3.3.2-1. The wood biomass and biochar product were characterised to analyse their compositions and calorific value (Section 3.4.1).

The grindability of biochar were then carried out using a lab-scale ball mill (Section 3.4.2) to examine size reduction of biomass and biochars. Biochar grindability data were benchmarked against that of Collie coal and biomass to demonstrate the excellent grindability of biochars, making biochars suitable to be ground using ball mills in coal-based power station. The bulk densities of various fuels were measured using method in section 3.4.3 to evaluate the effectiveness of fuel energy densification. Particle size distributions (PSDs) of various samples were analysed using a laser-diffraction particle size analyser (Section 3.4.4).

The ground biomass, biochar and coal samples were examined using SEM analysis as described in Section 3.4.5. Image analysis were then carried out on the collected SEM micrographs using a tool described in Section 3.4.6 for particle shape/roundness analysis. Milling power consumption is estimated based on lab experiments (Section 3.4.2) as an indication of energy saving. The results and discussion for this work are presented in Chapter 4.

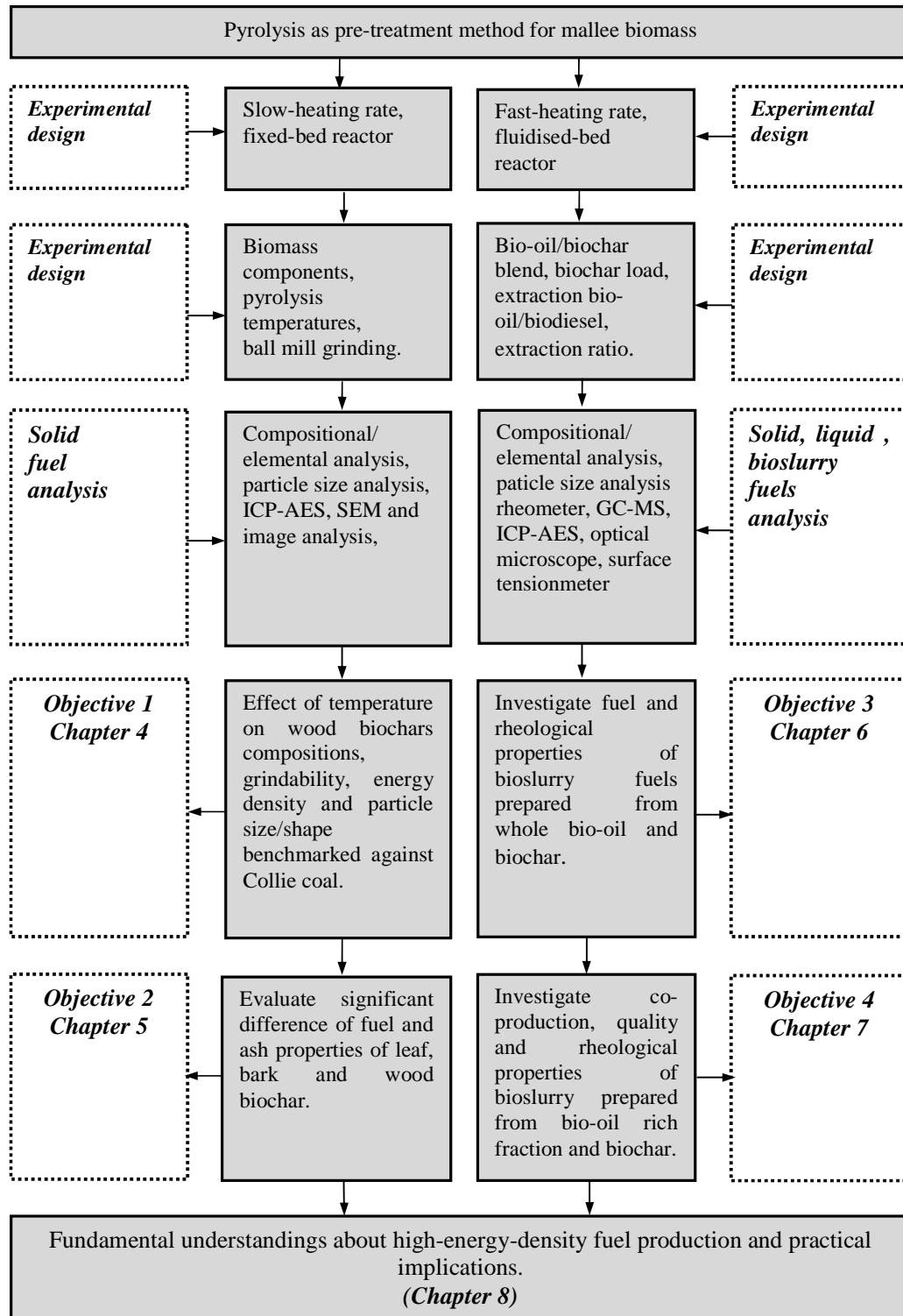


Figure 3-1 Research Methodology

3.2.2 Differences in Fuel Quality and Ash Properties of Biochars from Various Biomass Components of Mallee Trees

Biochar samples were produced from main mallee components i.e. wood, leaf and bark under slow pyrolysis (see detailed descriptions on sample preparations in Section 3.3.1-a and pyrolysis condition in Section 3.3.2-1). All biomass components and biochars were characterised to analyse their elemental compositions (Section 3.4.1) and major ash forming species as described in Section 3.3.7. The significant differences in fuel chemistry were assessed to evaluate the implications of biochar application, especially for ash-related problems and emissions. Grindability of biochar produced from each component was then carried out using a lab-scale ball mill (Section 3.4.2) and the grindability of various biochars was benchmarked against those of biomass. Energy consumption during fuel grinding were estimated as an indicator in energy saving during grinding. The bulk densities of various fuels were measured using the method described in Section 3.4.3. The particle size distributions (PSDs) of ground samples were analysed using a laser-diffraction particle size analyser (Section 3.4.4). SEM analysis (Section 3.4.5) was used to examine the microstructure of intact fuel samples and ground biochar particles. Chapter 5 presents the results and discussion for this work.

3.2.3 Bioslurry Production from Mallee Wood Fast Pyrolysis Oil and Biochar

For this part of work, mallee wood (sample preparation described in Section 3.3.1-b) was pyrolysed using a fluidised-bed reactor under fast heating conditions (as described in Section 3.3.2-2) to produce bio-oil and biochar. Various fuel properties of biochars were analysed, including fuel chemistry and calorific value (Section 3.4.1), grindability (Section 3.4.2) and PSDs (Section 3.4.4), in order to prepare bioslurry fuels. The biochar's surface area, porosity and ability to soak bio-oil (i.e. soakability) were also characterised using a method described in Section 3.4.8. Bioslurry fuels were prepared by mixing whole bio-oil with biochar at various loading levels of ground biochar (Section 3.4.9-1). The method in Section 3.4.3 for bulk density measurement was also used to measure bulk density of bioslurry fuels and further estimate energy densification. Inorganic species in fast pyrolysis bio-oil, biochar and bioslurry were quantified using a wet oxidation method and analysed using an ICP-AES (Section 3.4.7). Static stability of the bioslurry was assessed using

a method described in section 3.4.13. The rheological properties were conducted at steady mode using a Haake Mars II rheometer described in section 3.4.15. Detail experimental conditions, results and discussion for this study are explained in Chapter 6.

3.2.4 Bioslurry Production from Biochar and the Bio-oil Rich Fraction after Bio-oil/Biodiesel Extraction

This part of work is covered in Chapter 7. Mallee bio-oil and biochar were prepared from the fast pyrolysis of wood biomass using a fluidised-bed pyrolysis at 500°C (see description in Sections 3.3.1-b and 3.3.2-2). The bio-oil was then blended with biodiesel at various mass ratios (see sample preparation in section 3.3.1 and extraction process in section 3.4.10). The chemistry and energy content of bio-oil, biodiesel and bioslurry fuels were determined according the procedure described in section 3.4.1. Microstructures of the resulted phases were observed with an optical microscope (section 3.4.11). A GC-MS analysis was conducted to qualitatively analyse selected compounds in the different fractions (Section 3.4.14). A ball mill (Section 3.4.2) was used to grind the biochar and the ground biochar particles were analysed to get a required biochar particle size distributions (Section 3.4.4). The ground biochar was then mixed with selected bio-oil rich phase to produce bioslurry fuel at a certain biochar concentrations (Section 3.4.9-2). Bioslurry fuels using whole bio-oil was also prepared (Section 3.4.9-1) for benchmarking. The fuel density and surface tension were determined using a pycnometer and a surface tensiometer, respectively (Section 3.4.12). Details about measurement conditions were further explained in Chapter 7. Static stability of the resulted bioslurry was assessed using a method described in section 3.4.13. The steady and dynamic rheological measurements of bioslurry were conducted using a Haake Mars II rheometer described in section 3.4.15 with detailed experimental conditions explained in Chapter 7.

The methodology described in Section 3.2.1-3.2.4 are summarised in Table 3-1.

Table 3-1 Summary of methodology

Sub sections	Experiment	Instrument and analytical technique
<p><i>Sub section 3.2.1</i> Properties and Grindability of Biochars Produced from Pyrolysis of Mallee Wood under Slow-Heating Condition</p>	<ul style="list-style-type: none"> • mallee wood biomass was pyrolysed under slow heating conditions at moderate temperatures • The grindability of biochar were assessed using a lab-scale ball mill and benchmarked against those of Collie coal 	<ul style="list-style-type: none"> • compositions and calorific value of wood biomass and biochar product were analysed • fuels bulk densities were measured. • particle size distributions of ground were analysed using a laser-diffraction particle size analyser • SEM analysis were carried out • image analyses of SEM pictures were conducted to determine particle shape/roundness • milling power consumption is estimated
<p><i>Sub section 3.2.2</i> Difference in Fuel Quality and Ash Properties of Biochars from Various Biomass Components of Mallee Trees</p>	<ul style="list-style-type: none"> • biochar samples were produced from wood, leaf and bark under slow pyrolysis • grindability of biochar produced from each component was then carried out using a lab-scale ball mill • grindability of various biochars are benchmarked against with biomass. 	<ul style="list-style-type: none"> • elemental compositions for all biomass components and biochars were characterised to analyse their major ash forming species • the significant differences in fuel chemistry were assessed • energy consumption during fuel grinding are estimated as an indicator in energy saving • the bulk densities of various fuels were measured • the particle size distributions (PSDs) of ground samples were analysed using a laser-diffraction particle size analyser • SEM analysis was used to examine the microstructure of intact fuel samples and ground biochar particles

Sub section 3.2.3

Bioslurry Production from Mallee Wood Fast Pyrolysis Oil and Biochar

- mallee wood was pyrolysed using a fluidised-bed reactor under fast heating conditions to produce bio-oil and biochar.
- bioslurry fuels were prepared by mixing whole bio-oil with biochar at various loading levels of ground biochar
- various fuel properties of biochars were analysed (including fuel chemistry, calorific value, grindability, PSDs in order to prepare bioslurry fuels.
- biochar's surface area, porosity and ability to soak bio-oil (i.e. soakability) were characterised
- bulk density of bioslurry fuels were measured to estimate energy densification
- inorganic species in fast pyrolysis bio-oil, biochar and bioslurry were quantified using a wet oxidation method and analysed using an ICP-AES
- static stability of the bioslurry was assessed
- the rheological properties were conducted at steady mode using a Haake Mars II rheometer

Sub section 3.2.4

Bioslurry Production from Biochar and the Bio-oil Rich Fraction after Bio-oil/Biodiesel Extraction

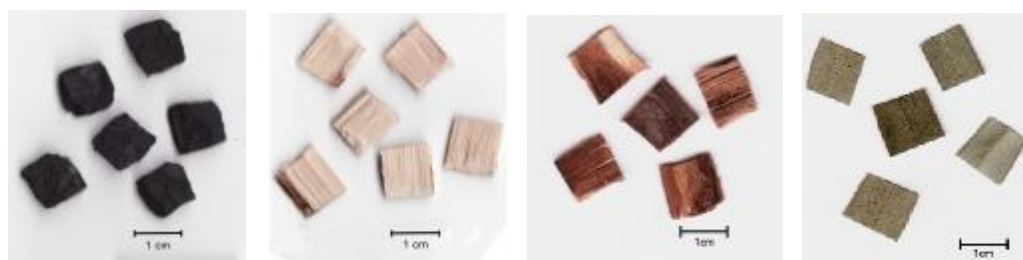
- mallee bio-oil and biochar were prepared from the fast pyrolysis of wood biomass using a fluidised-bed pyrolysis at 500°C
- the bio-oil was blended with biodiesel at various mass ratios
- ball mill was used to grind the biochar and analysed to get a required biochar particle size distribution
- the ground biochar was mixed with selected bio-oil rich phase to produce bioslurry fuel at a certain biochar concentrations
- bioslurry fuels using whole bio-oil was also prepared for benchmarking
- the chemistry and energy content of bio-oil, biodiesel and bioslurry fuels were determined
- microstructure of the resulted phases was observed with an Optical Microscope
- Gas Chromatograph-Mass Spectroscopy (GC-MS) analysis was conducted to qualitatively analysed selected compounds in the different fractions
- the fuel density and surface tension were determined using a pycnometer and a surface tensiometer, respectively
- static stability of the resulted bioslurry was assessed
- the steady and dynamic rheological properties of bioslurry were conducted using a Haake Mars II rheometer

3.3 Experimental

3.3.1 Biomass and Fuel Preparation

Biomass and coal samples. Two species of mallee *Eucalypt* were employed in this study. The preparation for each biomass is as follows:

- (a) *Slow pyrolysis experiment.* Green mallee trees (age: ~ 6 years; species: *E. polybractea*; moisture: 45%) were harvested from Narrogin in the wheatbelt area of Western Australia. The whole trees were separated into leaf, bark and wood components. Samples were then prepared from each component with a size of ~ 1 cm x 1 cm x 0.3 mm (length x width x thickness). The dried biomass was stored in freezer under -4 °C before experiments. For experiment explained in Chapter 4, Collie coal sample was used as a benchmark to compare wood biochar grindability performance. To prepare the coal, as mined Collie coal sample was also cut to similar size. In this study, the biomass samples were dried at 40 °C and Collie coal sample was dried at 105 °C in oven to reduce the moisture contents of all fuels to be around 4 - 5%. Figure 3-2 shows photo of the prepared *E. polybractea* biomass components and Collie coal samples.



Collie coal

E. polybractea

E. polybractea

E. polybractea leaf

wood

bark

Figure 3-2 Biomass and Collie coal samples

- (b) *Fast pyrolysis experiment.* For this experiment, mallee wood from species *E. loxophleba* (*ssp. lissophloia*) milled to a particle size 180-425µm was used. The biomass was dried at 105°C overnight before fast pyrolysis experiments.

Biodiesel, fast pyrolysis bio-oil and biochar. The biodiesel (Gull Bio-D 100%, rape seed oil methyl esters) used in the extraction process was kindly supplied by Gull

Western Australia (www.gullpetroleum.com.au). The biodiesel were used within 6 months from production date. Bio-oil and biochar produced from fast pyrolysis experiment (Section 3.3.2-1) was employed to prepare bioslurry.

3.3.2 Reactor Systems for Pyrolysis Experiment

1. Slow-Heating Conditions. The slow pyrolysis experiments were carried out in a fixed-bed reactor (length: 136 mm; ID: 102 mm), similar to the ones used in previous studies on the pyrolysis of Collie coal at slow heating rates.^{136,137} The reactor was externally heated by an electric furnace, with a thermocouple inserted in the sample bed for temperature control (Figure 3-3). Briefly, a biomass sample (~80g) were charged into the reactor at room temperature and the reactor was heated at 10°C/min to 105°C and hold for 20 min for drying before further heated to a desired pyrolysis temperature and maintained at the temperature for 30 minutes. Nitrogen was used as carrier gas at a flow rate 2.00 L min⁻¹ throughout the experiment. Biochar samples were prepared at pyrolysis temperatures of 300-800 °C. After each experiment, the biochar sample were cooled, collected and stored in a desiccator.

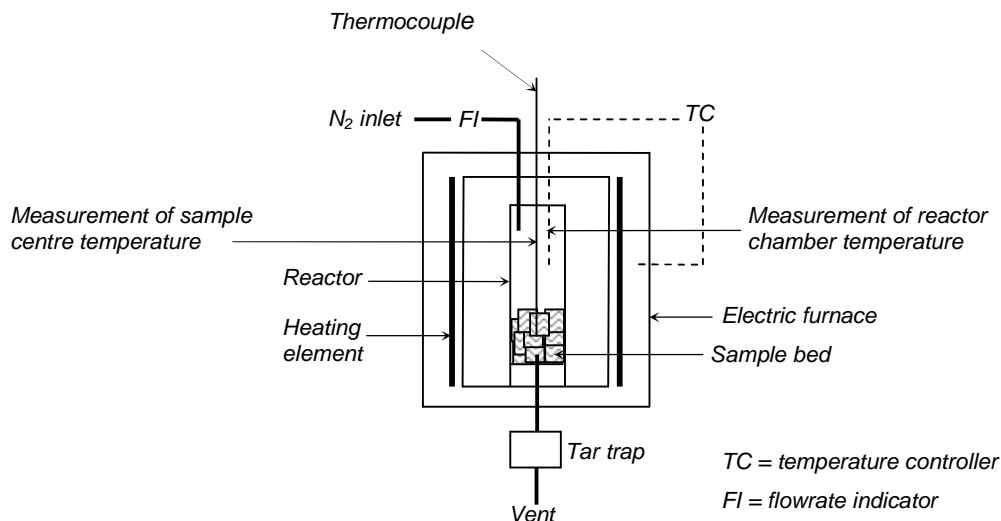


Figure 3-3 A schematic diagram of fixed-bed pyrolysis reactor

2. Fast-Heating Conditions. The fast pyrolysis experiment was carried out using a fluidised-bed reactor and systems for biomass feeding, char collection, vapour condensation, bio-oil recovery and gas analysis. The reactor (Figure 3-4) was made

of stainless steel and comprised of two sections: a cylindrical part that has dimension 102 mm i.d. \times 320 mm long and a conical part with a height of 198 mm. Silica sand (size 351-401 μ m) was used as inert bed solid. Nitrogen was used as fluidisation gas and the flow rate of nitrogen was varied to obtain a constant fluidisation velocity of $>$ 2 times the minimum fluidisation velocity. The feeding system consists of a sealed hopper of 0.033m³ nominal capacity, a stirrer and a screw feeder. A feeding rate of \sim 1 kg/h is used. The biomass (180-425 μ m size) was directly fed into the sand bed 5 min after the desired temperature was achieved and heated up rapidly to bed temperature. The char particles were separated using two cyclones in series. The vapour residence time in the reactor and cyclones was estimated to be \sim 1.4 and \sim 0.7s, respectively. Bio-oil condensation and collection were conducted in three sequential steps comprised of two condensers and an aerosol filter. More detailed descriptions can be found elsewhere.⁹⁹ Fast pyrolysis experiment at final reactor temperature 500°C was conducted to produce bio-oil and biochar samples for preparation of bioslurry fuels described in section 3.4.9 - 3.4.10, Chapter 6 and 7.

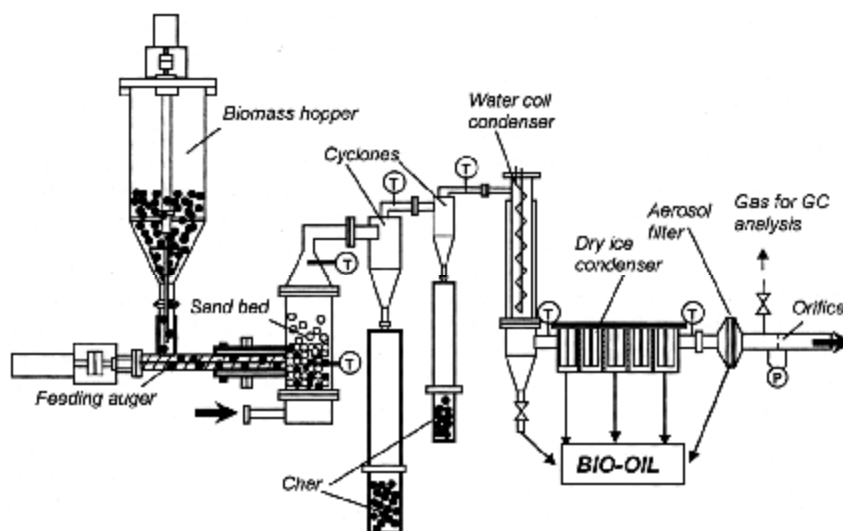


Figure 3-4 A schematic diagram of the fluidised-bed pyrolyser used in this study⁹⁹

3.4 Instruments and Analytical Techniques

3.4.1 Proximate, Ultimate and Calorific Value Analysis

The proximate, ultimate and calorific value analysis of fuel samples were conducted at HRL Laboratory (Melbourne, Australia). Moisture, volatile matter and ash were determined by a Leco MAC analyser following the Australian Standards AS1038.6.4

and AS2434.2. Elemental analysis of carbon, hydrogen and nitrogen were measured with a Leco CHN analyser (Australian Standard AS2434.8). Water in liquid fuel samples were determined using Karl Fischer titration method according to ASTM E203. The calorific value of bioslurry is the summation of the fuels and biochar equivalent low heat value (LHV, GJ/Tonne).

3.4.2 Grindability of Solid Fuels

The most common grindability test for coal is the Hardgrove Grindability Index (HGI) following the standard test method ASTM D409-02. However the HGI method was not successfully adopted to indicate grinding performance for biomass.⁹³ Therefore in this research, a method that employed ball-mill grinding and direct particle size analysis (see section 3.4.4) was developed to assess mallee biofuels grindability. A series of grindability experiments using a laboratory ball mill (Retsch Mixer Mill MM400, 150 watt) of adjustable frequency and time was carried out for dried biomass and biochar. The ball mill has a pair of grinding cell that run simultaneously at a similar frequency. A sample (mass ~ 0.5 g) was charged into the grinding cell and the ball mill operated at a grinding frequency 15 Hz with 15 mm ball size. During grinding, a similar amount of sample was charged in the cells for all fuels. Various grinding time was considered. Multiple milling experiments were carried out in order to produce sufficient amount of ground samples for subsequent analysis. The milling energy consumption for grinding was also estimated based on electricity usage during sample milling, serving as indicators on the potential energy saving in grinding, benchmarking against different fuel samples.

3.4.3 Bulk Density

Bulk density of all solid fuel samples (unground and ground) were determined using a filling and tapping procedure.¹³⁸ Briefly, a fuel sample is loaded in discrete portions into a glass column with known volume. After filling of each portion, the cylinder was tapped onto a bench until no volume change observed. The final volume and sample weight were recorded. Multiple measurements were done for each sample. For bulk density measurements, the standard error is 1.5%.

The bulk density of slurry fuels was measured by determining the weight of the slurry at a constant volume using a graduated measuring cylinder. Repeated measurements were performed with an error bar of 1%.

3.4.4 Particle Size Analysis

Ground fuel samples were sieved into two fractions. One is the fraction size > 1.8 mm and the other fraction of size < 1.8 mm. The < 1.8 mm size fractions were analysed using a laser-diffraction particle size analyser (Malvern Mastersizer2000, Worcestershire U.K). The sample was mixed with sodium hexametaphosphate solution (10% w/v) to aid dispersion of fine particles before loading into the measuring chamber. Repeated measurements were done to get an average number and the standard error is $< 1\%$. The particle size distributions (PSDs) were then constructed and the results are reported as cumulated and fraction volume percentage curves.

3.4.5 Scanning Electron Microscope

The detailed structure of slow pyrolysis biochars and dried biomass were examined using a Scanning Electron Microscope (Philips XL30). The microscopic structures of biochars/dried biomass particles were observed in cross-sections. To prepare the sample specimen, a piece of selected intact biochar or dried biomass of each component was arranged longitudinally then set in the epoxy resin. The specimen was then polished, dried in the oven ($\sim 50^{\circ}\text{C}$) overnight and coated with carbon to get a conductive medium for SEM observation. For selected ground samples, particles of a sample were also spread on a stub which was then carbon coated for surface observation.

3.4.6 Particle Shape Analysis

Particle shape analysis were carried out for selected ground fuels using a combined technique of SEM and image analysis, which is commonly used for the characterisation of char, fly ash, ash cenospheres, ash deposits and other solid samples.¹³⁹⁻¹⁴⁴ The obtained SEM images for ground samples (section 3.2.8) were further analysed using the UTHSCSA *Image Tool* program (freely available from the Department of Dental Diagnostic Science at the University of Texas Health Science

Center, San Antonio, Texas) for particle shape analysis. Detail descriptions of particle shape analysis are explained in Chapter 4.

3.4.7 Quantification of Ash-forming Species in Solid and Liquid/Slurry Fuels

The contents of AAEM (Ca, K, Mg and Na) and other inorganic species (Al, Fe, P and Si) in solid fuels (biomass components and biochars obtained with slow pyrolysis experiment) were analysed using an ICP-AES.¹⁴⁵ The biomass/biochar samples were firstly ashed at a temperature-time program with very slow heating rates to a final temperature of 600°C. The ash was then fused with borate (X-ray flux @: 35.3% lithium tetraborate and 6.7 % lithium metaborate) in a platinum crucible at 950°C for 2h. The ratio of ash to borate was about 1:15. The fusion bed was dissolved in dilute redistilled nitric acid (10% v/v) and subjected to the ICP-AES analysis.

Inorganic species in bio-oil and biochar (produced from fast pyrolysis experiment) also bioslurry were analysed following a wet oxidation procedure used in a previous study.¹⁴⁶ A fuel sample was first oxidized with HNO₃ (65%) before further digested with HClO₄ (70%). The wet oxidization experiment was carried out at 150°C. The residue was also dissolved in 10% HNO₃ for ICP-AES analysis. The ICP-AES analysis was conducted at Marine and Freshwater Research Laboratory, Murdoch University in Perth, Australia and complies with the NATA accreditation.

3.4.8 Biochar Surface Area, Porosity and Soakability

The surface area and apparent density of ground fast pyrolysis biochar were measured using Dubinin-Astakhov surface area and mercury intrusion porosimetry methods. The analysis were conducted at HRL Laboratories (Melbourne, Australia). The ability of biochar to soak up bio-oil was determined by adding discrete portions of ground biochar into bio-oil (weight predetermined) in a closed container. After each addition, the slurry was left to stand for 5 minutes to reach equilibrium soaking of bio-oil by biochar. In this experiment, the soakability of biochar is defined as the mass ratio of biochar to bio-oil whereby absolutely no free flowing of slurry is visually observed upon the addition of biochar into bio-oil.

3.4.9 Preparation of Bioslurry

The preparation of bioslurry fuels were conducted using two methods:

1. *With whole bio-oil.* To prepare the bioslurry, the biochar was first ground in a laboratory ball mill and the biochar particle size distribution was determined using a laser-based particle size analyser (see section 3.4.2 and 3.4.4). The optimum particle size of the biochar was investigated at various grinding time. A series of bioslurry fuels were prepared by suspending various mass concentrations of fine biochar particles into bio-oil (Chapter 6).
2. *With bio-oil rich fraction from extraction of biodiesel/bio-oil process.* Bioslurry fuels were prepared by suspending fine biochar similarly ground as description above into selected bio-oil rich phase solution resulted from the extraction process in section 3.4.10 (Chapter 7).

3.4.10 Extraction of Bio-oil/Biodiesel

A series of biodiesel/bio-oil blend was prepared by mixing various mass percentage of bio-oil to biodiesel. The blends were kept in sealed vials and stirred continuously using a magnetic stirrer at room temperature for 2 hours. After that, the blends were left to settle overnight. A 5 ml syringe is used to separate the bio-oil rich fraction (bottom layer) and biodiesel rich fraction (top layer) and the mass of fractions were again recorded. Selected bio-oil rich fraction was employed to prepare bioslurry using method in section 3.4.9-2. The detail procedures are explained in Chapter 7.

3.4.11 Optical Microscope

The microstructure of bio-oil and bio-oil rich fraction were investigated using a Nikon Eclipse ME600 Optical Microscope equipped with a Nikon Digital Camera DXM 1200F and Image-Pro Plus 5.1 software.

3.4.12 Density and Surface Tension

Fuel density was determined with a pycnometer (5 mL) and the measurement was done multiple times with error bar of <1 %. The surface tension of liquid and slurry fuels were measured using a KSV Sigma 701 Surface Tensiometer using Wilhelmy method with a round platinum rod (diam. 1 mm) as probe. The sample's temperature

is controlled with a water bath. Sample was left for 5 min in the measuring chamber to reach the desired temperature before taking the first reading. The surface tension values reported in Chapter 7 were an average and standard deviation of 50 data points after the surface tension reached equilibrium. More details experimental conditions are explained in Chapter 7.

3.4.13 Static Stability

Examination of bioslurry stability was carried out using a standard method for coal water slurry.¹¹⁶ A bioslurry sample (50 ml) was kept in a closed container and left to stand in room temperature (25°C) for 15 days. The slurry was then poured slant way for 30 seconds into a clean vial. The slurry container then turned upright for 4 minutes to let the slurry flow adequately into the vial. Then, the mass of non flowing part of the bioslurry was determined. The stability of bioslurry can then be calculated using the equation $SB_{sta} = (1 - M_B/M_S) \times 100$, where SB_{sta} is the static stability (%), M_S is the initial mass of the bioslurry sample (g) and M_B is the mass of the non flowing bioslurry (g) after 15 days. In this experiment, bio-oil without biochar addition was used as a blank. Repeated measurements were done on selected samples with an error bar of $\leq 0.3\%$.

3.4.14 Gas Chromatography-Mass Spectroscopy (GC-MS)

Chemical compounds in the fuels were qualitatively identified using a GC-MS (Agilent 6890 series GC Agilent 5973 MS detector, m/z range: 10-550amu) with a capillary column (0.25 μ m HP-5MS phase, 30m X 0.25 mm id). The temperature program was to reach an initial temperature 40°C, hold 3 min, ramp 15°C/min, final temperature 300°C and hold 5 min. The split ratio for the injector was 15:1 and the solvent delay time was 3 min.

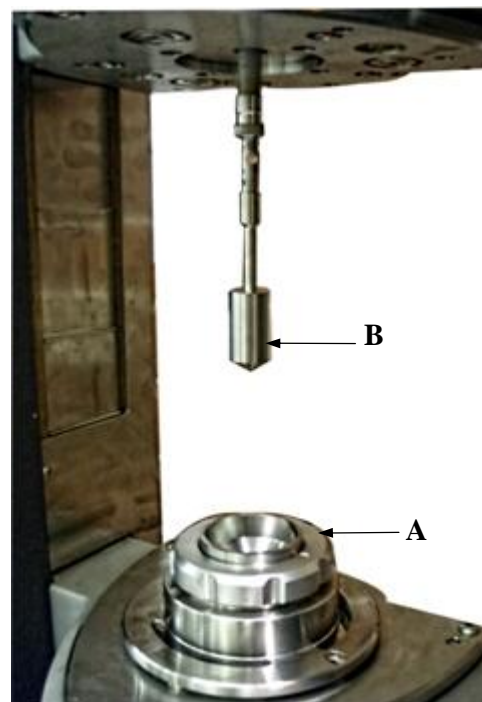
3.4.15 Rheological Study

The liquid/slurry fuels rheological properties were characterised using A Haake Mars II rheometer fitted with a Z20 cylinder sensor system (Figure 3-3). The instrument was pre-calibrated by the manufacturer and equipped with Haake Thermocontroller TC501 to control sample temperature. With this fixture a sample volume of 8.2 mL is required for each measurement and placed in a cup that was inserted into a

tempering unit (Figure 3-3 A). During the measurement, the gap between the tip of the sensor (Figure 3-3 B) and the cup base was set at 4.200 mm. The fuels rheological behaviour was examined under steady and dynamic mode. Details programme for the steady, dynamic measurement and regression equation are explained in Chapter 6 and 7.



Haake Mars II rheometer



Z20 cylinder sensor and cup

Figure 3-3 Haake Mars II rheometer and Z20 sensor system

3.5 Summary

The present research uses pyrolysis as a pre-treatment step to convert biomass into high-energy-density fuels under slow- and fast-heating conditions using fixed-bed and fluidised-bed reactor systems respectively. The biochar, bio-oil and bioslurry fuels were characterised using an array of analytical instruments. Such analysis include fuel chemistry, grindability, particle size distribution, SEM, image analysis, ICP-AES, GC-MS, Optical Microscope, surface tensiometer and rheometer.

CHAPTER 4

PROPERTIES AND GRINDABILITY OF BIOCHAR PRODUCED FROM THE PYROLYSIS OF MALLEE WOOD BIOMASS UNDER SLOW-HEATING CONDITIONS

4.1 Introduction

The main objectives of biomass pre-treatment are to drastically enhance biomass grindability and improve biomass composition to a low moisture, low H:C/O:C ratio and increase heating value to match with coal properties. Biomass upgrading on these critical aspects need to substantially increase biomass bulk density and volumetric energy density and improve feeding/handling properties as these are the key factors in realising substantial reduction in logistics cost associated with biomass utilisation for power generation (Chapter 2).

This chapter aims to investigate the properties of biochar produced from the pyrolysis of mallee wood biomass (species *E. polybractea*) under slow-heating conditions and the possibility to use biochar as a solid fuel, addressing key issues associated with the direct use of biomass as a fuel, including being bulky, of high moisture, low-energy-density and poor grindability. A laboratory size ball mill was employed in grindability experiment to evaluate biochar grinding performance as well as the possibility of conducting biochar grinding with conventional ball mill in coal-based power stations. Fuel bulk density was measured to estimate the improvement of volumetric energy densification achieved via grinding. Biochar fuel properties and grindability data were benchmarked against Collie coal. It should be noted that Collie coal is the only coal currently being mined for power generation in Western Australia so that it makes sense to use this coal as a benchmark.

4.2 Methodology

Mallee wood biomass and Collie coal samples were prepared as described in Section 3.3.1-a in Chapter 3. These samples are referred as “dried wood biomass” sample and “Collie” coal sample. Biomass samples were treated at temperatures of 300, 320, 330, 350, 400, 450 and 500°C under slow-heating conditions according to method in Section 3.3.2-1 to produce biochar. These biochar samples are referred as “WCxxx” chars, where “xxx” indicates the pyrolysis temperature in degree Celsius. It should be noted that different to the raw biomass and coal samples, no drying was carried out on the biochar samples.

The biochar was subjected to a series of grindability experiment (see Section 3.3.4.2) at various grinding time (1, 2 and 4 minutes). Grinding experiments were also carried out for the dried wood biomass and Collie coal samples under the same grinding conditions. Grinding at longer grinding time (8 and 15 minutes) were done for the dried wood biomass and the WC300 char for comparisons. Method described in Section 3.4.3-3.4.4 was used to analyse particle size of the ground fuels and bulk density/volumetric energy density determination respectively.

The particle shapes analysis was carried out for ground fuel samples using a combined technique of SEM and image analysis (Section 3.4.5-3.4.6). For each sample, a minimum of 200 particles were analysed. Four parameters were analysed, including a) *area* - the area of the object, which is then converted into sphere diameter; b) *major axis length* - the length of the longest line that can be drawn through the object; c) *minor axis length* - the longest line that can be drawn through the object perpendicular to the major axis; and d) *roundness*, which has a value between 0 and 1 and a greater value indicating the object being rounder. The roundness of a perfect circle is 1 and as the roundness decreases from 1, the object departs from a circular form.

4.3. Results and Discussion

4.3.1 Biochar Yield and Properties of Biochar as a Fuel

Figure 4-1 presented the biochar yield of mallee wood biomass as a function of pyrolysis temperature. As expected, the biochar yield decreases with increasing

pyrolysis temperature. A similar trend was also observed in previous studies on the pyrolysis of various biomass materials under similar conditions.^{103,147-149} It should be noted that with temperature increasing from 300 to 450°C, biochar yield decreases from ~56% to ~27 % dry base (db) and the biochar yield levels off with further temperature increase.

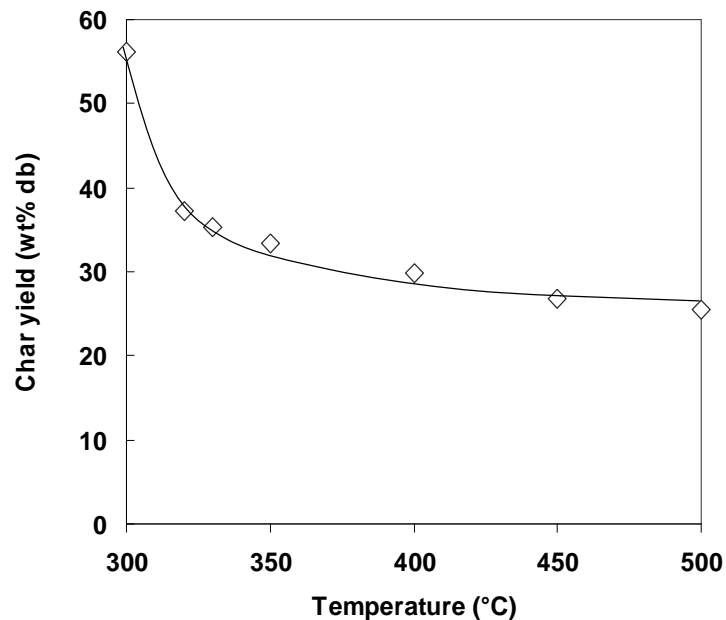


Figure 4-1 Biochar yield of mallee wood pyrolysis in a fixed-bed reactor at various temperatures

Proximate and ultimate analysis of biochars and the dried wood biomass are given in Table 4-1, along with those of Collie coal for benchmarking. It is interesting to see in Table 4-1 that even at a pyrolysis temperature as low as 320°C, the proximate and ultimate analysis of the biochar produced is similar to the Collie coal sample. Further increase in the pyrolysis temperature leads to the production of biochars with better fuel qualities. Biochar also has lower moisture, lower ash, and lower sulphur and nitrogen contents compared to Collie coal. It should be noted that the as-mined Collie coal (used to prepare the Collie coal sample in Table 4-1) and the green biomass (used to prepared the DWB sample in Table 4-1) have much higher moisture contents, that is ~25% and ~45%, respectively. The results indicated that, in comparison to the green biomass and as-mined Collie coal samples, biochars have better fuel qualities.

Table 4-1 Proximate and ultimate analysis of various fuels

Code	Sample	Proximate analysis (% , ar)				Ultimate analysis (% , db)				
		Moisture	Ash	FC	VM	C	H	N	S	O ^a
DWB	dried wood biomass	4.5	0.6	15.5	79.4	49.1	6.1	0.13	0.02	44.70
WC300	Char 300°C	4.6	0.7	35.3	59.5	60.3	5.3	0.18	0.02	34.14
WC320	Char 320°C	2.9	0.9	56.9	39.3	72.9	4.6	0.24	0.02	22.21
WC330	Char 330°C	2.7	1.1	59.2	37.0	73.6	4.5	0.27	0.03	21.52
WC400	Char 400°C	4.5	1.2	69.9	24.4	79.1	3.7	0.29	0.04	16.80
WC450	Char 450°C	4.0	1.4	75.3	19.3	82.9	3.3	0.32	0.03	13.38
WC500	Char 500°C	4.5	1.3	79.8	14.4	85.5	3.0	0.34	0.03	11.14
Collie	Collie coal	5.5	8.5	51.1	34.9	74.0	4.3	1.30	0.60	19.80

M,Moisture; FC, fixed carbon; VM,volatiles matter; ar, as received; daf, dry ash free. ^a By difference

On the basis of the data in Table 4-1, the atomic H/C and O/C ratios of biochars, biomass and Collie coal are also plotted in a van Krevelen diagram for further comparisons, as shown in Figure 4-2.

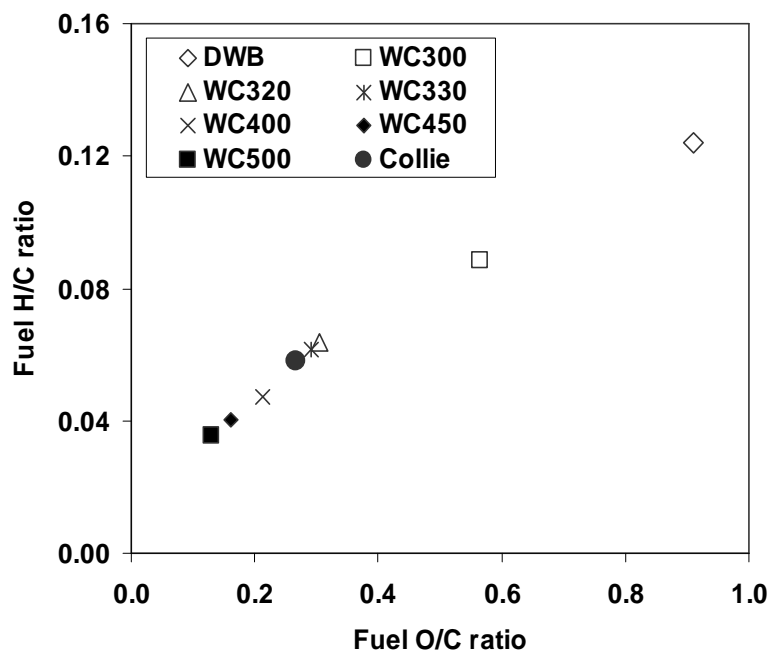


Figure 4-2 Relationship between fuel H/C and O/C ratios for various solid fuels. Legends: DWB, dried wood biomass; WCxxx, biochar prepared from the pyrolysis of the dried wood biomass at xxx °C; Collie, Collie coal

It is known that from the combustion point of view, fuels with low H/C and O/C ratios are favourable since it reduces energy loss, smoke and water vapour.⁴⁸ Figure 4-2 has clearly showed that in comparison to the parent biomass, biochars have significantly lower H/C and O/C ratios, which decrease with increasing pyrolysis temperature. The pyrolysis reactions lead to a significant increase in the mass energy density of biochars (see part A of Figure 4-3). This can be explained with regard to higher energy contained in carbon-carbon bonds than in carbon-oxygen and carbon-hydrogen bonds. Figure 4-2 also has demonstrated that biomass pyrolysis at temperatures as low as 320°C produces biochars with H/C and O/C ratios similar to Collie coal. The data in the van Krevelen plot are in agreement with the measured mass energy density of various fuels, as shown in part A of Figure 4-3.

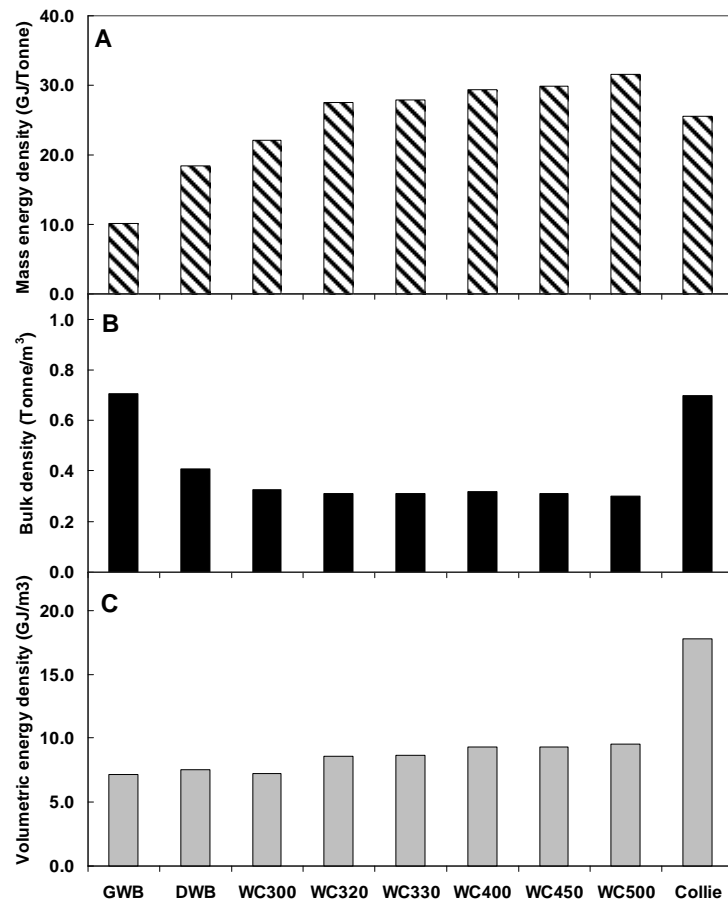


Figure 4-3 Mass energy density (A), bulk density (B), and volumetric energy density (C) of various fuels. GWB, green wood biomass; DWB, dried wood biomass; WCxxx, biochar prepared from the pyrolysis of the dried wood biomass at xxx °C; Collie, Collie coal

It is obvious that the mass energy density of biochars increases with increase pyrolysis temperature, due to more intensive pyrolysis reactions at higher temperatures. For example, the mass energy densities are 22, 28, and 32 GJ/tonne for the biochars produced at pyrolysis temperature of 300, 330 and 500°C, significantly higher than those of the DWB (~ 18 GJ/tonne) and the green biomass (~10 GJ/tonne). It can also be seen that, even at a pyrolysis temperature as low as 320°C, the biochar mass energy density (~28 GJ/tonne) is even higher than that of Collie coal (~26 GJ/tonne). Therefore, biochar as a fuel achieves significant mass energy densification.

However, fuels with high mass energy densities do not always mean that such fuels are not bulky, that is of high bulk densities. Disadvantages of fuels with low fuel bulk densities are well known, including low volumetric energy densities, process control difficulties, increased storage costs, expensive transportation and other technology limitations.⁶ In this study, experiments were then carried out to measure the bulk densities then to work out the volumetric energy densities of various fuels and the results are plotted in part B and C of Figures 4-3. It is interesting to see that, although the mass energy densities of biochars have been increased substantially in comparison to biomass (part A of Figure 4-3), biomass pyrolysis actually leads to a reduction in fuel bulk densities. This is mainly due to the fact that the fuel particles experienced little changes in its size and shape after pyrolysis while volatiles were released. These two opposite effects, that is an increase in mass energy density and decrease in bulk density, lead to only a slight increase in the fuel volumetric energy density, from ~7 GJ/m³ of the green biomass to ~9 GJ/m³ of various biochars depending on pyrolysis temperature. Such biochar volumetric densities are significantly lower than those of Collie coal (~17 GJ/m³), suggesting that transport of biochar obtained from pyrolysis is still not suitable.

4.3.2 Grindability of Biochar

Part C of Figure 4-3 therefore indicates that further densification processes are still needed to improve the volumetric energy density of biochars. This means that biochar size reduction via grinding is necessary to increase bulk density, which in turn requiring the biochars to have a good grindability. Additionally, one of key issue

associated with the use of biomass as a fuel in applications such as co-firing⁷¹ is biomass's poor grindability. It is therefore strongly desired for biochars to have a good grindability. A series of experiments was then carried out to investigate the grindability of the biochars, biomass and Collie coal samples using a laboratory ball mill, considering various grinding time including 1, 2 and 4 minutes. All fuel samples have a similar starting size and shape before grinding so that the grindability can be assessed based on the particle size distribution after grinding. In other words, after the same period time of grinding, the smaller particle size distribution a fuel sample gets the better grindability the fuel is. A specification for particle size used in coal combustion i.e. 80% <74-75 μm ¹⁶ was used as a guideline. Figures 4-4 presented the cumulative particle size distributions of the ground dried wood biomass, selected biochars, and Collie coal at various grinding time.

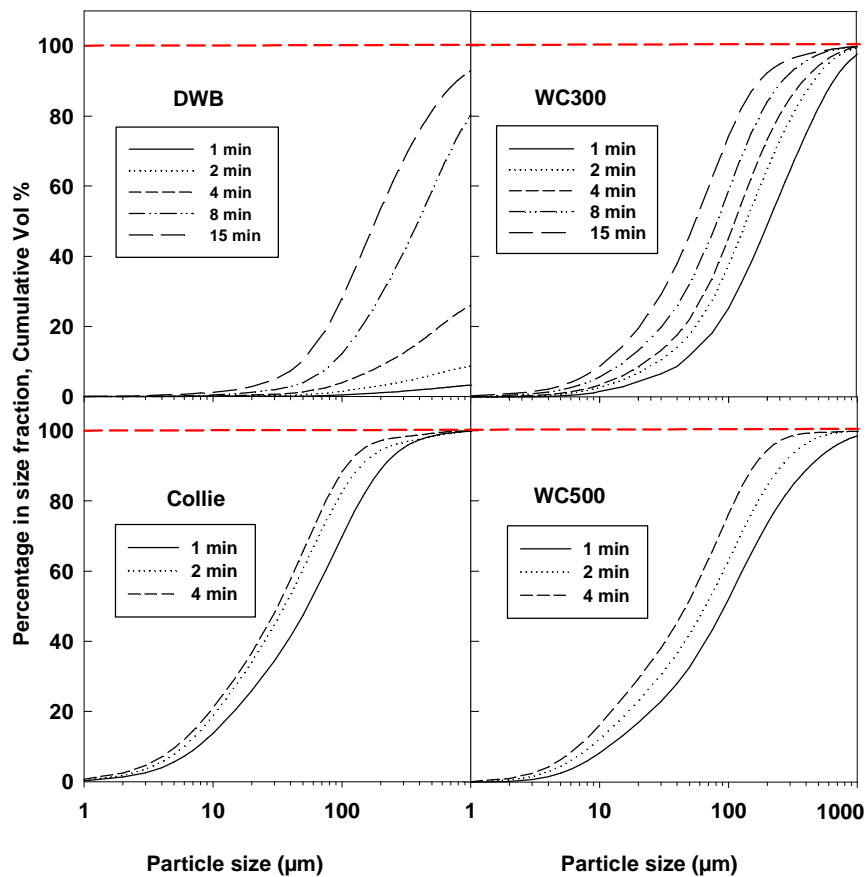


Figure 4-4 Particle size distributions of selected ground fuels. DWB, dried wood biomass; WCxxx, biochar prepared from the pyrolysis of the dried wood at xxx °C; Collie, Collie coal

Figure 4-5 showed the particle size distributions of various fuels at 4 min grinding time. Several important observations can be made based on the data in these figures. First, as expected, the dried wood biomass exhibits a poor grindability. After grinding for 2 minutes, the size reduction is very small, with over 90% of the particles of sizes >1.8 mm. In fact, because the dried woody biomass is also hard to be ground, even after 15 minutes grinding, the cumulative percentage of the ground sample only reaches 19% for particles of sizes less than $75\ \mu\text{m}$ (Figure 4-4). On the contrary, biochars have excellent grindability, indicating that the pyrolysis reactions weakening the wood fibre structure and biochars become brittle and easily ground into fine powders.

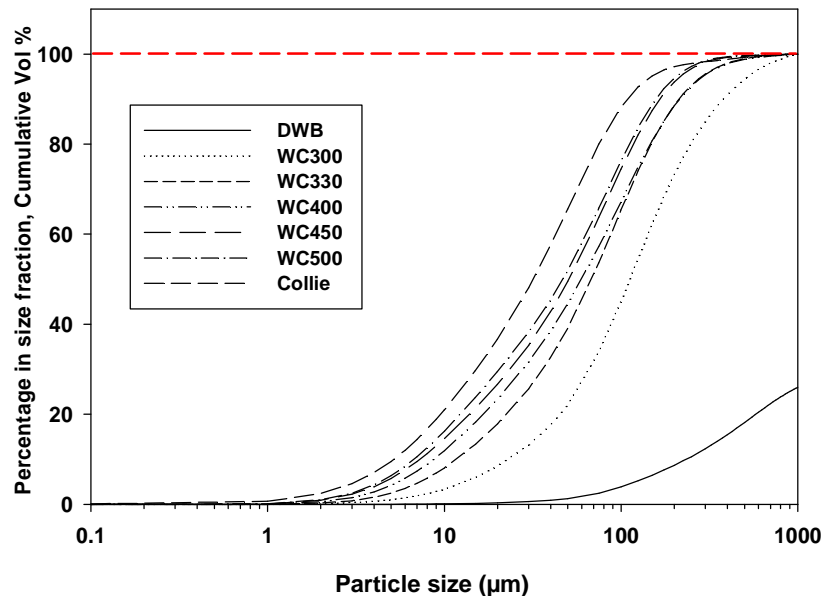


Figure 4-5 Particle size distributions of selected ground fuels at 4 mins grinding time. DWB, dried wood biomass; WCxxx, biochar prepared from the pyrolysis of the dried wood at xxx °C; Collie, Collie coal

Second, Figure 4-4 also demonstrated that the particle size distributions of all fuel samples (dried wood biomass, biochars, and Collie coal) decrease with grinding time. For each fuel sample, a grinding limit seems to exist beyond which additional grinding only leads to slightly further size reduction. In other words, once the grinding limit is reached, what can be ground under the grinding conditions would

have been mostly ground. The dried wood biomass for example, takes 15 min to reach the grinding limit, whereas for the biochars only 2 min grinding time are needed, indicating a better grindability of biochars in comparison to biomass.

Third, it is interesting to note in Figure 4-5 that, compared to the dried wood biomass, even mild treatment by pyrolysis at a temperature as low as 300°C leads to a significant increase in the fuel grindability, resulting in ~28% of the particles in the ground WC300 biochar sample being less than 75 µm after only 2 minutes grinding. An increase in the pyrolysis temperature from 300 to 330°C leads a further apparent increase in biochar grindability but higher pyrolysis temperature only slightly enhance biochar grindability. The data suggested that thermal treatment of biomass at temperature <330°C lead to biochar structure changes that have significant impacts to fuel grindability.

Lastly, Figure 4-5 indicated that the grindability of biochars is similar to, although is not as good as, that of Collie coal. Under the current grinding conditions, Collie coal gives the highest size reduction (74% cumulative percentage particle below 75 µm) after 2 minutes, among all fuel samples. Whereas the build-up problem on ball charges bed is often seen during the grinding of dried woody biomass, the problem diminishes during biochar grinding. Such an observation is of critical importance to practical applications. It is well known that ball mill, which is widely used in coal-fired power stations, is less suitable for grinding biomass because its gravity impacts and tumbling actions only flatten rather than shortening biomass fibres, as experienced in the previously unsuccessful trials⁷¹⁻⁷⁴ (Table 2-3 Chapter 2). The excellent grindability of biochars opens the opportunity to use ball mill systems to co-mill coal and biochars, addressing the key issue of poor milling performance associated with the direct use of biomass as a fuel in the co-utilisation processes of biomass and coal. According to the electricity usage of the ball mill during grinding, further calculations were also conducted to illustrate the potential energy saving achievable during milling of biochar in comparison to biomass. It is estimated that biochar grinding requires an electricity consumption of 2.5-10.0 kWh/kg (similar to Collie coal) compared to over 37.5 kWh/kg for biomass grinding, indicating a drastic milling energy saving of ~73-93%, depending on the pyrolysis temperature at which

the biochar was produced. Certainly, the excellent grindability of biochars would also help to address other related issues e.g. fuel blockage, feeder limitation and so forth. The bulk density and volumetric energy density of the ground fuel samples, prepared from dried woody biomass, biochars and Collie coal at various grinding times, are plotted in Figure 4-6.

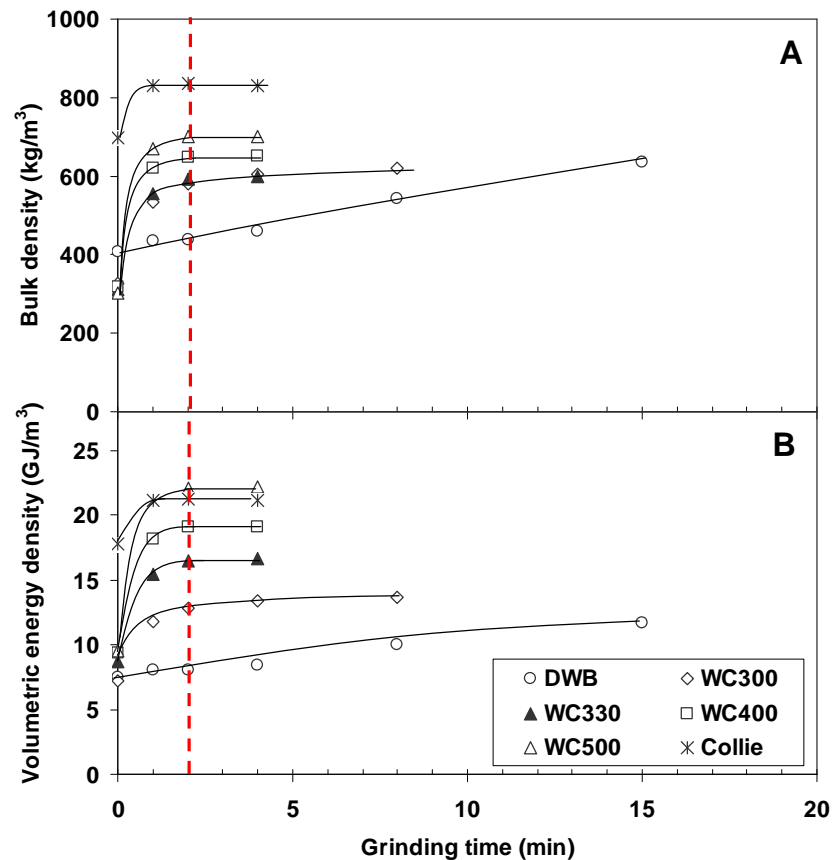


Figure 4-6 Bulk energy density (A) and volumetric energy density (B) of various fuels as a function of grinding time. DWB, dried wood biomass; WCxxx, biochar prepared from the pyrolysis of the dried wood biomass at xxx °C; Collie, Collie coal

As results of size reduction of fuel samples after grinding, the bulk density and volumetric density of all fuel samples first increase with grinding time and then level off with further grinding. In the case of the dried wood biomass, considerably long grinding time (15 minutes) is required to reach the plateau values of the bulk density and volumetric energy density, and only 2 minutes grinding is required for biochars. Part A of Figure 4-6 clearly indicated that the rapid size reduction of

biochars during grinding as results of the excellent grindability of biochars can achieve significant increases in the bulk density of the ground biochars after a grinding time as short as 1 or 2 minutes. Apparently, the size reduction of biochars after grinding leads to a significant removal of the inter- and intra-particle voids, which are commonly experienced by large biomass particles during packing. Part A of Figure 4-6 showed that the bulk densities of biochar samples after 2 minutes grinding are 600-700kg/m³, which are only slightly lower than that of the ground Collie coal (~830 kg/m³), but this is already a significant improvement from the unground biochars (~300 kg/m³). The increase of biochar bulk density closer to that of the Collie coal sample has significant economic impact to the improvement of biomass/coal fuel handling characteristics especially for blending process control as mixing fuels of similar densities can avoid sedimentation problem and produce a homogenised mixture.

As results of the excellent grindability of biochars, the significant increase in the bulk densities of biochars after grinding also leads to the significant increase in the volumetric energy densities of biochars after grinding. Part B of Figure 4-6 clearly demonstrated that, after only 1 to 2 minutes grinding, the volumetric energy densities of the ground biochars prepared from the pyrolysis at a temperature of 330°C or higher are ~17 – 23 GJ/m³, which are already equal or better than ~17 GJ/m³ of unground Collie coal sample and 10 GJ/m³ for the green biomass as well as significant increases from ~7 – 9 GJ/m³ for the unground biochars. Similar to the trend observed for the bulk density, the volumetric energy density of biochars and Collie coal reached the plateau values after grinding for 2 minutes. Therefore, the use of biochar has the potential to reduce biochar transport costs to be at least at a similar level of Collie coal. In Figure 4-6, the bulk and volumetric energy densities of WC300 leveled after 4 minutes grinding. For subsequent grindability experiment, 4 minutes are then taken as the optimal grinding time for all wood biochars.

4.3.3 Particle Shape

The grinding of various fuel samples may also produce particles of largely-different shapes. The SEM micrographs of all ground samples are shown in parts (a) to (h) of Figure 4-7.

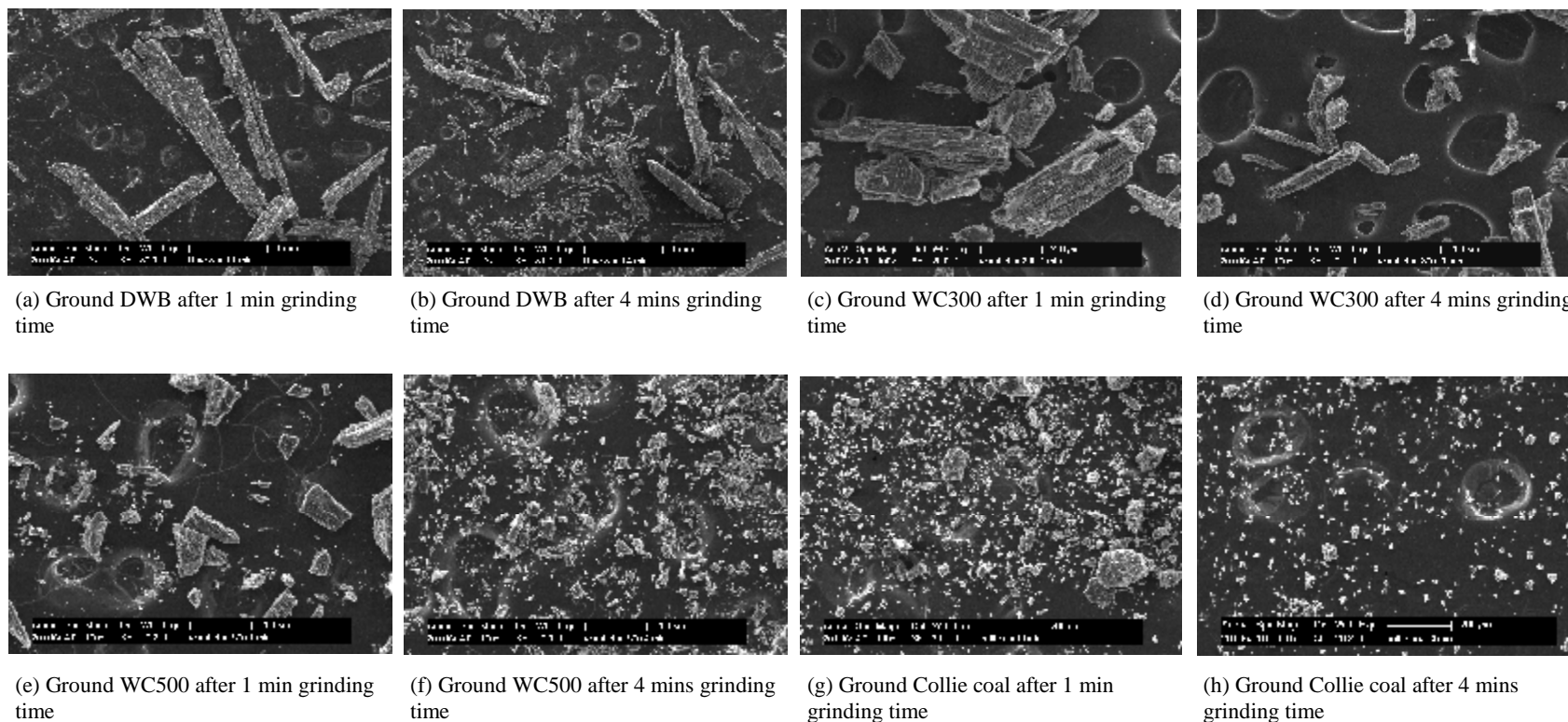


Figure 4-7 Images of ground fuel samples. (Legends: DWB, dried wood biomass; WCxxx, biochar prepared from the pyrolysis of the dried wood biomass at xxx °C; Collie, Collie coal)

It can be seen in part a of Figure 4-7 that the wood biomass particles have anisotropic nature which means wood strength is with the grain and same along the directions of fibres. Because of its fibrous nature, grinding of the dried wood biomass produces long fibrous particles. Although the particles > 1.8 mm were removed by sieving, the length of some particles in the ground biomass sample was still many times larger. This is because when the ground biomass particles are sieved manually, the orientation of long thin particles enable them escape through the specified sieve holes as the shortest dimension of the particles are typically much less than the size of the mesh. Parts c-h Figures 4-7 showed that compared to dried woody biomass, ground particles derived from biochars and Collie coal sample are much shorter and the shapes appear rounder.

A quantitative assessment was then carried out on key shape parameters (i.e. roundness and major/minor axis length ratio, MMALR) for the particles in the ground samples of the dried wood biomass, selected biochars and the Collie coal sample. A low roundness and high MMALR indicated that the particle is long and fibrous. On the contrary, a high roundness and low MMALR reflected that the particle is short and round. Figure 4-8 presented the results of the dried woody biomass, biochars and the Collie coal sample at 1 and 4 minutes grinding time.

Figure 4-8 clearly showed that the particles in the ground biomass sample are large, long and fibrous. An increasing grinding time leads to reduced particle size while the MMALR remains high. In contrast, the particles of the ground biochars and the Collie coal sample are much shorter and rounder. Increasing the grinding time from 1 to 4 min leads to only slight changes in the particle shapes of the ground biochars. Figure 4-8 also indicated that at the same grinding time, the particles in the ground biochars prepared at a high pyrolysis temperature generally have a higher roundness and a lower MMALR. Therefore, biochar as a fuel not only has an excellent grindability but also leads to the production of short and round particles after grinding. Compared to the long and fibrous particles in the ground biomass sample, the short and round shapes of ground biochar particles are favourable in many practical applications particles of such characteristics are known to enhance fluidisation behaviour³⁴ and have desired fuel frictional properties.¹⁵⁰

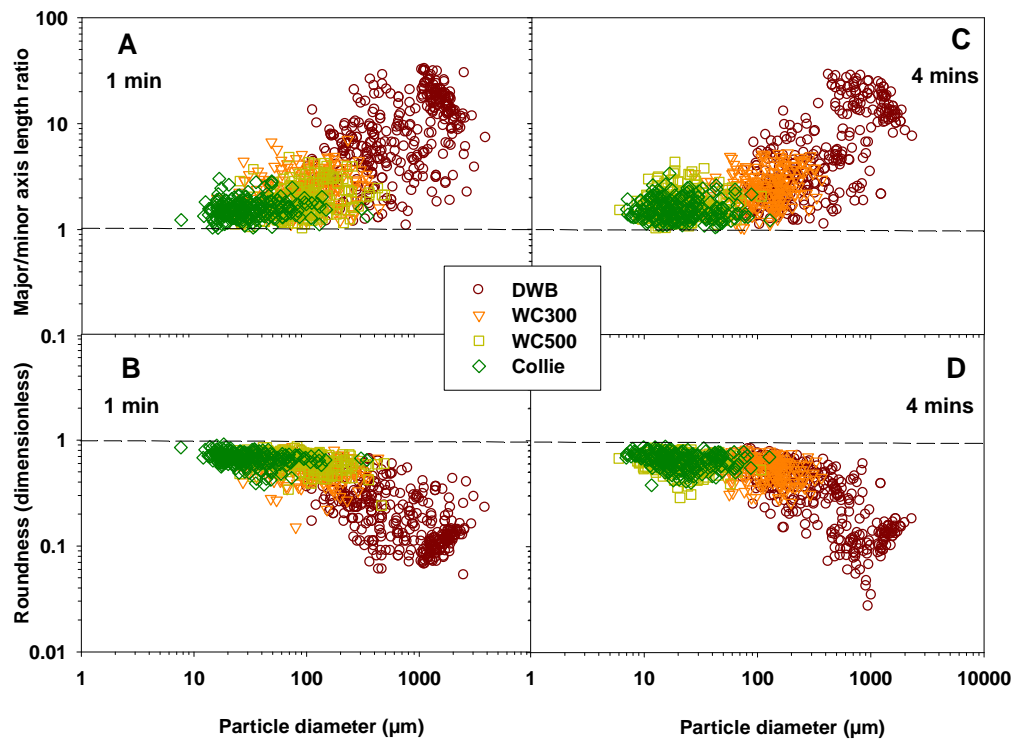


Figure 4-8 Major/minor axis length ratio and roundness of fuel particles after grinding for 1 min (A and B) and 4 mins (C and D). DWB, dried wood biomass; WCxxx, biochar prepared from the pyrolysis of the dried wood biomass at xxx °C; Collie, Collie coal

Most importantly, in applications such as gasification and liquefaction, particle quality similar to those obtained in this study was found to positively improve combustibility, reactivity and process efficiency.⁸²

4.4 Conclusions

The use of biomass directly as a fuel suffers from low bulk density, low energy density and poor grindability. This study shows that biochar produced from biomass pyrolysis can be a good fuel, addressing the key issues associated with biomass utilisation. Biochar has a high mass energy density but is still bulky. The excellent grindability of biochars enables it to be earlier ground to achieve a similar volumetric energy density to coal. Grinding of biochars is of low energy consumption also produces biochar particles that are short, round and favourable for practical applications.

CHAPTER 5

SIGNIFICANT DIFFERENCES IN FUEL QUALITY AND ASH PROPERTIES OF BIOCHARS FROM VARIOUS BIOMASS COMPONENTS OF MALLEE TREES

5.1 Introduction

A main strategy in biomass pre-treatment is to transform wide streams of biomass into a more homogenised fuel (Chapter 2) to benefit fuel handling and process design. The first step of this transformation requires fundamental understanding on unique properties of each biomass components/types of interest. Mallee biomass is produced from the harvest and chipping of whole mallee trees so that it contains three main components i.e. wood, leaf and bark. For power generation, mallee biomass can either be partitioned or used as a whole biomass. The latter approach is more likely to be applied in future large scale application.²⁰ The data in Chapter 4 demonstrated that the biochars derived from slow pyrolysis of mallee wood exhibit improved fuel properties, grindability and volumetric energy density and closely matched to those of Collie coal. With regard to different scenarios of mallee biomass application, properties of fuel derived from other mallee components also need to be understood. This chapter continues the work in Chapter 4 and focuses on investigating the key differences in the fuel quality and ash properties of biochars produced from the slow pyrolysis of various mallee components. The objective of this chapter is to identify advanced fuel characteristics and undesirable issues that each component might impose in various scenarios of mallee biomass utilisation. This corresponds to the second thesis objective outlined in Chapter 2.

5.2 Methodology

Firstly, sample from various components of mallee trees were prepared as described in Section 3.3.1-a in Chapter 3. Biochar samples were prepared at pyrolysis temperatures of 300-800°C (Section 3.3.2-1). These biochar samples were referred as “LCxxx”, “BCxxx” or “WCxxx” chars, where the prefix “LC” refers to leaf char, the prefix “BC” denotes bark char, and “WC” represents wood char, while the suffix “xxx” indicates the pyrolysis temperature (in degree Celsius).

The grindability of the biochars were assessed using a ball mill (see Section 3.4.2) at 4 minutes grinding time, that is the optimal grinding time for wood biochars as explained in Chapter 4. Fuel particle size, bulk and volumetric energy density were determined according to method in Section 3.4.3-3.4.4. The detailed structure of biochars and dried biomass were examined using SEM (Section 3.4.5). The contents of AAEM (Ca, K, Mg and Na) and other inorganic species (Al, Fe, P and Si) in biomass components and biochars were analysed using an ICP-AES following ash fusion with borate (Section 3.4.7).

5.3. Results and Discussion

5.3.1 Partition and Compositions of Mallee Biomass Components

On a dry basis, the whole mallee tree samples comprised mainly of wood (60 wt% dry basis (db), leaf (27 wt% db) and a smaller fraction of bark (13 wt% db). Table 5-1 presented proximate and ultimate analysis of dried leaf, wood and bark.

Table 5-1 Proximate and ultimate analysis of biomass

Dried biomass	Proximate analysis (% ar)				Ultimate analysis (% daf)				
	M	Ash	FC	VM	C	H	N	S	O ^a
leaf	4.8	4.1	18.5	72.6	54.3	6.7	1.15	0.09	37.8
bark	6.6	7.1	17.6	68.7	43.1	5.2	0.31	0.04	51.4
wood	4.5	0.6	15.5	79.4	49.1	6.1	0.13	0.02	44.7

^a by difference

Concerning the biomass ash content, bark notably has the highest ash followed by leaf. It is generally accepted⁷⁶ that high ash level in bark and leaf is an indicator of the nutrient concentration (especially K) within an actively metabolizing part of a tree. It is known that, for many *Eucalyptus* species,¹⁵¹ seasonal bark shedding occurs where old bark is shed and replaced with new tissues. In leaf and tree crown, nutrients from the soil are fixed before being relocated to other parts of the tree.⁷⁶ For volatile matter, wood has the highest level although the differences among the three components are not as pronounced as ash. Knowledge of the biochar ash properties and where it originates is essential for the design of appropriate reactors and the understanding on ash-related issues such as fly ash and ash deposit formation or logistics concerning ash disposal/storage/utilisation.¹⁵² Leaf biomass obviously shows high level of nitrogen and sulphur. During combustion, nitrogen in fuel is largely responsible for nitric oxides (NO_x) while sulphur mainly form SO_x and sulphates with AAEM species. Not only NO_x and SO_x contribute to emission problem, high concentration of SO_x in flue gas during combustion could also cause serious corrosion in heat exchanger parts.¹⁵²

5.3.2 Differences in Biochar Yield and Fuel Chemistry

The biochar yield decreases with increasing pyrolysis temperature, as shown in Figure 5-1. Within the temperature range studied, bark pyrolysis gives the highest char yield (~60% db at 300°C, ~38% db at 500°C) while wood is the lowest. Despite higher char yield, the bark biochar (Table 5-1) has a high ash content, which increased with increase pyrolysis temperature. Although bark only contributes to 13 wt% db of the entire biomass of mallee trees, the high ash level is expected to potentially impose ash-related problems. As expected, in terms of moisture, C, H, O and volatiles, the data in Tables 5-1 and 5-2 clearly show that biochars in general have better fuel qualities than dried biomass.

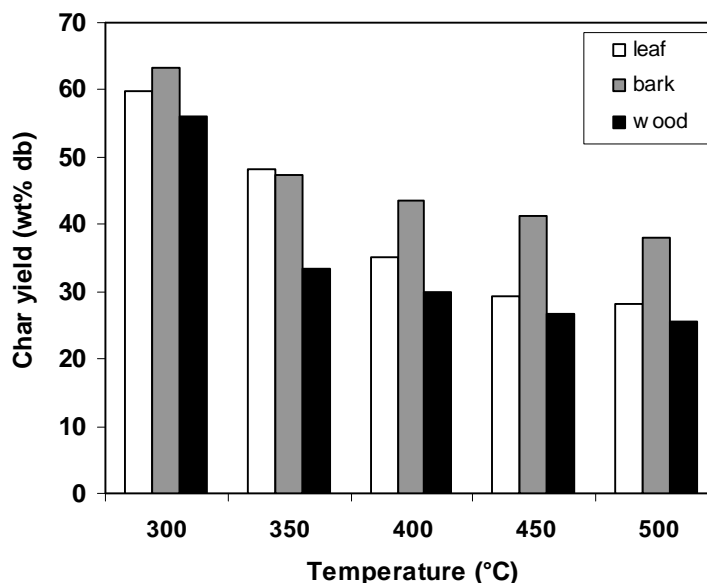


Figure 5-1 Biochar yield of mallee partitions in a fixed-bed reactor at various temperatures. (Legends: LC, biochar prepared from leaf component; BC, biochar prepared from bark component; WC, biochar prepared from wood component)

Table 5-2 Proximate and ultimate analysis of biochars

Biochar	Proximate analysis (% ar)				Ultimate analysis (% daf)				
	M	Ash	FC	VM	C	H	N	S	O ^a
Leaf Component									
LC300	3.4	6.5	28.8	61.3	64.2	5.8	1.62	0.07	28.3
LC400	4.2	10.3	51.4	34.1	65.4	3.8	1.84	0.02	28.9
LC500	4.2	11.9	63.3	20.6	70.2	2.5	2.09	0.08	25.1
Bark Component									
BC300	5.2	10.6	31.4	52.8	51.4	4.1	0.46	0.02	44.0
BC400	5.8	13.9	45.3	35.0	55.3	2.9	0.47	0.01	41.3
BC500	3.3	17.9	52.9	25.9	61.1	2.1	0.56	0.06	36.2
Wood Component ^b									
WC300	4.6	0.7	35.3	59.5	60.3	5.3	0.18	0.02	34.1
WC400	4.5	1.2	69.9	24.4	79.1	3.7	0.29	0.04	16.8
WC500	4.5	1.3	79.8	14.4	85.5	3.0	0.34	0.03	11.1

^a by difference, ^b data taken from Chapter 4

All biochar have low moisture content (~ 3-6%), which is desired in thermochemical processes. The oxygen and volatiles in biochars decrease with increasing pyrolysis temperature; however there is no significant difference of all biomass components. A combination of high oxygen and volatiles content could potentially enhance the release of inorganic vapours during combustion.⁶⁵ As mentioned previously, N and S content in leaf are higher than bark and wood. For leaf biochars obtained at 300, 400 and 500°C, N content in the leaf biochars increased significantly with pyrolysis temperature. Sulphur contents in all biochars are typically low. As a rule of thumb,¹⁵² sulphur-related emission problems are not expected to be an issue when the sulphur content in the fuel is less than 0.2 wt% db, which is indeed the case for the biochars produced from all biomass components.

5.3.3 Significant Differences in Biochar Grindability

After 4 minutes grinding, the particle size distributions (PSDs) for selected ground biochars are shown in Figure 5-2. Generally, the grindability of all of the biochars is increased with pyrolysis temperature. In Figure 5-2, BC300 followed a similar trend with wood biochars (see discussion in Chapter 4). The volumetric percentage of particle size < 50 µm obtained from ground BC300, BC400 and BC500 were a few time higher than WC300, WC500 and WC500 which indicated that bark biochars were easier to grind than wood biochars. Almost all particles in the ground biochars of bark and wood components fall between 0.5 to 1000 µm in volumetric size. However, leaf biochars behaved differently during grinding. By sieving, the total percentage of ground LC300 < 1.8 mm size is ~69% (similar with ground dried leaves), compared to 100% for ground BC300 and WC300. In Figure 5-2, the PSD curves of ground leaf biochars typically have distinct multiple peaks, in comparison to overlapping curves of bark and wood biochars giving ground BC and WC a more even particle size distributions. For example, the PSD curve of LC400 biochar shows two peaks: one in the size range of 0.5-500 µm and the other is in the size range of >500 µm. A similar 'tail' also appears even in the PSD curves of the ground LC500 and LC800 biochars. The data suggested that leaf contain special structures which are hard to grind.

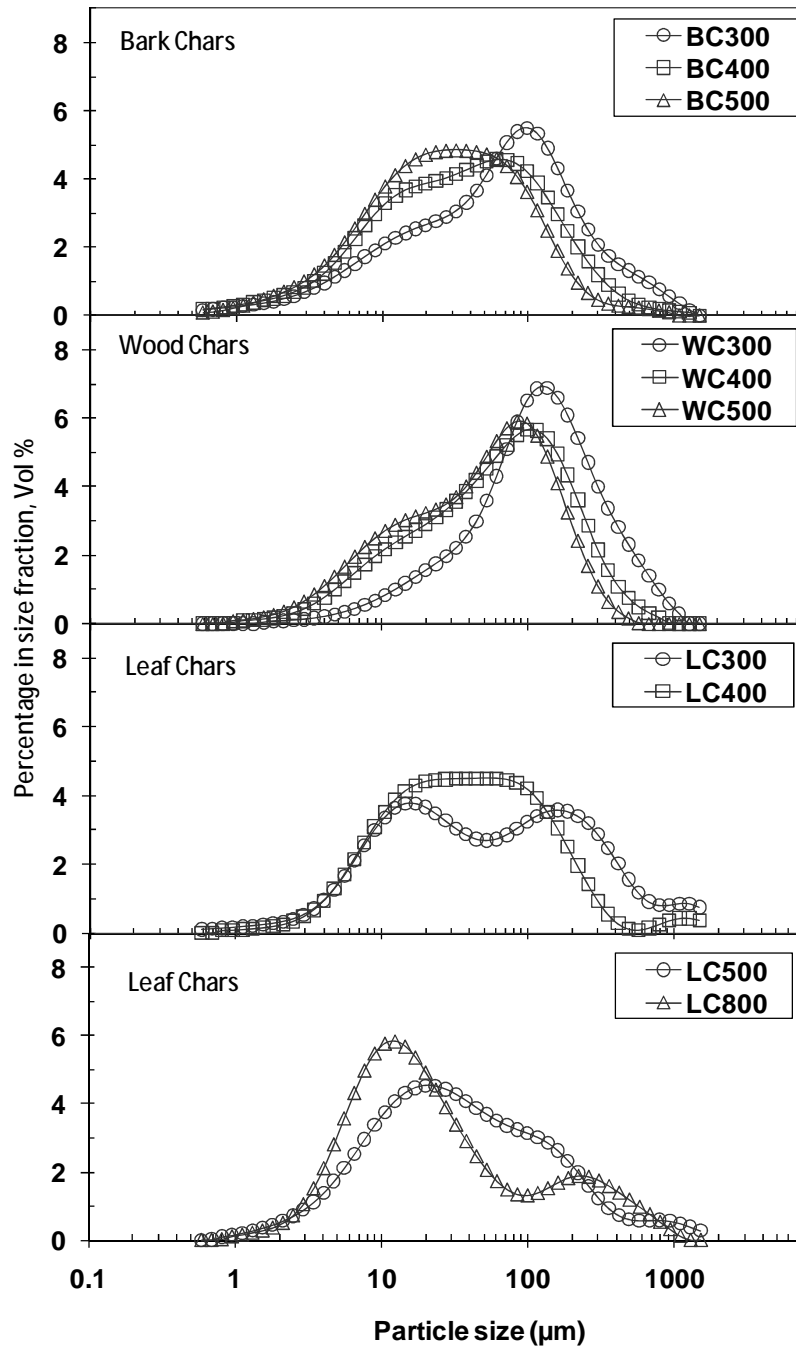


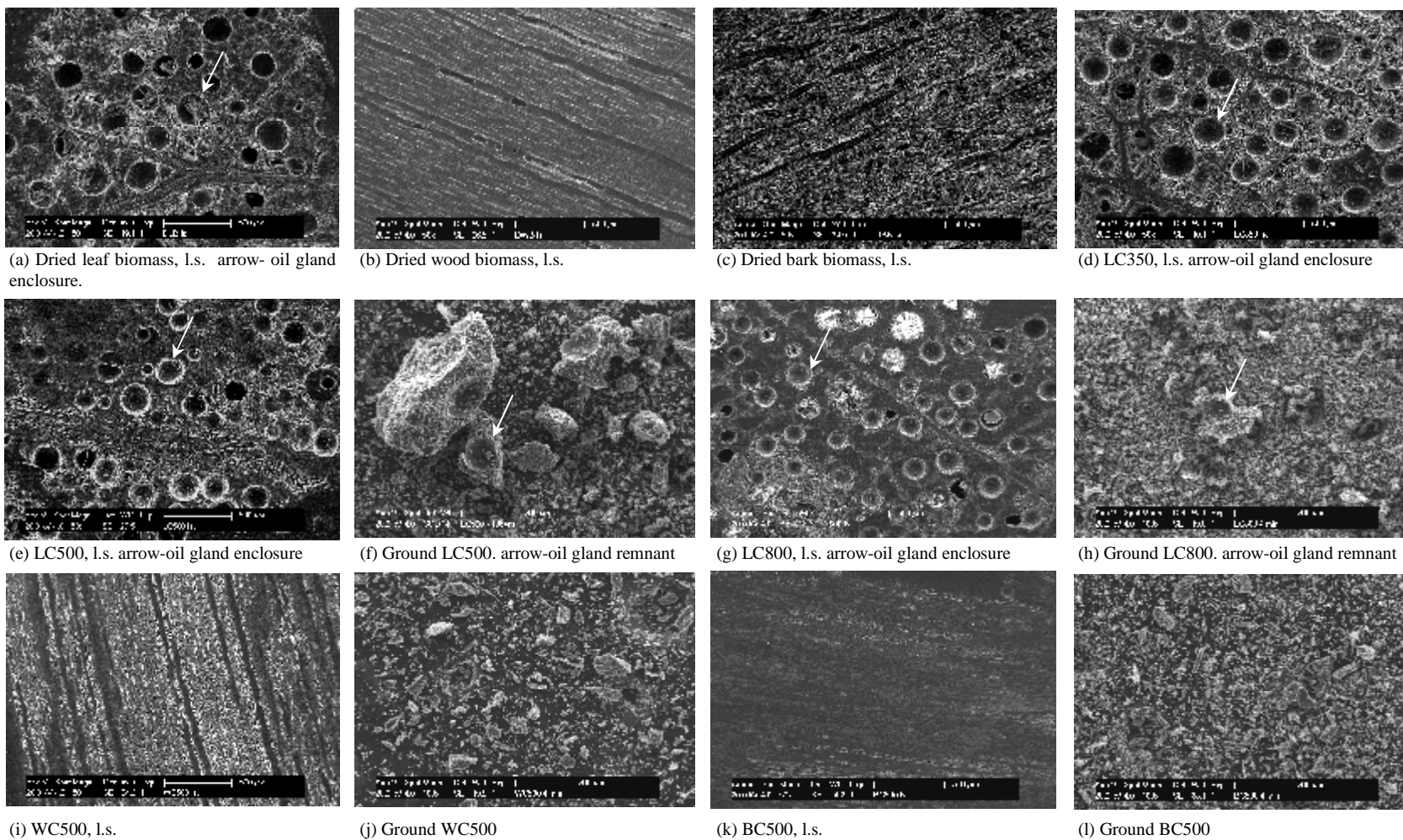
Figure 5-2 Particle size distributions (PSDs) of selected ground biochars. (Legends: LC, biochar prepared from leaf component; BC, biochar prepared from bark component; WC, biochar prepared from wood component)

5.3.4 SEM Imaging

Further efforts were then taken to examine the microstructure of biomass and biochars using SEM and the images are shown in part a to l of Figure 5-3. The SEM images in Figure 5-3 clearly shown the abundance of oil glands in mallee leaf. It is known that *E. polybractea* (blue mallee) leaf has relatively high density of oil glands,¹⁵³ ranging from ~260 to 500 glands/cm² (i.e. around 3000 to 3260 glands per leaf). It was also found that the oil gland's diameter is positively correlated with leaf age.¹⁵³ As shown in the image of longitudinal section (l.s.) of dried leaf (Figure 5-3 a), oil glands in the leaf of this study are scattered enclosures ~ 200-250 μm in diameter. Part d-h of Figure 5-3 clearly demonstrated the presence of large fragments of oil glands in the ground leaf biochars at all temperatures, suggesting that the oil gland structures are strong and proved to survive thermal degradation at 350°C, 500°C even as high as 800°C.

When subjected to milling, the presence of tough oil glands in leaf is the main reason of the observed poor grindability of leaf biochars. For example, large fragments of oil gland walls are the sources of large particles (>100μm) in the ground leaf chars, (e.g. LC500 sample, see part f of Figure 5-3). Such SEM observation is consistent with the observed 'tail' in the PSD curves of leaf biochars, as shown in Figure 5-2, although an absolute conclusion cannot be withdrawn because the particle size determination mentioned in Section 5.3.3 was based on volumetric size (i.e. irregularly shaped particles were measured and converted into its equivalent sphere volumes) compared to SEM imaging, which is of an area-based size.

The data in Figure 5-2 and SEM images in Figure 5-3 clearly demonstrated that the biological structure of the parent biomass plays a key role in the grindability of the biochars prepared from the pyrolysis of this biomass. In the case of leaf chars, a possible key limiting factor of grindability is the abundance of oil glands present in the leaf and heterogeneity of its cellular structures. Besides oils glands, the leaf is formed by epithelium, spongy mesophyll cells, and vascular bundles.⁵⁴ Mallee wood biomass (see Figure 5-3 b) clearly showed its anisotropic and fibrous nature. Dried bark was observed as loosely packed fabric cells (Figure 5-3 c).



(a) Dried leaf biomass, l.s. arrow- oil gland enclosure.

(b) Dried wood biomass, l.s.

(c) Dried bark biomass, l.s.

(d) LC350, l.s. arrow-oil gland enclosure

(e) LC500, l.s. arrow-oil gland enclosure

(f) Ground LC500. arrow-oil gland remnant

(g) LC800, l.s. arrow-oil gland enclosure

(h) Ground LC800. arrow-oil gland remnant

(i) WC500, l.s.

(j) Ground WC500

(k) BC500, l.s.

(l) Ground BC500

Figure 5-3 Images of unground and ground fuel samples. (Legends: LC, biochar prepared from leaf component; BC, biochar prepared from bark component; WC, biochar prepared from wood component)

Biologically, wood components of a tree comprised mainly of dead hollow vascular tissue whose major function is to transport water and minerals to the upper part of the tree. Bark contains cork cells, which is a spongy hydrophobic material that protects the tree.⁵⁴ Unlike leaf biochars, bark and wood biochars seems to have a more homogenous appearance. In this set of experiments, the distinct structural differences among leaves, bark and wood, either biological or chemical, are believed to contribute towards the general difference in grindability, because biomass components may differ not only of cellular organisation but cell wall compositions. Comparing intact bark/wood biochars with their parent biomass (see Figures 5-3 b, 5-3 c as well as Figures 5-3 i and 5-3 k), cell boundaries of biochars (especially BC500) are no longer clearly visible, which suggests severe thermal degradation of biomass after slow pyrolysis. Grinding of BC500 and WC500 resulted in small and more even size particles (see Figure 5-3 j and 5-3 l).

However, in LC500 and LC800 char samples (Figure 5-3 e and 5-3 g), the oil glands enclosure seems to remain intact after thermal treatment which later significantly affected leaf biochars grindability as mentioned previously. The grindability data and SEM observation of leaf, bark and wood biochars are valuable to predict how whole mallee biochar may behave during milling. Wood biochars with its high grindability is desirable to give good fuel handling characteristics and reduce milling energy (see discussion in Chapter 4). The data in Figures 5-2 shows that grindability of bark is similar to that of wood. As in a fuel processing unit, biochar will be subjected to milling and cutting as a crucial step to reduce its size.¹⁶ The size reduction problems including high milling energy/cost and low bulk/volumetric density are likely be imposed by leaf due to the presence of dense and tough oil glands in leaf and structural heterogeneity.

5.3.5 Differences in Biochar Energy Densities

Figure 5-4 presented the bulk and volumetric density of the biochars before and after grinding for 4 minutes. In Figure 5-4, the bulk density of fuels before grinding (0 min) indicated that slow pyrolysis of leaf and wood biomass actually produced biochars with lower bulk density compared to dried biomass. Bulk densities of bark biochar are only slightly higher than bark biomass. This indicated that in spite of

significant mass loss occurred during pyrolysis, there are little changes in particle size and shape.

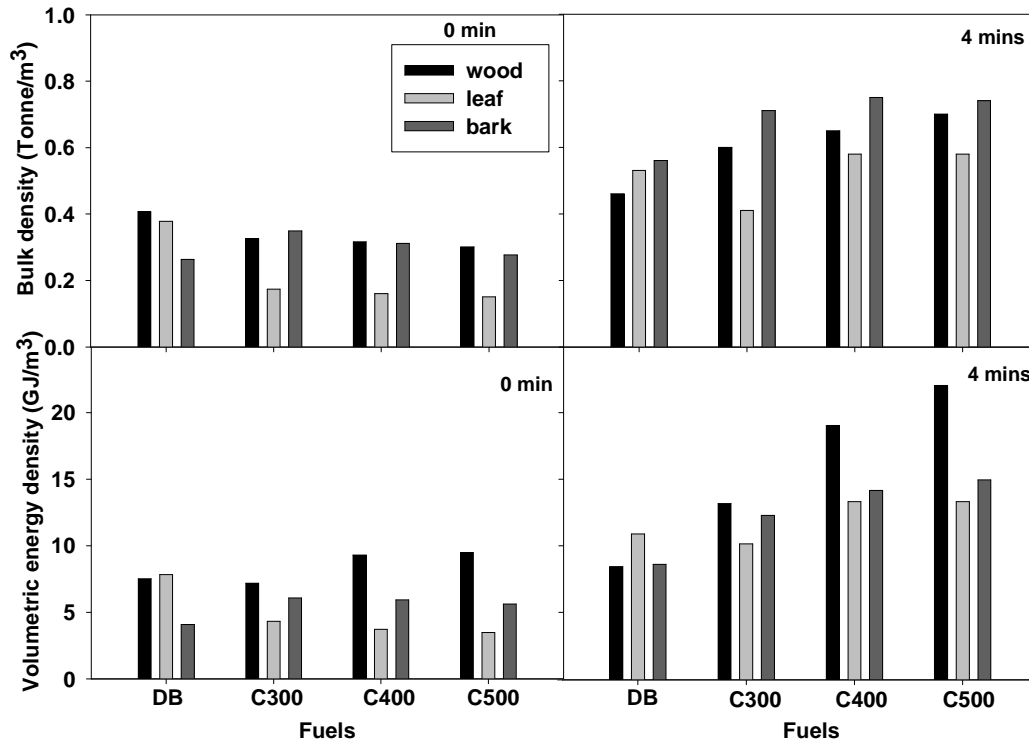


Figure 5-4 Bulk density and volumetric energy density of various fuels. (Legend: DB, dried biomass, and Cxxx, biochar prepared at xxx°C)

After 4 minutes grinding, all fuels have improved bulk density. With the exception of leaf biochars, bulk density of ground bark and wood biochars have increased substantially after grinding. The similar trend in bulk density of the bark and wood biochars is consistent with that in the grindability in the bark and wood biochars (see discussion in Section 5.3.3). Largely attributed to the oil glands remnants, the bulk densities of the leaf chars are only slightly higher or even lower (e.g. LC300) than that of the dried leaf.

The significant difference in the compositions, heating value and grindability after pyrolysis lead to significant differences in the volumetric energy density of biochars prepared from bark, wood and leaf. As shown in Figure 5-4, the unground wood

biochars (0 min) obtained at 300, 400 and 500°C have the highest volumetric energy density among all fuels. The unground bark biochars also have a slight higher volumetric energy density of the dried bark biomass. Besides fuel chemistry, ash contents and grindability are the other two key factors which can significantly influence the volumetric energy density of a biochar after grinding (see Figure 5-4 d). Due to the ash content is negatively correlates to heating value,⁸³ one would expect that bark biochars would have the lowest energy density compared to wood biochars and leaf biochars. However, as results of the excellent grindability of bark biochars, the volumetric energy density of bark biochars are actually higher than leaf biochars. For example, BC500 has a volumetric energy density of $\sim 15 \text{ GJ/m}^3$, in comparison to $\sim 14 \text{ GJ/m}^3$ of LC500 and $\sim 22 \text{ GJ/m}^3$ of WC500.

It is interesting to note that in Figure 5-4, unground dried leaf has the highest volumetric energy density among the raw components. Dried leaf biomass contains eucalyptus oil⁷⁶ which contributes to its high gross heating value. During pyrolysis, volatilisation of extractives proceeds as temperature increases. As mentioned in Section 5.3.3, the grindability of LC300 has not improved much, while mass loss proceeds at this low temperature, therefore resulting in a reduction of the bulk and volumetric energy densities of LC300 in comparison to that of the ground dried leaves. There is only a slight increase in the volumetric energy density of leaf biochars until the pyrolysis temperature increases to 400°C, suggesting that the poor grindability limits the potential of leaf biochars for energy densification via grinding. Certainly, such limitations may also have significant implication to the design of transport, storage facilities and the overall supply chain of these fuels.

5.3.6 Differences in Biochar Ash Properties

The key inorganic species in dried biomass and biochars are presented in Table 5-3. Bark biomass and biochars have the highest calcium content among all fuels samples analysed. Leaf biomass and biochars have high contents of K and Na while wood biomass and biochars have low contents of ash and AAEM species.

Table 5-3 Contents (wt% db) of inorganic species, including AAEM species in fuel samples

Samples	Inorganic Species (wt% db)							
	Ca	K	Mg	Na	Si	Al	Fe	P
DWB	0.104	0.090	0.041	0.012	0.0027	0.0021	0.0018	0.0138
DLB	1.152	0.438	0.113	0.452	0.1037	0.0464	0.0226	0.1247
DBB	4.010	0.258	0.220	0.125	0.0335	0.0087	0.0090	0.0310
WC300	0.178	0.158	0.071	0.023	0.0031	0.0007	0.0012	0.0308
WC350	0.299	0.274	0.115	0.041	0.0015	0.0007	0.0015	0.0460
WC400	0.363	0.333	0.145	0.055	0.0027	0.0012	0.0021	0.0545
WC450	0.328	0.356	0.150	0.047	0.0022	0.0011	0.0021	0.0547
WC500	0.421	0.370	0.164	0.056	0.0023	0.0016	0.0043	0.0623
LC300	1.933	0.733	0.188	0.752	0.1389	0.0711	0.0317	0.1777
LC350	2.154	0.875	0.236	0.875	0.1885	0.0875	0.0377	0.2222
LC400	3.412	1.267	0.331	1.365	0.2340	0.1170	0.0517	0.3022
LC450	3.367	1.638	0.419	1.456	0.2639	0.1456	0.0637	0.4095
LC500	3.907	1.474	0.403	1.596	0.2773	0.1447	0.0639	0.3496
BC300	6.326	0.423	0.374	0.194	0.0241	0.0085	0.0092	0.0413
BC350	7.935	0.529	0.463	0.248	0.0193	0.0106	0.0098	0.0546
BC400	7.938	0.582	0.484	0.308	0.0277	0.0104	0.0135	0.0588
BC450	8.599	0.609	0.537	0.287	0.0502	0.0107	0.0107	0.0681
BC500	10.527	0.732	0.595	0.325	0.0300	0.0150	0.0148	0.0731

Figure 5-5 showed retentions of Ca, K, Mg and Na at all pyrolysis temperature are ~100%, suggesting all AAEM species in the biomass are retained in the biochars after pyrolysis. This is expected under the pyrolysis conditions in this study, which used large biomass particles and a slow-heating rate.

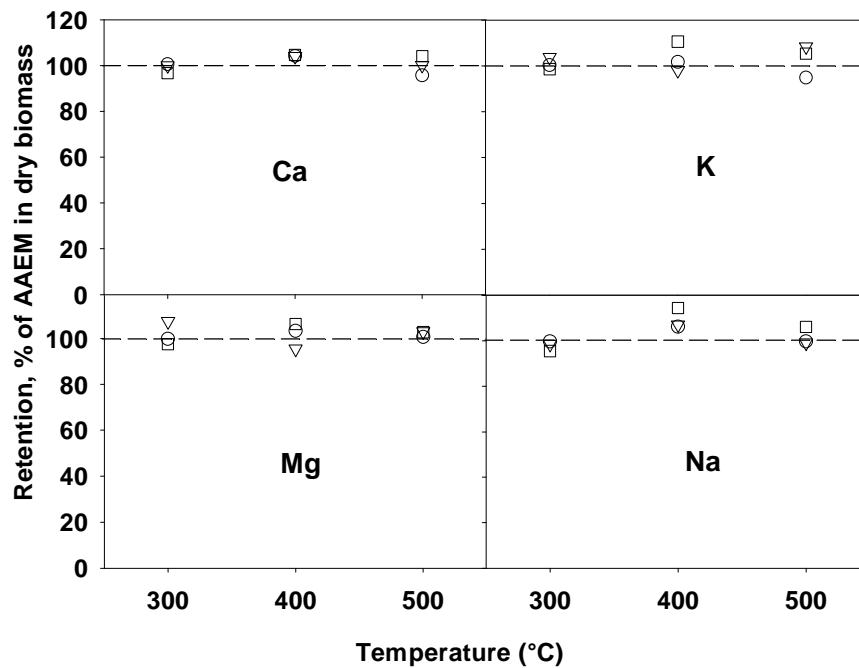


Figure 5-5 Retention of AAEM species in (○) leaf biochar, (□) wood biochar, and (▽) bark biochar as a function of pyrolysis temperature

Several indices (Table 5-4) have been developed for relating fuel chemistry to propensity of ash fouling and slagging. It has been suggested that indices used in combustion study (e.g. alkali indices) must be determined directly from the fuel sample instead of calculating backward from elemental analysis of ash as the latter technique is prone to error.¹⁵⁴ Based on our data in Figure 5-5, relevant to the present scope of work, the ratios of Si/K and Ca/K are considered and of interest to evaluate the slagging propensities of mallee biochars as fuels. Thermodynamically, formation of Ca-silicates is more favoured than of Mg-silicates and K-silicates.¹⁵⁵ Because the melting point of Si-oxides and Ca-silicates are much higher than K-carbonate and chloride, fuels with higher Si/K and Ca/K ratios generally have a low propensity of slagging and fouling during combustion. Therefore, the ratios of Si/K and Ca/K for leaf, bark and wood biochars are presented in Figure 5-6.

Table 5-4 Indices in applications of biomass for fuel generation

Indications	Indices	Computation and unit	Threshold value
Fouling, slagging behaviour, biomass combustion properties ⁶⁵	Alkali index	$(1/Q)Y_f^a(YK_2O^a + YNa_2O^a)$ kg alkali GJ ⁻¹ or lb alkali MMBtu ⁻¹ Q = heating value of fuel Y _f ^a = mass fraction of ash in fuel YK ₂ O ^a + YNa ₂ O ^a = mass fractions of K ₂ O and Na ₂ O in ash	>0.17 kg alkali GJ ⁻¹ (0.4 lb alkali MMBtu ⁻¹) -fouling is probable > 0.34 kg alkali GJ ⁻¹ (0.8 lb MMBtu ⁻¹)-fouling is certain
Potential fraction of alkali could be reacted as chloride and sulphate by Cl and S from fuel, biomass combustion properties ⁶⁵	Stoichiometric ratios of Cl and S to K and Na in fuels	$(Cl + 2S)/(K+Na)$ molar	Ratio value of 1 or above– sufficient Cl and S in fuel to completely react with the alkali Ratio value below 1 – excess of alkali
Fouling tendency of fuel ash, biomass combustion properties ⁶⁵	Base- to-acid ratio (R _{b/a})	$(Fe_2O_3 + CaO + MgO + K_2O + Na_2O) / (SiO_2 + TiO_2 + Al_2O_3)$ label for each compound = its weight concentration in ash dimensionless	For coal, minimum R _{b/a} = 0.75 For biomass, minimum R _{b/a} tends to appear at < 0.75
Slagging tendency, energy crops quality ^{17,79}	Ratios between K, Ca and Si	dimensionless Si/K and Ca/K	High Si/K or Ca/K - lower slagging tendency
Slagging reasons in stemwood pellets combustion ¹⁵⁶	Compositions of Si, Al and Fe oxides of fuel ash	dimensionless Weight concentration of SiO ₂ , Al ₂ O ₃ and Fe ₂ O ₃ of fuel ash Weight % of fuel ash	~20-25 wt% SiO ₂ , ~ 4-5 wt% Al ₂ O ₃ and Fe ₂ O ₃ of fuel ash – slag/deposits formed

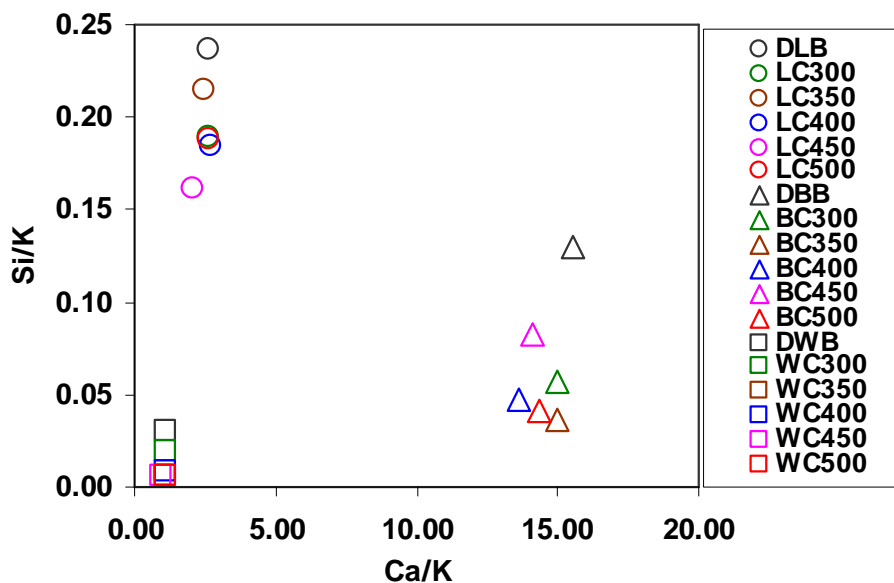


Figure 5-6 Relationship between fuel Si/K and Ca/K ratios. LCxxx-biochar prepared from dried leaf biomass at xxx °C; BCxxx-biochar prepared from dried bark biomass at xxx °C; WCxxx-biochar prepared from dried leaf biomass at xxx °C. DLB-dried leaf biomass; DBB- dried bark biomass; DWB- dried wood biomass

It is interesting to see that leaf, bark and wood biochars as fuels could be placed into three distinct groups in terms of ash properties, i.e. wood or wood biochars has low Si/K and Ca/K ratios; bark and bark biochars have a high Ca/K ratio but a low Si/K ratio; and the leaf and leaf biochars have high Si/K and Ca/K ratios. Therefore, biochars produced from the wood biomass component seem to have a high slagging propensity, followed by bark biochars and leaf biochars.

5.4. Conclusions

This chapter reports the significant differences in the fuel quality and ash properties of biochars produced from the slow pyrolysis of various mallee biomass components. This enables the potential biomass components which may cause problems in downstream utilisation of whole mallee biomass. Compared to the parent biomass components, it is obvious that biochars of all mallee components as fuels have better fuel qualities, such as low moisture, good grindability and high energy density. There are significant differences in the grindability of different biochars. Leaf biochars

have the poorest grindability among all biochars, due to the presence of abundant tough oil glands in leaf. Even at a pyrolysis temperature of 800°C, after grinding, the oil gland enclosures remained intact. There are also significant differences in ash properties of biochars as fuels. Wood biochars have low Si/K and Ca/K ratios hence may have a high propensity of slagging in comparison to bark and leaf biochars. Therefore, in using the bulk biochar of the whole mallee biomass, grinding problem is more likely to arise from leaf fraction while ash related problems could be more likely to be due to the wood and bark components.

CHAPTER 6

FUEL AND RHEOLOGICAL PROPERTIES OF BIOSLURRY PREPARED FROM THE BIO- OIL AND BIOCHAR OF MALLEE BIOMASS FAST PYROLYSIS

6.1 Introduction

Previous investigations were conducted on using biomass directly to prepare biomass-based slurry fuels (see those included in Table 6-1). However, for bioslurry fuels prepared from bio-oil and biochar from biomass fast pyrolysis, little technical information can be found in the literature, although the concept was attempted by commercial developers (e.g. “BioOil Plus” from Dynomotive¹²⁶ and “Bioliq” from Karlsruhe¹²⁵). For mallee biomass, so far no work has been conducted on the production and properties of bioslurry from this abundant biomass in WA. Based on the requirements of slurry fuels as listed in Tables 2-6 and 6-1, developments of bioslurry fuels from mallee bio-oil/char components will be more likely targeted for boilers and gasifiers systems since the characteristics of bio-oil and biochar individually are suitable for these applications.

This study focuses on investigating the key fuel properties of bioslurry fuels prepared from bio-oil and biochar of mallee biomass fast pyrolysis as outlined in the third thesis objective in Chapter 2. The main objectives are to produce bioslurry fuels with not only good fuel properties but also stable at optimum biochar loading, with desirable rheological behaviour. Besides the characterisation of fuel properties and stability, temperature and time-dependent steady rheological measurements were conducted at room and elevated temperatures. Other important aspects, such as inorganic species in bioslurry fuels, were also measured and benchmarked against the specifications of slurry fuels for combustion and gasification applications.

Table 6-1 Summary of reviews in recent developments of biomass-derived slurry fuels

Reference	Type of slurry fuel	Preparation and study	Slurry fluid behaviour	Key findings
Al-Amrousi et al. ¹⁵⁷	fuel oil-water-charcoal emulsion.	charcoal derived from camphor. Effect of surfactants: anionic (dodecylbenzenesulfonic acid sodium salt), non ionic (dodecylphenol ethoxylate) on slurry stability, viscosity and corrosion inhibition.	emulsion viscosity increased with increased of charcoal content, viscosity decreased with increased of water content.	stable emulsion obtained at 15-20 wt% charcoal with 15-20 wt% water and 65 wt % fuel oil, slurry calorific value between 31-42 GJ/Tonne, non anionic surfactants showed higher efficiency of stabilizing properties and corrosion inhibition in steel tanker.
Benter et al. ¹²⁷	biomass-diesel-kerosene slurry	mixture of diesel, kerosene and ground <i>Pinus radiata</i> wood: preparation of slurry in uncontrolled temperature (min 15°C, max 25°C), effect of addition of non anionic surfactant (Sapogenat T-080/ T-139 and castor-oil based thickener (Rheocin) on slurry stability and viscosity.	all slurries showed pseudoplastic behaviour.	adding ethanol and water (15-20 wt %) with 20 wt % wood loading produce stable suspension for more than 30 days, similar effect with addition of Rheocin. Slurry with smaller wood mean particle diameter (35 µm) showed increase sedimentation stability than large particle (68 µm mean diameter).
Natarajan et al. ¹⁵⁸	corn starch-water slurry (CSWS)	effect of corn starch concentration and thickener (polyacrylic acid) on slurry stability, rheology and viscosity.	a minimum viscosity observed at 45°C due to swelling of biomass. Beyond 60°C, slurry gelled	slurry with 0.15% polyacrylic acid and 40% corn starch have favourable rheological property for injection and pumping. Slurry with ≥ 0.15% polyacrylic acid is stable on storage for 2 months.
Henrich and Weirich ¹²⁵	bio-oil/biochar slurry	test performance of gasification of bioslurry in Pressurised Entrained Flow Gasifier. Bioslurry produced using 2 steps method: fast pyrolysis of straw at 500°C to produce bio-oil and char, char and bio-oil are then mixed as bioslurry.	viscosity decreased with increasing char particle size	energy content in slurry up to 90% of the biomass energy. The two steps process of bioslurry production is feasible for dry herbaceous biomass, maximum char size 0.3 mm, stable slurry with 25 wt% char loading was prepared from beechwood pyrolysis.

Raju et al. ¹⁵⁹	biomass-water slurry	synthesis of transportation fuel from biomass (agricultural waste) -water slurry.	pumpable slurry at 40 and 60 wt% biomass in water.	improvement of slurry production by mixing of water and biomass are at low temperature ~200°C under nitrogen (150 psi). Slurry contained 60% solid or 38% carbon by weight.
He et al. ¹⁶⁰	biomass-water slurry	coal-water slurries, biomass water slurries and commingled biomass and coal water slurries: rheological properties, effect of hydrothermal process to increase solid loading.	larger particle size slurries have better pumpability. Slurry pumpability decreases with increase concentrations of biomass.	hydrothermal process increase solid loading to 35% of biomass water-slurry and to 45 % solid loading in commingled slurries with viscosity less than 700mPa.s.
Li et al. ¹⁶¹	algae-coal-water slurry	preparation of coal slurry with algae: pre-treatment method to reduce viscosity of algae, rheological properties, gasification characteristics.	slurry exhibits pseudoplastic behaviour and shear thinning.	pre-treatment method: anaerobic fermentation, chemical treatment, high speed shearing and heating result to decrease algae viscosity and increase algae solid loading. Max solid loading 62.5 wt%, stability higher than coal-water slurry. Algae slurry promote gasification rate.

6.2 Methodology

6.2.1 Preparation of Bioslurry

The bio-oil and biochar for preparing the bioslurry samples were freshly produced from the fast pyrolysis of mallee wood of species *Eucalyptus loxophleba* (spp *lissophloia*) according to method described in Section 3.3.2-2, Chapter 3. To prepare the bioslurry, the biochar was first ground in a laboratory ball mill (see Section 3.4.2) and the biochar particle size distribution was determined using a laser-based particle size analyser using method in Section 3.4.4. The optimum particle size of the biochar is investigated at various grinding time i.e. 2, 6, 8, 10 and 20 minutes. The surface area, apparent density and soakability of ground biochar were determined according to descriptions in Section 3.4.8 (Chapter 3).

A series of bioslurry fuels were prepared by suspending various mass concentrations of fine biochar particles into whole bio-oil (see Section 3.4.9-1). Based on the present fast pyrolysis yields of bio-oil (61% db) and biochar (14% db), bioslurry with various char loading ranging from 8 to 20 wt% were prepared. The slurries were stirred and kept in closed plastic vials to avoid vaporizations or sample loss. Bulk density and static stability of bioslurry were measured using method explained in Sections 3.4.3 and 3.4.13. The calorific value of slurry is the summation of the bio-oil and biochar equivalent low heat value (LHV, GJ/Tonne). Inorganic species in biochar, bio-oil and the resulted bioslurry fuels were measured using a wet oxidation method and ICP-AES (Section 3.4.7)

6.3 Results and Discussion

The rheological properties of bioslurry were characterised using a Haake Mars II rheometer equipped with a Z20 cylinder sensor system (see Section 3.4.15). In this experiment, the changes of viscosity and shear stress as a function of shear rate at 25°C and 50°C were determined at maximum shear rate of 500s⁻¹ under steady measurement. The curve of shear stress versus shear rate were fitted by the Power Law $\tau = K\dot{\gamma}^n$, where τ is shear stress (Pa), $\dot{\gamma}$ is the shear rate (s⁻¹), K and n are rheological constants, referred to as the fluid consistency coefficient and flow behaviour index respectively. For $n = 1$, the equation reduces to Newton's law of

viscosity. Therefore departure of n from 1 indicates the degree of deviation from Newtonian behaviour. The behaviour is pseudo-plastic for $n < 1$ and dilatant for $n > 1$.¹⁶² To validate the effect of time-dependent /thixotropy behaviour of the bioslurry, a plot of shear stress versus shear rate was made as the shear rate was increased to a maximum of 300 s^{-1} , then hold at this shear rate for 30s before decreased to the starting point. The thixotropy test was also measured at 25°C and 50°C . Fresh bioslurry samples were used for all measurements described in this experiment.

6.3.1 Properties of Ground Biochar for the Preparation of Bioslurry Fuels

The particle size distributions (PSD) of the biochar sample at various grinding times are shown in Figure 6-1. As mentioned in Table 2-6 (Chapter 2), the applications of coal slurry in boilers require coal particle size of $80\% < 74\text{-}75 \mu\text{m}$.^{109,110,115,163} Figure 6-1 shows that with the present laboratory ball mill, desirable size reduction of biochar can be achieved within an optimal grinding time of 8 mins. Increased grinding time up to 20 mins further reduced the size only slightly. For example, biochar ground after 8 mins has 88% of all particles with size $< 75\mu\text{m}$, in comparison to only slight increase to 92% after 20 mins grinding.

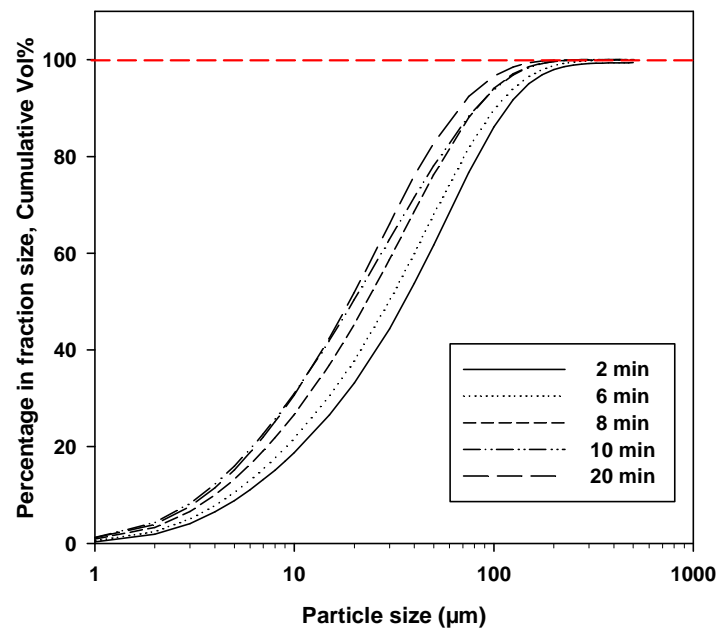


Figure 6-1 Particle size distributions of ground biochar at various grinding time

Since 8 mins grinding time produced biochar particle that met the requirement for boiler fuels, biochar powder obtained at this grinding time is used to prepare bioslurry throughout the study. The PSD of ground biochar at 8 mins is given in details in Figure 6-2. The PSD has 10, 50 and 90 % under size (D_{10} , D_{50} , D_{90}) of 3.94, 22.72 and 79.60 μm respectively. As shown in the previous investigation biochar clearly has excellent grindability in comparison to biomass (see Chapter 4 and 5). The excellent biochar grindability not only alleviates problems like fuel blockage and incomplete burnout but most importantly, the data showed that preparation of bioslurry from biochar is a better option than the slurry fuels prepared from biomass (e.g. biomass-water slurry fuels in a previous study ¹²⁷). The extensive energy requirement for grinding biomass to the required fine size dictated that biomass-water slurry fuels are not feasible

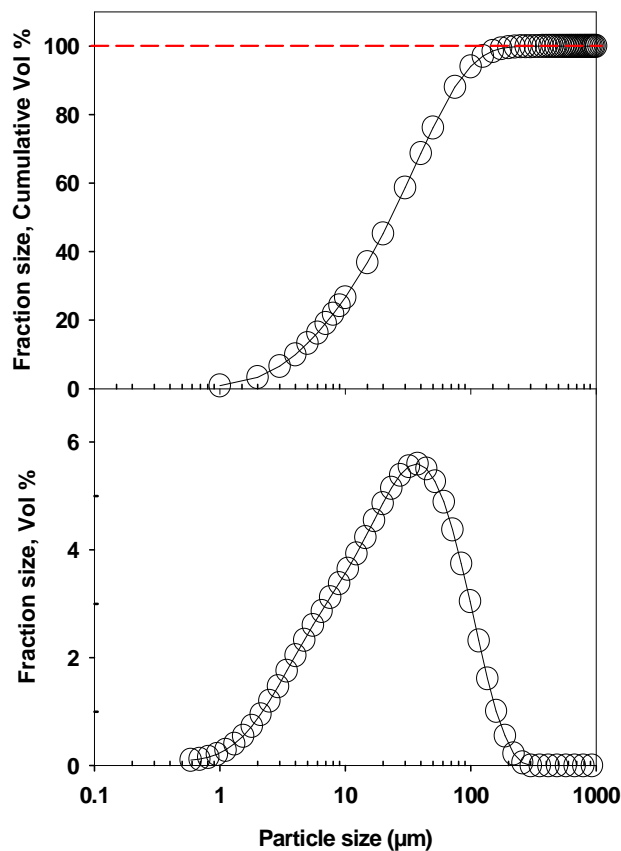


Figure 6-2 Particle size distributions of ground biochar at 8 mins grinding time

Biochar surface area measured using Dubinin-Astakhov method was 244 m²/g. It was also found that biochar porosity is primarily due to macropores (65%) and mesopores/transitional pores (35%). Volume in pores with radius greater than 1.00µm (macropores), radius between 0.01-1.00µm (mesopores) and radius smaller than 0.01µm (micropores) are 0.7312, 0.4007 and 0.0001 cc/g respectively, giving the total pore volume 1.1320 cc/g. The porosity of biochar suggests mallee biochar is a good candidate for slurry preparation since it was reported previously¹⁶⁴ that coals having about 35-55% of their total open pore in the transitional range are most suitable for adsorption of organic molecules from solution. After grinding, the biochar has an apparent density of 538 kg/m³. The experimental data show that the biochar soaked up to 1.4 times bio-oil of the biochar's weight at the maximum before sufficient interparticle lubrication was achieved to form flowing slurry, enabling significant volumetric energy densification.

6.3.2 Fuel Properties and Significant Energy Densification via the Preparation of Bioslurry

The ash content in biochar (Table 6-2) was much higher than bio-oil. This is expected as at the pyrolysis temperature (500°C), the majority of inorganic species in biomass were mostly retained in biochar during fast pyrolysis process.

Table 6-2 Ultimate and proximate analysis of biomass, biochar and bio-oil

Fuel	Proximate analysis (% ar)				Ultimate analysis (% daf)			
	MC	Ash	VM	FC	C	H	N	O*
biomass [^]	-	0.5	81.9	17.6	48.4	6.3	0.1	45.2
biochar	4.4	4.0	20.5	71.1	71.2	3.1	0.41	16.6
bio-oil ^{af}	21.1	0.03	Nd	Nd	40.9	7.2	0.13	51.7

[^]- dry base (data was taken from ref⁹⁹), nd- not determined, *- by difference.

It should be noted that there was ~0.4 wt% char fines entrained in bio-oil during the condensation process, contributing to the presence of ash in bio-oil. Compared to bio-oils reported previously (10-35 wt%, wet basis),^{121,128,165} the moisture content in the bio-oil in this study is ~21%, which itself is below the maximum water content (<32 wt%, see Table 2-6 Chapter 2) allowed for applications in engines. The nitrogen contents in the biochar and bio-oil are much lower than the limits for combustion in

boilers (Table 2-6 Chapter 2), and that of ultra clean coal (N content ~1.07 %) as reported previously.¹¹¹

Figure 6-3 showed the bulk and volumetric energy densities of bioslurry, along with bio-oil (denoted as 0 wt% char loading in the figure) and green chipped biomass (BM).

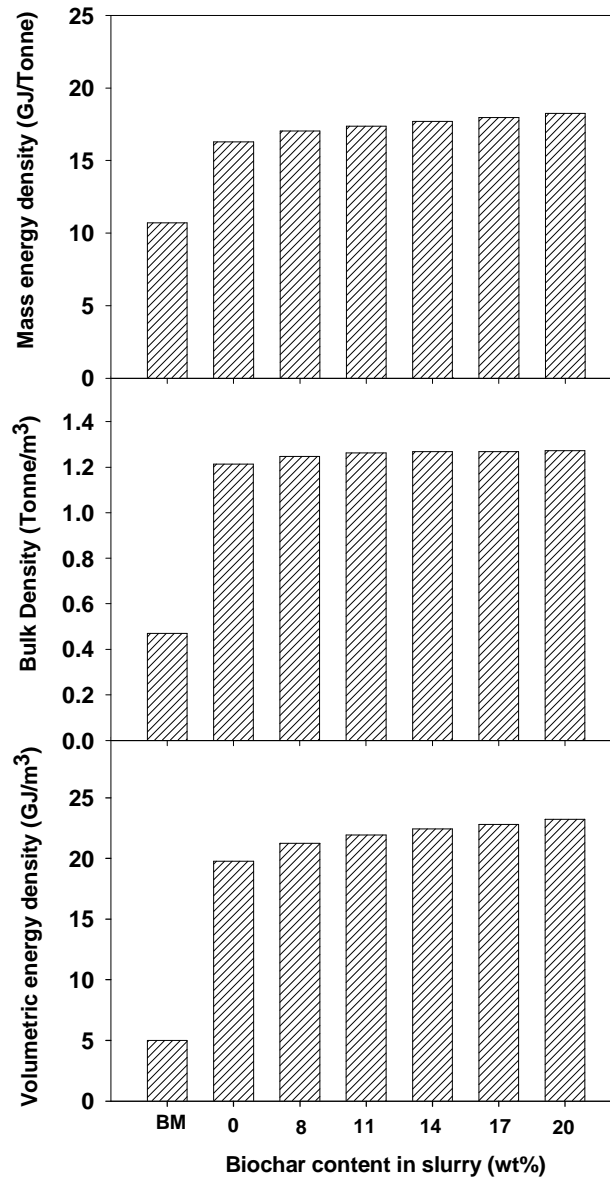


Figure 6-3 Mass energy, bulk and volumetric energy densities of fuels. BM- biomass

Obviously, bioslurry have higher bulk and energy densities than biomass and bio-oil. At 20 wt% biochar loading, the bioslurry has a bulk density of 1.27 Tonne/m³ and a volumetric energy density of ~23 GJ/m³, achieving significant volumetric energy densification from ~5 GJ/m³ of the green chipped biomass. Although there is only a slight increase in bulk density compared to bio-oil, the addition of biochar with a higher mass energy density has resulted in an increase in volumetric energy density of bioslurry being 14% (at 20% char loading) higher than bio-oil. The data have significant implications towards the cost reduction in fuel logistics (collection, handling, transport and storage). For example, a typical 20 MW straw-fired power station requires 150,000 wet tonnes/yr of biomass involving 40 road transport vehicle delivery per day. Biomass fuels with relatively higher bulk densities such as coppice requires 135,000 wet tonnes/yr biomass with around 50% lesser lorry movement.²¹ In case of mallee green biomass, the transport cost increase almost linearly as feedstock collection distance increase.²⁰ It was estimated that mallee green biomass transportation cost has increased from A\$32.0 gt⁻¹ at 10 km to almost doubled (A\$47.5gt⁻¹) at 100km and to A\$73.5gt⁻¹ at 250 km. Therefore, a much higher density bioslurry is expected to substantially reduce the transportation cost of mallee green biomass.

6.3.3 Inorganic Species in Bioslurry Fuels

Table 6-3 presents the contents of various inorganic species in biochar, bio-oil and selected bioslurry fuels. It can be seen that the inorganic elements in biochar and bio-oil are predominantly alkali and alkaline metallic (AAEM) species, i.e. calcium, potassium, magnesium and sodium. For bioslurry, the data are reported as both directly measured and estimated based on the percentage of biochar and bio-oil in the slurry. As expected, it can be seen in Table 6-3 that both the measured and estimated values are in good agreement. This suggests that the inorganic species in bioslurry fuels can be estimated directly from their initial concentrations in biochar and bio-oil.

It is known that one of the major issues for biomass combustion are ash-related problems associated with AAEM species which can form alkali sulphates, chlorides or alkali silicates.⁴⁵ The lower melting points (<700°C) of alkali sulphates and

silicates form deposits on the reactor wall and particles bed leading to bed sintering and defluidisation^{27,69}. The highly stable potassium chloride is one of the major causes of slagging and fouling problems in combustion.⁶⁵ To minimise the ash-related problems such as sintering, agglomeration, erosion, deposition and corrosion, it has been suggested¹⁵² that the contents of Ca, K and S in fuels need to be below accepted limits, i.e. <35 wt% for Ca and < 7.0 wt% (db) for K, as well as S <0.1 wt%(db) for sulphur related corrosion and <0.2 wt%(db) for SO_x emission.

Table 6-3 Elemental analysis of fuels

Element (wt% ar)	Fuels					
	bio-oil	biochar	bioslurry, 8 wt% biochar	bioslurry, 14 wt% biochar	bioslurry, 20 wt% biochar	
Ca	measured	0.0008	1.3429	0.1112	0.1952	0.2493
	estimated			0.1030	0.1906	0.2572
K	measured	0.0016	0.6661	0.0469	0.0878	0.1121
	estimated			0.0512	0.0938	0.1308
Mg	measured	0.0019	0.2893	0.0228	0.0437	0.0547
	estimated			0.0238	0.0420	0.0589
Na	measured	0.0045	0.2077	0.0182	0.0241	0.0258
	estimated			0.0200	0.0333	0.0448
Fe	measured	0.0006	0.0996	0.0081	0.0145	0.0167
	estimated			0.0081	0.0147	0.0163
P	measured	<0.0200	0.1181	0.0097	0.0176	0.0231
	estimated			0.0090	0.0170	0.0234
S	measured	0.0060	0.0313	0.0068	0.0096	0.0104
	estimated			0.0079	0.0096	0.0108

The data in Table 6-3 showed that the concentrations of these species in the bioslurry fuels prepared are all below the guideline limits, suggesting that the combustion of bioslurry will probably not go to impose significant ash-related problems associated with the species listed in Table 6-3. In fact, the S content in bio-oil, biochar and bioslurry are also very low compared to coals (ultra clean coal S~0.25%, Jincheng coal S~ 0.49 %) and sewage sludge (0.88%)¹¹¹ used to prepare other slurry fuels, a clearly advantageous in utilising bioslurry in state of the art combustion systems.

6.3.4 Bioslurry Static Stability

In the literature, various settling tests were conducted for characterising bioslurry stability. For example, it can be done via measuring the volume ratio of clear to sediment phase,^{127,166} or rod drop method¹¹¹ to determine the formation of sediment over time (usually in hours) and weight ratio of bottom part to top part after settling is allowed to occur for a certain period.^{116,162} Due to the dark brown colour nature of the bioslurry in this study, determining meniscus between clear and sediment layers was difficult. Rod drop method was found unreliable as the bioslurry tends to stick to the glass rod leading to loss of substantial amount of sample during measurement. Therefore, this study adapted a standard method for coal water slurry¹¹⁶ to assess bioslurry stability. The static stability of bioslurry at different biochar loading is presented in Figure 6-4.

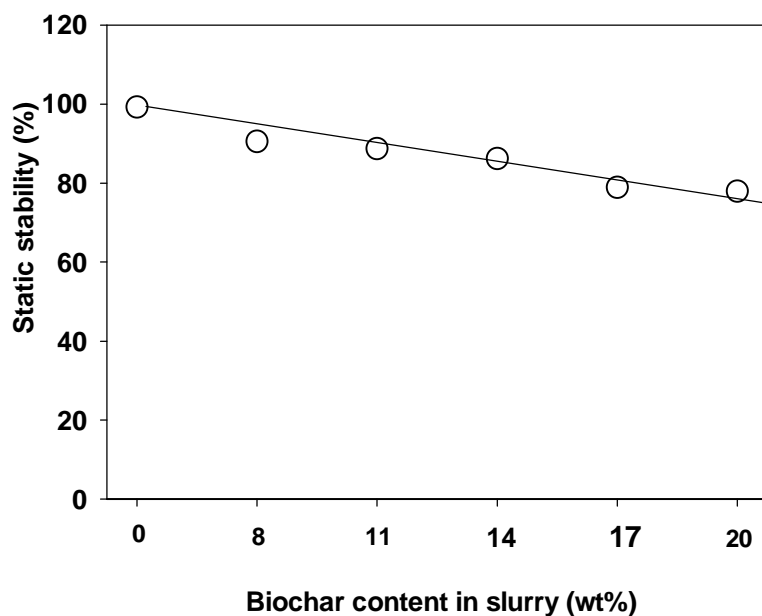


Figure 6-4 Static stability of fuels

The stability of bioslurry was found to decrease steadily with the increase of solid loading but all bioslurry samples have good stability (>70% as required for coal-water-slurry). It was also observed that the soft sediment settled at the bottom of the container can be easily mixed back with the liquid part by stirring. The static stability data has significant impact on process design and handling of bioslurry especially in

the aspect of continuous stirring requirement and/or the use of stabilizing agent to minimise settling.

6.3.5 Rheological Property of Bioslurry

The changes of shear stress and viscosity of the slurry as a function of shear rate are demonstrated in Figure 6-5. At 25°C, the bioslurry generally exhibits non-Newtonian behaviour especially for biochar loading 11-20 wt%. The shear thinning or pseudoplastic behaviour is characterised with the decrease of viscosity as the shear rate increase. This type of fluid behaviour is common in COM, CWS, coal-algae slurry, coal-sewage sludge slurry and to a certain extent coal-biomass slurries.^{110,112,115,160,162}

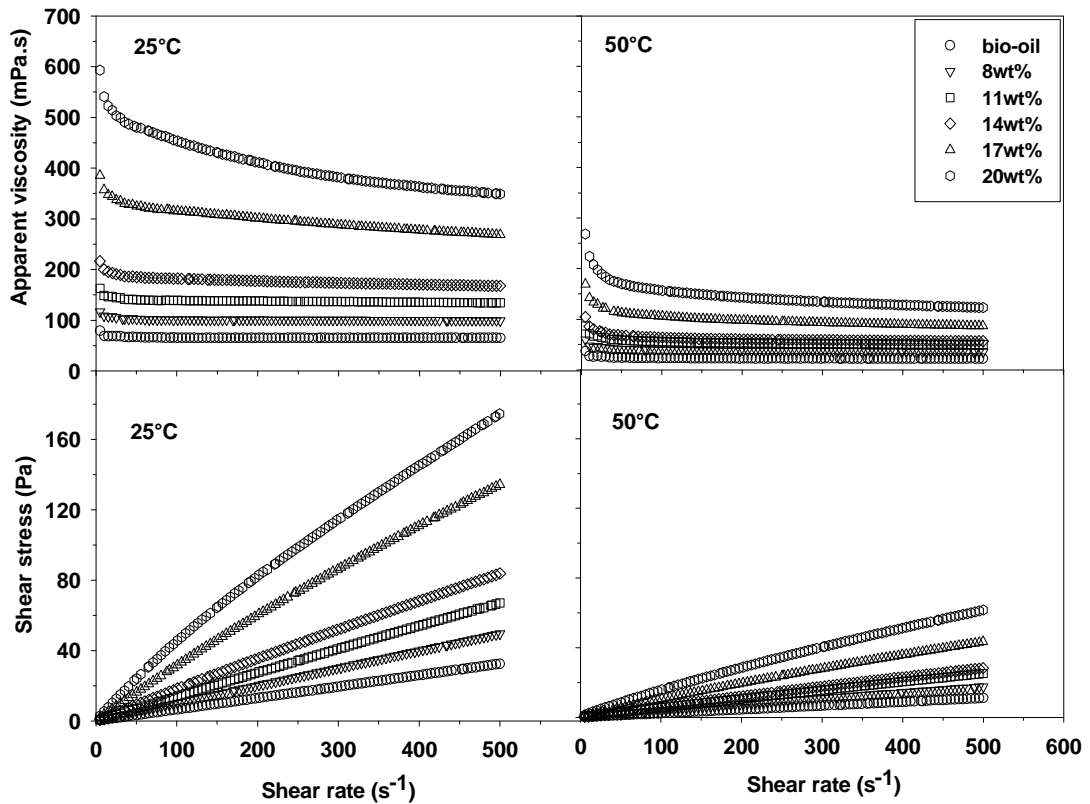


Figure 6-5 Shear stress and apparent viscosity of fuels as a function of shear rate

For bioslurry at 8 wt% concentration and bio-oil, slight shear thinning occurs at low shear rate (below 30s⁻¹) but the overall behaviour is predominantly Newtonian. A similar behaviour is also observed at 50°C. The data for shear stress dependent on

shear rate for non-Newtonian bioslurry (11-20 wt%) at 25°C were fitted with the Power Law equation as described in Section 6.2.1. The values of the flow behaviour index n for the slurry fuels are given in Table 6-4.

Table 6-4 Flow behaviour index, n of bioslurry (25°C)

Bioslurry	Biochar loading (wt%)			
	11	14	17	20
flow behaviour index, n	0.9746	0.9447	0.8913	0.8344

All of the n values are less than 1.00, indicating the bioslurry show pseudoplastic behaviour. With the increasing of biochar concentration, the n values become smaller, showing increasing deviation from Newtonian behaviour. The understanding of fluid behaviour for bioslurry is useful to predict bioslurry spraying and atomisation characteristics. For instance, the Sauter mean diameter (SMD) of a spray for Newtonian fluids increase as the viscosity increase. The SMD for non-Newtonian fluids however can be affected by the elasticity and shear thinning behaviour.¹⁶⁷ The high pressure accumulator-type injection system also requires pseudoplastic behaviour to produce desirable spray pattern.¹⁶⁸

The apparent viscosity for bioslurry obtained at shear rate 100s^{-1} measured at 25 and 50°C are presented in Figure 6-6. An earlier study suggested that the maximum viscosity for safe handling of CWS in boilers is $1000\text{ mPa}\cdot\text{s}$ at 100s^{-1} .¹¹² For a pressurised gasification reactor, the maximum viscosity is $\sim 700\text{ mPa}\cdot\text{s}$.¹⁶⁰ In Figure 6-6, the maximal viscosity is $\sim 453\text{ mPa}\cdot\text{s}$ for the highest concentration of biochar (20 wt%) at 25°C. At 50°C, the viscosity is reduced to $\sim 300\text{ mPa}\cdot\text{s}$. This data indicated that bioslurry can be easily pumped at 25°C and elevated temperature in both boilers and pressurised gasifiers thus open the opportunity for deploying these fuels in those applications. To minimise aging reactions, it is also desirable to have targeted viscosity number at room temperature.

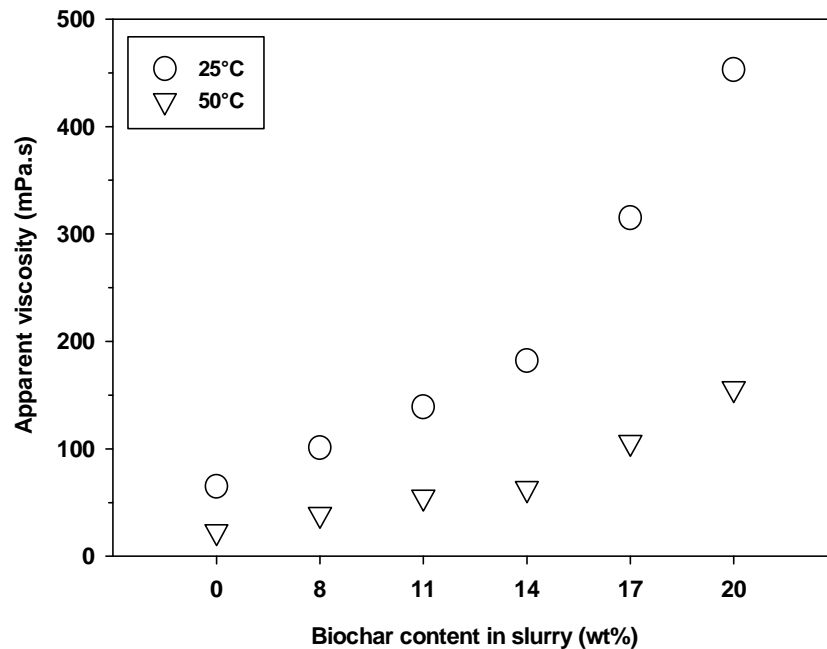


Figure 6-6 Apparent viscosity of fuels at shear rate 100s^{-1} . Guideline limit: 1000 mPa.s in boilers, 700 mPa.s in pressurised gasifier

Bioslurry fuels at biochar concentration 14-20 wt% also exhibit thixotropic behaviour at both measured temperatures. For these bioslurry fuels, the shear thinning behaviour also depends on time. For thixotropic fluids, the viscosity decrease with time at a constant shear rate and can be characterised with a hysteresis loop (see descriptions in a previous publication¹⁶⁹) as shown in Figure 6-7. The area of hysteresis loop for biochar concentration of 20 wt% is larger than 14 wt% concentration. This type of fluid behaviour is also prevalent at high concentration of COM,¹¹⁰ indicating the amount of biochar/solid plays an important role in forming a spatial structure in the multiphase bio-oil/ liquid medium.¹⁶⁷ It is believed that along the upward ramp, the shearing effect broke the agglomerated char in bioslurry giving the shear thinning effect. Since the spatial structure has been broken permanently, the changes of shear stress were no longer same during the downward ramp. The agglomerated char structure is suggested to loosen more easily at higher temperature.¹⁶⁷ Therefore, the area of hysteresis loop for biochar concentration 20 wt% at 50°C is smaller than 25°C.

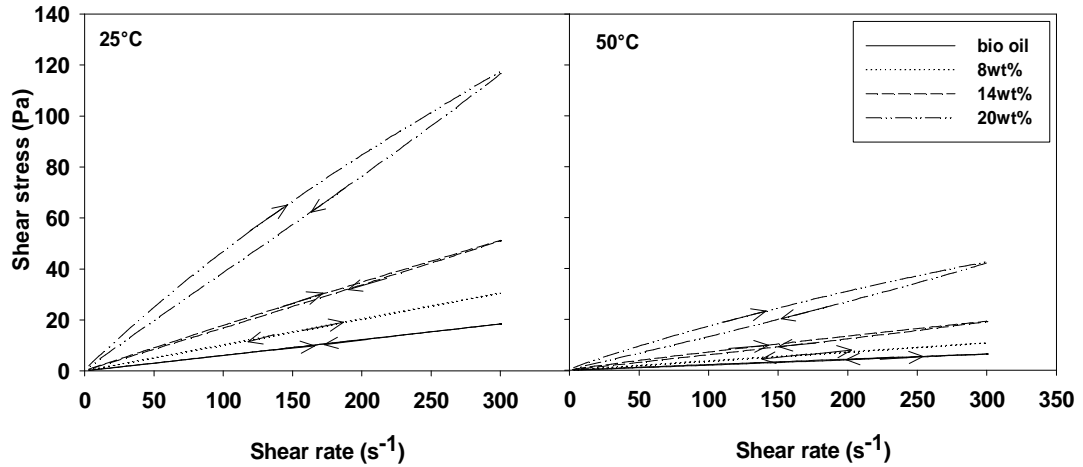


Figure 6-7 Thixotropic behaviour of fuels

6.3.6 Benchmarking of Bioslurry against Other Slurry Fuels and Implications

Table 6-5 listed a summary of the results in this study, benchmarking against the requirements of slurry fuels for combustion application. It is clear that the fuel and rheological properties of the bioslurry fuels prepared in this study can meet the slurry fuel specifications for applications in combustion/gasification systems especially boilers and gasifiers. The results suggested that a bioslurry-based bioenergy supply chain is competent to replace fossil-based slurry fuels in large-scale coal-based power plants for substantial emission reduction.

Table 6-5 Benchmarking of bioslurry against fuel requirements^{51,109-116,118-121,123-126,170,171} in combustion

Property	Bioslurry in this study	Fuel requirements in combustion/gasification ^{51,109-116,118-121,123-126,170,171}
particle size distribution	88% < 75 μm	80% < 74-75 μm
porosity	35% are transitional pores	35-55% transitional pores is suitable for adsorption of organic molecules
bulk density, Tonne/m ³	1.25-1.27	0.6-0.9 or higher
inorganic species, wt%		
N	<0.4	<0.6
S	<0.011	<0.1
Ca	<0.25	<35
K	<0.13	<7.0
static stability, %	79-90	>70
fluid behaviour	non-Newtonian pseudoplastic	non-Newtonian pseudoplastic
viscosity at shear rate 100 s ⁻¹	max 453 mPa.s	max 1000 mPa.s in boiler 700 mPa.s in pressurised gasifier

6.4 Conclusions

This study demonstrates that bioslurry has desirable fuel properties which meet specifications for combustion/gasification applications. The excellent grindability of mallee wood biochar enables the preparation of bioslurry at the desired size requirement instead of grinding raw biomass. Bioslurry has high volumetric energy density which is expected to significantly reduce logistic cost often associate with utilising green biomass. Bioslurry is also relatively stable with 50% less than viscosity number required in boilers and pressurised gasifiers. At high biochar concentrations (e.g. 11-20 wt%), bioslurry fuels are non-Newtonian fluids with pseudoplastic behaviour. The contents of AAEM, N and S in the bioslurry fuels are also well below the limits. Therefore, bioslurry can potentially replace conventional fuel use in large-scale coal-based energy plants, particularly applications in boilers and gasifiers.

CHAPTER 7

PREPARATION OF BIOSLURRY FUELS FROM BIOCHAR AND THE BIO-OIL RICH FRACTIONS AFTER BIO- OIL/BIODIESEL EXTRACTION

7.1 Introduction

Chapter 6 illustrates the favourable fuel and rheological properties of bioslurry fuels, produced from bio-oil and bio-char that are products of mallee biomass fast pyrolysis, for combustion and gasification applications. However, so far the preparation of such bioslurry fuels use the whole bio-oil produced from the fast pyrolysis of biomass such as mallee. Such an approach may not be the best option for bio-oil utilisation. It is known that bio-oil contains a wide range of components and some of which are suitable for value-added applications.^{52,55} For example, significant R &D have been carried out to develop various technologies for bio-oil upgrading and refining for the production of liquid transport fuels, including direct biodiesel extraction,¹⁰⁶ esterification,^{172,173} catalytic upgrading,^{129,132} hydrotreating^{174,175} and emulsification with diesel^{123,133} or biodiesel^{134,135} with the aid of a surfactant.

Particularly, it is worth to note that García-Perez et al¹⁰⁶ developed a method that used biodiesel to extract some of the best fuel fractions of bio-oil, resulting in a biodiesel/bio-oil fuel blend that is proven to be a good transport fuel. Monolignols, furans, sugars, extractive-derived compounds and a small fraction of oligomers were the main bio-oil compounds extracted in biodiesel. The addition of these bio-oil fractions to biodiesel did not seem to greatly influence the calorific value of resulting bio-oil/biodiesel blend. A subsequent investigation was also carried out to apply the same method for extracting bio-oil produced from mallee biomass fast pyrolysis, leading to similar conclusions.¹⁷⁶

Therefore, instead of using the whole bio-oil for preparing bioslurry fuels, it is plausible to use biodiesel for bio-oil extraction first that enable a better use of bio-oil. The best (high-quality) components in the bio-oil can be extracted into the produced biodiesel/bio-oil blend that can be used as a liquid transport fuel (as shown in previous studies^{106,176}). The residue bio-oil rich fraction (low-quality) after biodiesel extraction can then be used to prepare bioslurry fuels. This is the idea proposed in this study as an alternative approach for bio-oil utilisation and bioslurry fuels preparation. Therefore, the main objectives of this work are to investigate the quality of the resulted bioslurry fuels benchmarked against those slurry fuels produced from whole bio-oil.

7.2 Methodology

This study employed three fuel samples i.e. biodiesel, fast pyrolysis bio-oil and biochar (see Chapter 3 Section 3.3.1-a). A series of bio-oil/biodiesel blend samples (method previously described in Section 3.4.9-3.4.10) were prepared by mixing 80, 60, 40 and 20 mass % of bio-oil to biodiesel, corresponding to 0.25, 0.67, 1.50 and 4.00 mass ratios of biodiesel to bio-oil, respectively. The blends were kept in sealed vials and stirred continuously using a magnetic stirrer at room temperature for 2 hrs. After that, the blends were left to settle. A 5 ml syringe is used to separate the biodiesel rich fraction (top layer) and the bio-oil rich fraction (bottom layer) and the mass of resulted fractions were recorded. Hereafter, the bio-oil rich and biodiesel rich fractions are denoted as BOR_{x.xx} and BDR_{x.xx} whereby “BOR” refers to “bio-oil rich fraction”, “BDR” means “biodiesel rich fraction” and “x.xx” refers to the initial mass ratio of biodiesel to bio-oil. The proximate and ultimate analysis of the fuels prepared are shown in Table 7-1. Bioslurry fuels were then prepared by suspending the fine biochar particles into bio-oil and the selected bio-oil rich fraction solutions resulted from the biodiesel extraction process (also see Section 3.4.9-3.4.10). Bioslurry fuels with biochar loading of 10 and 20 wt% were prepared. Hereafter, the bioslurry fuels prepared with the original bio-oil are denote as “BO-10%” and “BO-20%” whereas bioslurry fuels prepared from the bio-oil rich phase are denoted as “BOR x.xx-10%” and “BOR x.xx-20%” corresponds to 10 or 20 wt% biochar loading, respectively.

The microstructures of bio-oil and the bio-oil rich fractions were examined using a Nikon Eclipse ME600 optical microscope (Section 3.4.11). Fuel density was determined with a pycnometer (5 mL) and the measurement was done multiple times with deviations of < 1%. The surface tension of fuels was measured using a KSV Sigma 701 Surface Tensiometer, following the Wilhelmy method (see Section 3.4.12). The sample temperature is controlled with a water bath. Sample was left for 5 min in the measuring chamber to reach the desired temperature before taking the first reading. The result reported was an average of 50 data points after the surface tension reached equilibrium with error bar <2%. Density and surface tension measurements were conducted at both 25°C and 40°C.

Chemical compounds in the fuels were qualitatively identified using a GC-MS (Section 3.4.14). A Leco AC350 calorimeter was used to measure calorific value of the fuels. The calorific values of bioslurry fuels are estimated based on the percentage of liquid fuels and biochar and their respective low heating values (LHV, GJ/Tonne). A standard method for coal-water-slurry¹¹⁶ was employed to examine bioslurry stability as described in Section 3.4.13. The fuels rheological properties were characterised using A Haake Mars II rheometer fitted with a Z20 cylinder sensor system (Section 3.4.15). Calibrations of the instrument were done before and after measurements to ensure the reliability of results in this study. In the steady mode, the changes of viscosity and shear stress as a function of shear rate was measured at a maximum shear rate of 1000s⁻¹. The fluid behaviour can then be characterised based on the shear stress versus shear rate relationship, typically fitted in the form of Power Law $\tau = K\dot{\gamma}^n$, K is fluid consistency coefficient and n is flow behaviour index. When $n = 1$, the Power Law equation is reduced to Newton's law of viscosity. The departure of n from 1 illustrates the degree of deviation from Newtonian behaviour; typically the behaviour is pseudo-plastic for $n < 1$ and dilatant for $n > 1$ ¹⁶².

This study also carried out the dynamic measurement of the storage (elastic) modulus G' and loss (viscous) modulus G'' as a function of stress and frequency on bioslurry fuels to examine viscoelastic behaviour. A stress sweep test was performed at 0.1Hz between shear stress 0.001-1000.00Pa to determine the linear viscoelastic region. For

selected bioslurry fuels, frequency sweeps between 0.1-10 Hz were conducted at 4.00Pa. All steady and dynamic measurements were carried out at 25°C and 40°C. Fresh fuel samples were used for all measurements conducted in this study.

7.3 Results and Discussion

7.3.1 Fuel Chemistry

Table 7-1 compares some fuel properties of the bio-oil, biodiesel, resulted bio-oil rich and biodiesel rich fractions.

Table 7-1 Fuel properties and heating values. BOR x.xx – bio-oil rich fraction obtained from biodiesel extraction at a biodiesel to bio-oil ratio of x.xx; BDR x.xx – biodiesel rich fraction obtained from biodiesel extraction at a biodiesel to bio-oil ratio of x.xx

Fuel	(wt %, ar)		Ultimate analysis (% daf)					Heating value
	water	ash	C	H	N	S	O*	LHV (GJ/Tonne)
bio-oil	33.7	0.09	42.3	7.3	0.06	0.02	50.3	17.3
BOR 0.25	33.7	0.04	41.4	7.6	0.07	0.02	50.9	16.9
BOR 0.67	34.1	0.03	43.3	8.1	0.11	0.01	48.5	17.1
BOR 1.50	35.0	0.04	40.2	7.8	0.11	0.01	51.9	16.4
BOR 4.00	38.7	0.06	37.9	7.8	0.14	0.01	54.2	15.4
biodiesel	0.3	<0.01	77.1	11.7	0.05	0.01	11.1	39.6
BDR 0.25	1.0	<0.01	75.0	11.0	0.02	0.01	14.0	38.4
BDR 0.67	1.1	<0.01	75.6	11.1	0.03	0.01	13.3	38.6
BDR 1.50	1.0	<0.01	75.7	11.2	0.02	<0.01	13.1	38.8
BDR 4.00	0.6	0.03	76.0	11.2	0.04	<0.01	12.8	39.2

* by difference;

LHV – low heating value

It is observed in Table 7-1 that the water content for resulted bio-oil rich fractions and biodiesel rich fractions were significantly increased compared to the original bio-oil and biodiesel before extraction. A similar trend of water content increase in biodiesel-rich phase was also reported for extraction of mallee bio-oil/biodiesel carried out at 60°C, 30 min previously which was related to extraction of water soluble compounds from bio-oil into biodiesel.¹⁷⁶ In such a case, supposedly the bio-oil rich fraction should have less water content after extraction instead of increasing as observed in Table 7-1.

In this experiment, the water content was determined with Karl Fischer Titration according to ASTM E203. Although the exact mechanisms are unknown at present,

there are at least two possible reasons responsible for the increase of fuels water content after extraction process. Firstly, it could possibly resulted from interference of certain chemicals such as aldehyde, ketones and acetic acid (which are known to exist in bio-oil⁵⁵) that react with methanol in the reagent during the titration process to form water.¹⁷⁷ Secondly, some mechanisms such as condensation reactions can increase the amount of water content in bio-oil (as reported previously during bio-oil aging¹⁷⁸). However in the present experiment, fresh bio-oil was used and the extraction process was conducted at room temperature to minimise aging reactions. Therefore the reactions in which water is formed as a byproduct can possibly occur during the extraction process itself as the increased water content is corresponding to decrease in the fuels heating value i.e up to ~11% in the case of BOR 4.00 (Table 7-1).

The data in Table 7-1 also suggested that a slight decrease in the carbon and hydrogen content and increase in the oxygen content of the biodiesel-rich fractions has limited impact on the fuel heating values of the biodiesel-rich fractions. This trend is in good agreement with previous results.¹⁷⁶ A van Krevelen plot in Figure 7-1 showed the relationship between fuel hydrogen to carbon ratio and oxygen to carbon ratio and further verifies the trend for LHV in Table 7-1. Figure 7-1 also suggests that biodiesel extraction at low extraction ratio (0.25 and 0.67) yielded bio-oil rich fractions with minimal changes in C, H and O contents and (therefore) with similar LHV in comparison to the whole bio-oil. Table 7-1 showed that all fuels have very low sulphur contents well below the guideline limit ($S < 0.1$ wt% as required for preventing corrosion¹⁵²). The nitrogen contents in the biodiesel rich fractions have decreased and an increase in nitrogen contents by more than twice are also evidenced in the bio-oil rich fractions. However, overall, the nitrogen contents in the fuels are still less than the guideline value ($N < 0.4$ wt% for combustion or gasification applications¹⁵²). From fuel requirements for practical applications (e.g. combustion and gasification) and supply chain point of view, fuel with low water content and high (volumetric) energy density is favoured for stable combustion/gasification, reducing flue gas volume (hence reactor sizes) and minimising fuel transport/handling cost which are the key hurdles limited biomass utilisation in the industry.^{6,19,121} Therefore, based on the data in Table 7-1 and Figure 7-1, bio-oil rich

fraction that has similar fuel chemistry and LHV with the whole bio-oil i.e BOR 0.67, was chosen as an example to prepare bioslurry fuels for further investigations, benchmarking against those bioslurry fuels prepared using the original whole bio-oil.

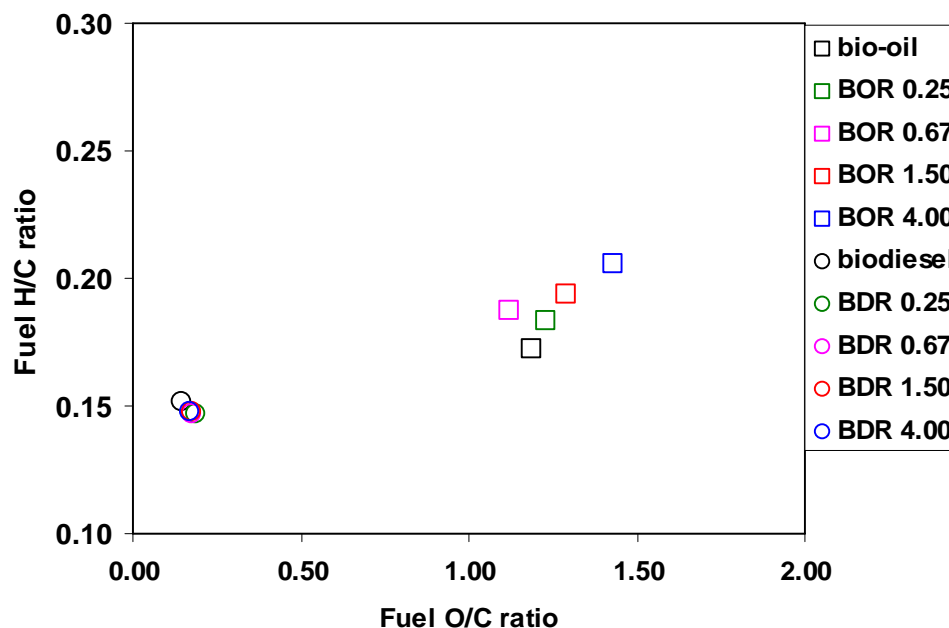


Figure 7-1 van Krevelen diagram showing relationship of fuel H/C ratio to O/C ratio. BOR x.xx – bio-oil rich fraction obtained from biodiesel extraction at a biodiesel to bio-oil ratio of x.xx, BDR x.xx – biodiesel rich fraction obtained from biodiesel extraction at a biodiesel to bio-oil ratio of x.xx

7.3.2 Solubility of Bio-oil in Biodiesel

The relationship of initial biodiesel/bio-oil ratio vs the ratio of biodiesel rich/bio-oil rich fraction is shown in a linear plot (Figure 7-2A). The slope (K) has been used as an indicator of the solubility of bio-oil in biodiesel^{106,176} with higher K value corresponds to increase bio-oil solubility. The average K value (K~1.32, deviations < 1%) obtained in this experiment is comparable to those obtained from sugar rich-polar oil obtained from Auger pyrolysis of pine chip ($1.0 < K < 1.4$)¹⁰⁶ and slightly higher than bio-oils extracted at 60°C in previous work (mallee bio-oil, K~1.2; pine bio-oil, K~1.23).¹⁷⁶

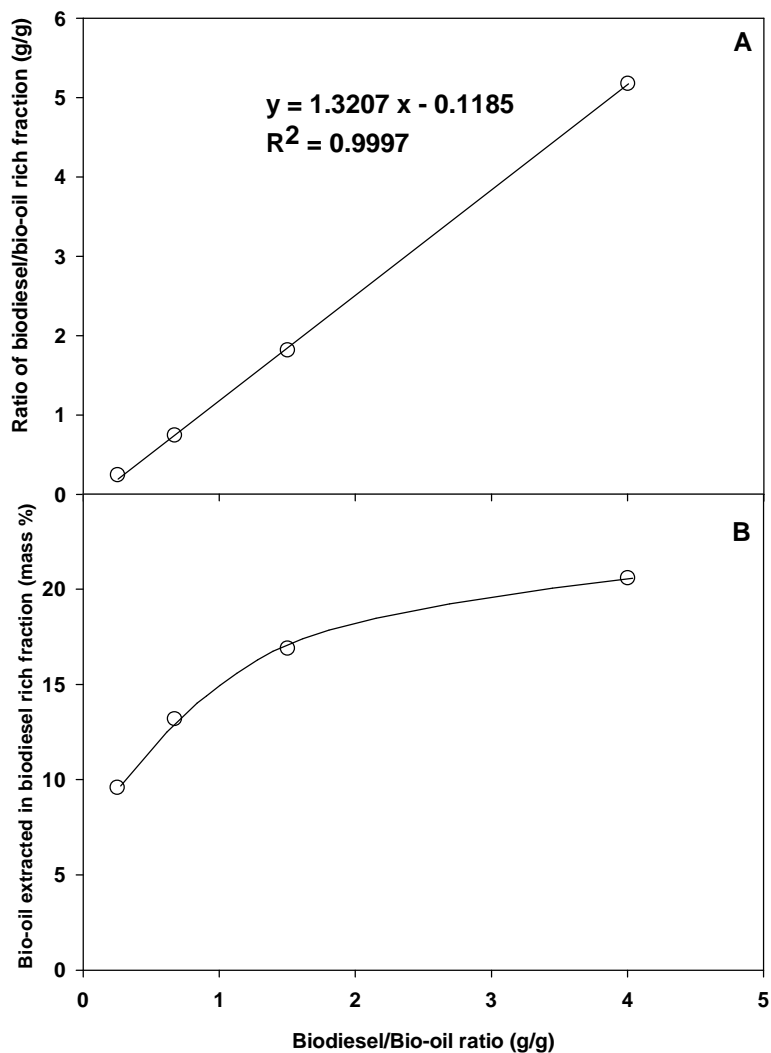


Figure 7-2 Extraction curve of biodiesel/mallee bio-oil blends

It is worth to note that in the extraction process, the separation of the resulted biodiesel and bio-oil rich phases was preliminary attempted using a glass separation funnel but was unsuccessful. The two layers/fractions were visibly separated at the bottom of funnel after an overnight standing period. However, during the separation process, it was observed that the bottom layer (bio-oil rich fraction) tends to stick on the funnel wall while the biodiesel rich fraction rushed down causing remixing of the fractions. Therefore, the separation process was preceded with a syringe instead. Even so, it was difficult to get a complete separation of the final thin biodiesel/bio-oil

interface. Fine char particles in bio-oil were observed to migrate to the interface that also made a complete separation almost impossible.

From the view point of fuel applications, it is more favourable to have the fine biochar particles retained in bio-oil rich fraction than in biodiesel rich fraction because the bio-oil rich fraction will be used to prepare bioslurry fuels. Therefore, after separation the resulted bio-oil rich fractions were left with a thin layer of biodiesel (~1 mm thick) on the surface. Close examinations with optical microscope of various fuel samples are shown in Figure 7-3 (200X magnification). In Figure 7-3 a, chars particles are finely disperse in the original bio-oil. In the bio-oil rich fractions (Figure 7-3 b to 7-3 d), the char particles were highly concentrated around the margin of biodiesel droplets, indicating the affinity of fine biochar particles to the bio-oil/biodiesel interface. This surface-active char behaviour was also reported in some of the previous studies on bio-oil.^{167,179} After the layer separation, only an increased mass of biodiesel rich fractions and decreased mass of bio-oil rich fractions were recorded and not vice-versa. The photomicroscopy evidence also shows that the biodiesel fraction is immiscible with bio oil rich phases. Therefore the solubility of biodiesel in bio-oil is limited.

The concentration of bio-oil fractions ($C_{bio-oil}$) in the biodiesel rich phase can be calculated from the K value using the equation $C_{bio-oil} = (K-1) / (K \times ((M_{biodiesel} / M_{bio\ oil}) + 1))$, where $M_{biodiesel}$ and $M_{bio\ oil}$ are the initial mass of biodiesel and bio-oil used for preparing the fuel blends.¹⁷⁶ Figure 7-2B shows the estimated concentration of bio-oil extracted in biodiesel rich phases. It can be seen that there is a substantial proportion (as high as ~21%) of bio-oil were extracted by biodiesel at a biodiesel/bio-oil ratio of 4.

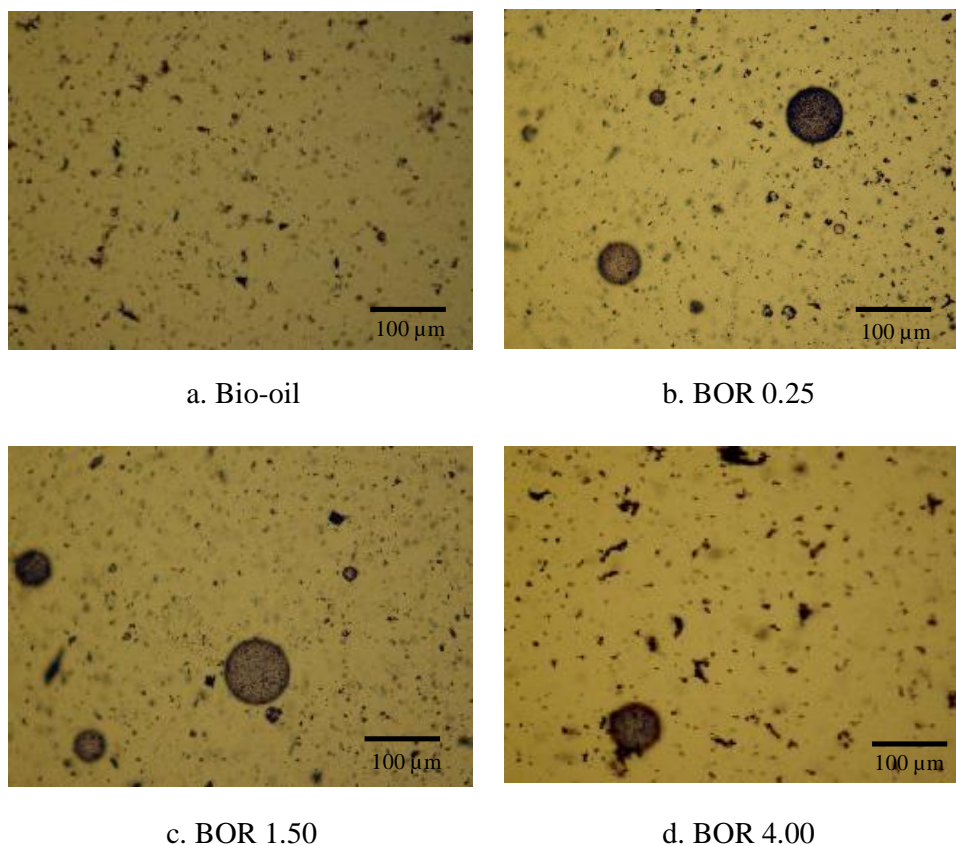


Figure 7-3 Photomicroscopy of fuels. BOR x.xx – bio-oil rich fraction obtained from biodiesel extraction at a biodiesel to bio-oil ratio of x.xx

7.3.3 Fuels Density, Surface Tension and GC-MS

Practical application of liquid fuels requires desired performance of sprays quality in atomisation, which is known to be determined by the fuel's surface tension, density and viscosity.¹⁸⁰⁻¹⁸² In general, spray atomisation quality is expected to degrade by high viscosity, density and surface tension.¹⁸² Table 7-2 presented the density of various fuels while Figure 7-4 shows the equilibrium surface tension obtained at 25°C and 40°C, benchmarking against those of medium and heavy fuel oils in practical applications.

Table 7-2 Fuel density and equilibrium surface tension. BOR x.xx – bio-oil rich fraction obtained from biodiesel extraction at a biodiesel to bio-oil ratio of x.xx; BDR x.xx – biodiesel rich fraction obtained from biodiesel extraction at a biodiesel to bio-oil ratio of x.xx; BO-10% and BO-20% – bioslurry fuels prepared from the whole bio-oil with 10 wt% and 20 wt% biochar loading, respectively; BOR 0.67-10% and BOR 0.67-20% – bioslurry fuels prepared from bio-oil rich fraction after biodiesel extraction (at a biodiesel to bio-oil ratio of 0.67) with 10 wt% and 20 wt% biochar loading, respectively.

Fuels	Density (Tonne/m ³)		Equilibrium surface tension (mN/m)	
	25°C	40°C	25°C	40°C
bio-oil	1.18	1.17	30.2	25.5
Biodiesel	0.87	0.86	32.7	31.5
fuel oil (medium) ¹⁸¹	NA	0.94	NA	23.0
fuel oil (heavy) ¹⁸¹	NA	0.97	NA	23.0
BOR 0.25	1.18	1.17	23.3	22.0
BOR 0.67	1.18	1.17	21.8	21.4
BOR 1.50	1.18	1.16	29.5	20.1
BOR 4.00	1.18	1.17	22.8	24.4
BDR 0.25	0.90	0.89	26.1	24.2
BDR 0.67	0.89	0.88	25.1	23.9
BDR 1.50	0.89	0.88	27.8	25.6
BDR 4.00	0.88	0.87	26.0	23.9
BO-10%	1.21	1.20	33.4	31.5
BO-20%	1.24	1.22	33.6	32.0
BOR 0.67-10%	1.22	1.20	33.2	32.4
BOR 0.67-20%	1.25	1.23	35.0	32.0

NA – data not available

It can be seen that extraction of bio-oil with biodiesel has minimal effect on density of the resulted fractions and the bioslurry fuels. As seen in Table 7-2 and Figure 7-4, it is also interesting to see that the resulted bio-oil rich fractions and biodiesel rich fractions have significant lower equilibrium surface tension than the original bio-oil and biodiesel used to prepare the blends. The surface tension of the biodiesel-rich fractions is up to 24% less than the original biodiesel although there is no apparent correlation between fuel surface tension reduction and the extraction ratio.

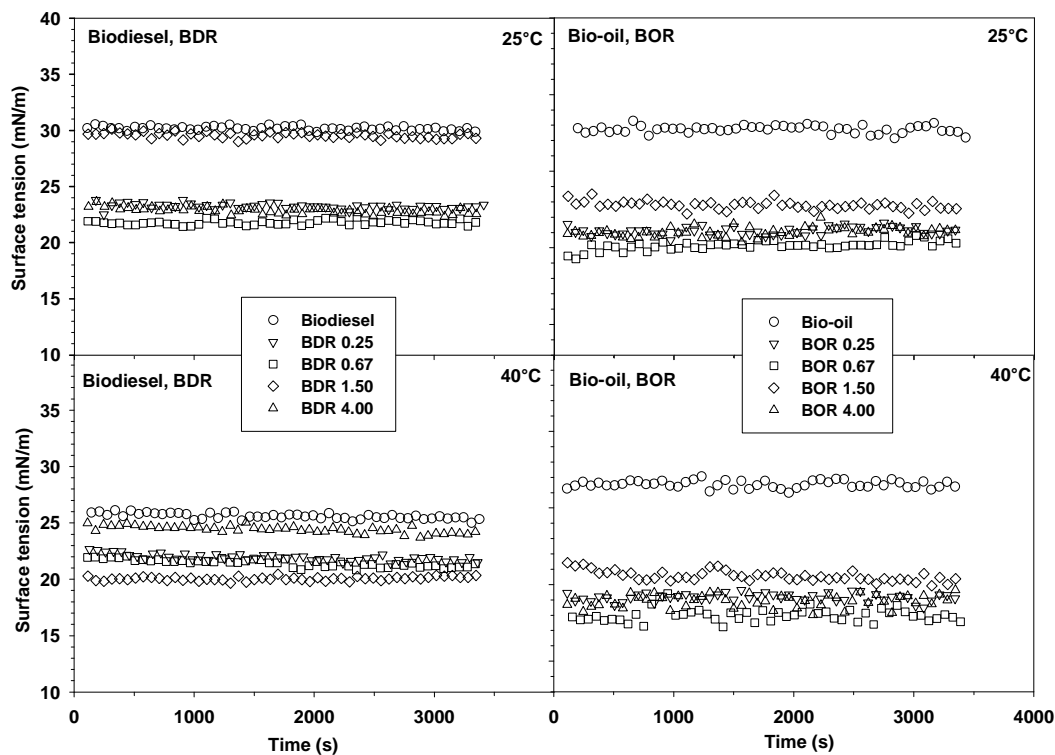


Figure 7-4 Surface tension of various fuels. BOR x.xx – bio-oil rich fraction obtained from biodiesel extraction at a biodiesel to bio-oil ratio of x.xx; BDR x.xx – biodiesel rich fraction obtained from biodiesel extraction at a biodiesel to bio-oil ratio of x.xx

Further GC-MS analysis was then carried out to provide insights on the key compounds (particularly of phenolic compounds and levoglucosan) in the fuels that may be responsible for such a reduction in the surface tension of these fuels. Figure 7-5 presented the GC-MS identified compounds of interest for bio-oil, biodiesel, and selected resulted fractions (BOR 0.67 and BDR 0.67). It should be noted that only compounds within the GC-MS detection capability are reported. For a similar mallee bio-oil, García-Perez et al.¹⁷⁶ estimated that chemical from phenols, furans and carboxylic acids families are the most solubilised in biodiesel and the extraction of phenolic compounds into biodiesel enhances the oxidation stability of biodiesel.

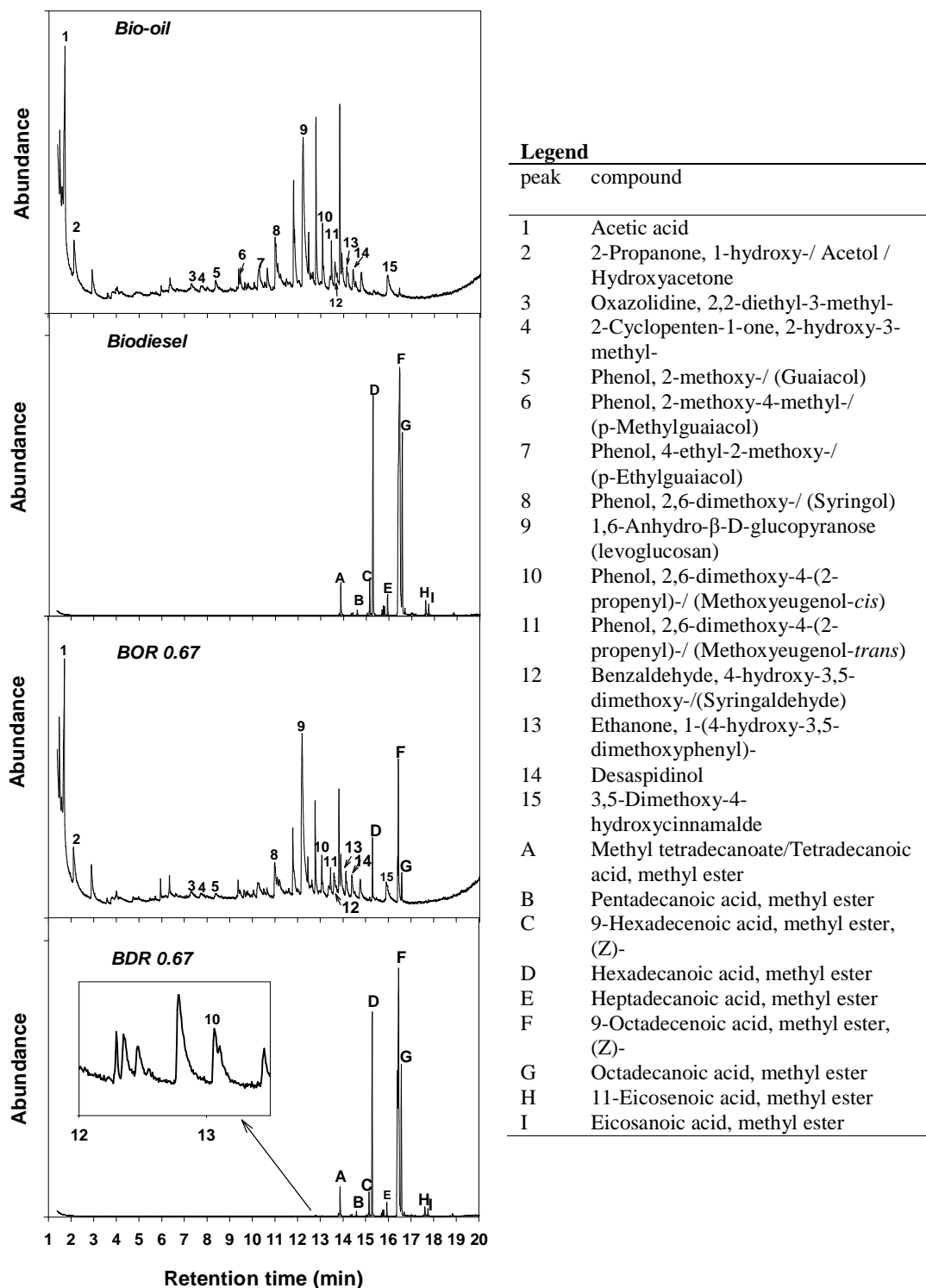


Figure 7-5 GC-MS of selected compounds in bio-oil, biodiesel and resulted fractions. BDR 0.67 – biodiesel rich fraction obtained from biodiesel extraction at a biodiesel to bio-oil ratio of 0.67; BOR 0.67 – bio-oil rich fraction obtained from biodiesel extraction at a biodiesel to bio-oil ratio of 0.67.

In Figure 7-5 - it is clearly evidenced that a phenolic compound (matched to peak 10 in bio-oil) was detected in BDR 0.67, indicating extraction of this compound from bio-oil to biodiesel rich-phase. It is known that emulsifiers developed from phenolates in bio-oil have surfactant characteristics that improve the stabilisation and handling of petroleum emulsions.¹⁸³ The results presented here appear to suggest that phenolic compounds may also have a positive role in reducing the surface tension of resulted biodiesel rich fractions as shown in Figure 7-4.

It is further noteworthy to highlight that the surface tension of bio-oil measured in this study is ~30 mN/m at 25°C, in consistence with the values reported in the literature for other bio-oils such as 29.2 mN/m for a bio-oil that its origin and the method used for surface tension measurement were not detailed in the reference,¹²⁸ 31-39 mN/m for a bio-oil from softwood bark and hardwood rich in fibers and measured using Du Nuoy ring method¹²⁰ and 34.66 mN/m for a bio-oil from a hardwood and measured using pendant drops method.¹⁶⁷ The surface tension of biodiesel measured in this study is ~25.5 mN/m at 40°C, which is similar to that of saturated methyl esters (carbon number 8:0) reported for biodiesel fuels.¹⁸⁴ It can also be seen in Figure 7-5 that some peaks for methyl esters are present in the BOR 0.67 sample, most likely resulting from the thin layer of biodiesel covering left after fraction separation as explained previously. The thin biodiesel covering is also likely responsible for the decreased surface tension of the bio-oil rich fractions as shown in Table 7-2 and Figure 7-4. However, it should be noted that such reductions in the surface tension of bio-oil rich fractions did not have significant effect on the surface tension of the prepared bioslurry fuels e.g. BOR 0.67-10% and BOR 0.67-20% which are almost similar to BO-10% and BOR-20%.

7.3.4 Fuel Volumetric Energy Density and Stability

The volumetric energy density of bio-oil, bio-oil rich fractions and bioslurry fuels are presented in Figure 7-6.

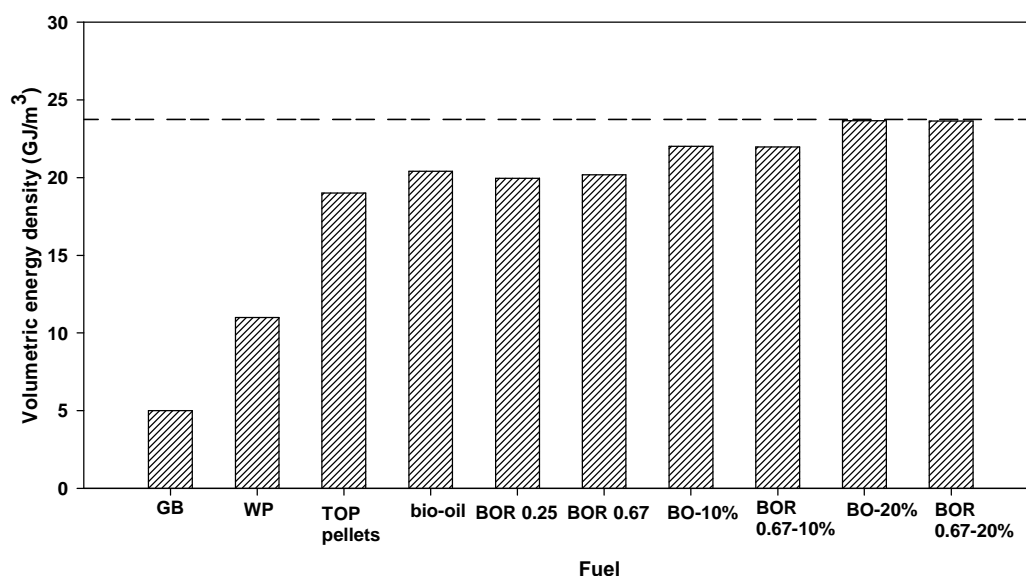


Figure 7-6 Volumetric energy density of various fuels. GB – green biomass; WP – wood pellets; TOP – torrefaction in combination with pelletizing; BOR x.xx – bio-oil rich fraction obtained from biodiesel extraction at a biodiesel to bio-oil ratio of x.xx; BDR x.xx – biodiesel rich fraction obtained from biodiesel extraction at a biodiesel to bio-oil ratio of x.xx; BO-10% and BO-20% – bioslurry fuels prepared from the whole bio-oil with 10 wt% and 20 wt% biochar loading, respectively; BOR 0.67-10% and BOR 0.67-20% – bioslurry fuels prepared from bio-oil rich fraction after biodiesel extraction (at a biodiesel to bio-oil ratio of 0.67) with 10 wt% and 20 wt% biochar loading, respectively.

In consistence with the data trend presented in Chapter 6, the result demonstrated that the preparation of bioslurry fuels via suspending fine ground biochar particles into bio-oil achieves a significant volumetric energy densification. The volumetric energy density of the various bioslurry fuels prepared is up to ~ 24 GJ/m³ (at 20 wt% biochar loading) in comparison to ~ 5 GJ/m³ of green chipped biomass (as reported previously (see Chapter 6)). The bioslurry energy density is reduced from 24 to 22 GJ/m³ when the biochar loading decreases 20 to 10 wt% in the bioslurry fuels. Overall, such a volumetric energy densification through bioslurry fuels is significant, in comparison to other biomass pre-treatment methods for energy densification such

as pelletizing and torrefaction in combination with pelletizing (TOP) that achieved moderate fuel volumetric energy densities (11-19 GJ/m³).¹⁹

An increase in biodiesel/bio-oil ratio during extraction from 0.25 to 0.67 leads to a minimal effect on the density and heating value of the bio-oil rich fractions (Table 7-1 and 7-2). The volumetric energy density of the bio-oil rich fractions is similar to that of the original bio-oil. Furthermore, bioslurry fuels prepared with BOR 0.67 at 10 wt% and 20 wt% biochar loading have a similar volumetric energy density in comparison to the bioslurry fuels prepared from bio-oil (i.e. BO-10% and BO-20% in Figure 7-6). These results have significant practical implications, suggesting that the preparation of bioslurry fuels from bio-oil rich fraction is indeed viable to produce equivalent high-energy density fuels favourable for transport. The bioslurry fuels prepared using BOR 0.67 also have similar stability in comparison to those using the original bio-oil. For example, the bioslurry fuels at 20 wt% biochar loading i.e BOR 0.67-20% and BO-20% have stability values of 71.7 % and 72.1%, respectively.

7.3.5 Rheology of Bioslurry Fuels Prepared from the Bio-oil Rich Fractions after Biodiesel Extraction

Commercial applications of slurry fuels depend upon a number of properties including slurry stability, pumpability and atomisation quality.^{112,116,160,185} It was suggested that the maximum viscosity for safe pumping of coal water slurry is 1000 mPa.s at 100s⁻¹ for combustion applications in boilers¹¹² and ~700 mPa.s for gasification applications in pressurised gasifiers¹⁶⁰. The results presented in Chapter 6 have demonstrated that bioslurry fuels prepared from the whole bio-oil are well within such specifications. Figure 7-7 shows the apparent viscosity of bio-oil rich fractions and bioslurry fuels obtained with max shear rate 1000 s⁻¹ at 25°C and 40°C. It can be seen that at 100s⁻¹, all fuels exhibit viscosity well below the guideline limits. At these temperatures, the viscosity of both the original bio-oil and bio-oil rich fractions are < 50 mPa.s while those of the bioslurry fuels are <300 mPa.s at 25°C and < 200 mPa.s at 40°C, respectively. Therefore, similar to the bioslurry prepared from the whole bio-oil, the bioslurry fuels prepared from the bio-oil rich fractions (after biodiesel extraction) can also be pumped safely at room temperatures, which is desired in order to minimise the bioslurry aging.¹³²

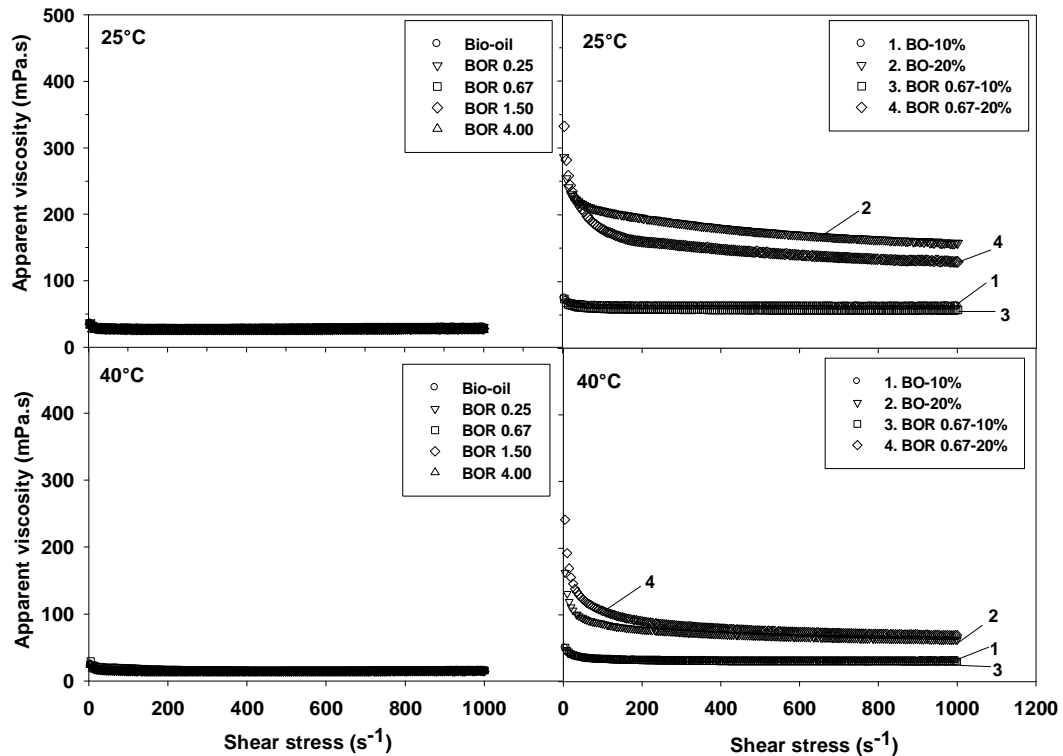


Figure 7-7 Apparent viscosity of various fuels as a function of shear rate. BOR x.xx – bio-oil rich fraction obtained from biodiesel extraction at a biodiesel to bio-oil ratio of x.xx; BO-10% and BO-20% – bioslurry fuels prepared from the whole bio-oil with 10 wt% and 20 wt% biochar loading, respectively; BOR 0.67-10% and BOR 0.67-20% – bioslurry fuels prepared from bio-oil rich fraction after biodiesel extraction (at a biodiesel to bio-oil ratio of 0.67) with 10 wt % and 20 wt % biochar loading, respectively.

A slight shear thinning effect is also evidenced in Figure 7-7 at very low shear rate ($<50 \text{ s}^{-1}$) for bio-oil and bio-oil rich phases but in overall the fluid behaviour are dominantly Newtonian. For bioslurry fuels i.e BO-10%, BOR 0.67-10%, BO-20% and BOR 0.67-20% the curves show non-Newtonian pseudoplastic behaviour, which is common for slurry fuels (eg. coal-oil mixture, coal-water slurry, coal-algae slurry, coal-sewage sludge slurry and coal-biomass slurries^{110,112,115,160,162}). While BO-20% has slightly higher viscosity than BOR 0.67-20% at 25°C, such differences diminish as temperature increases to 40°C (see Figure 7-7).

Fuel atomisation involves conversion of a volume of liquid into waves, ligaments and ultimately small droplets.¹⁸⁵ The prediction of atomisation quality can be made using slurry viscosity measured at high shear rate 1000-10 000 s⁻¹,¹⁸⁵ followed by the estimation of the spray droplets' Sauter Mean Diameter (SMD) that largely depends on slurry properties via the Ohnesorge number.^{181,185} Ohnesorge number relates the fuel viscous forces to inertial and surface tension forces and can be estimated using the following equation, Ohnesorge number (dimensionless) = $\eta_F / (\sigma_L \rho_F D_F)^{0.5}$, where η_F is the apparent viscosity of fuel, σ_L is the surface tension of liquid, ρ_F is the density of fuel and D_F is the diameter of fuel passage).^{181,185} Fuels with a higher Ohnesorge number are expected to produce larger SMD after spray.

Table 7-3 presented the Ohnesorge number of fuels estimated based on fuels density, viscosity and surface tension at 40°C as comparison to heavy fuel oil under similar operating conditions. It can be seen that the bio-oil rich fractions and BOR 0.67-20% have a slightly higher Ohnesorge number than the whole bio-oil and BO-20%. However, in comparison to heavy fuel oil, atomisation of BO-20% and BOR 0.67-20% is estimated to produce much smaller droplets (favourable for practical applications), with significantly reduced SMDs by ~51% and ~46% respectively.

The viscosity curves of bioslurry fuels are then fitted with the Power Law equation (Section 7.2) to estimate the flow behaviour index n , as shown in Table 7-4. In general, the flow behaviour index n decrease with increasing biochar loading in the bioslurry fuels. It is also evidenced that bioslurry fuels prepared from bio-oil rich phases (BOR 0.67-10% and BOR 0.67-20%) show more deviations from Newtonian behaviour in comparison to those (i.e. BO-10% and BO-20%) prepared from the whole bio-oil.

Table 7-3 Estimation of Ohnesorge number based on fuel properties at 40°C. BOR x.xx – bio-oil rich fraction obtained from biodiesel extraction at a biodiesel to bio-oil ratio of x.xx; BO-10% and BO-20% – bioslurry fuels prepared from the whole bio-oil with 10 wt% and 20 wt% biochar loading, respectively; BOR 0.67-10% and BOR 0.67-20% – bioslurry fuels prepared from bio-oil rich fraction after biodiesel extraction (at a biodiesel to bio-oil ratio of 0.67) with 10 wt% and 20 wt% biochar loading, respectively

Fuel	Density Tonne/m³	Surface tension (mN/m)	Viscosity at 1000 s⁻¹ (mPa.s)	Ohnesorge number (dimensionless)
bio-oil	1.17	31.5	15.6	0.31
BOR 0.25	1.17	24.2	15.8	0.36
BOR 0.67	1.17	23.9	15.8	0.36
BOR 1.50	1.16	25.6	14.6	0.32
BOR 4.00	1.17	23.9	14.4	0.33
BO-10%	1.20	32.4	31.4	0.60
BOR 0.67- 10%	1.20	31.5	29.7	0.58
BO-20%	1.22	32.0	62.7	1.20
BOR 0.67- 20%	1.23	32.0	69.4	1.33
heavy fuel oil ¹⁷⁵	0.97	23.0	567.0 [^]	61.50

[^] shear rate not specified

Table 7-4 Flow behaviour index, *n* of various fuels. BO-10% and BO-20% – bioslurry fuels prepared from the whole bio-oil with 10 wt% and 20 wt% biochar loading, respectively; BOR 0.67-10% and BOR 0.67-20% – bioslurry fuels prepared from bio-oil rich fraction after biodiesel extraction (at a biodiesel to bio-oil ratio of 0.67) with 10 wt% and 20 wt% biochar loading, respectively

Temperature (°C)	Flow behaviour index, <i>n</i> for bioslurry			
	BO-10%	BO-20%	BOR 0.67-10%	BOR 0.67-20%
25	0.9978	0.8619	0.9889	0.8571
40	0.9906	0.8624	0.9706	0.8369

The dynamic measurement is used to evaluate viscoelasticity behaviour of a material. The viscoelastic behaviour properties of a material are represented by the moduli G' , G'' and the phase angle/ loss tangent ($\tan \delta$) parameter. The storage (elastic) modulus G' measures the deformation energy stored in the material during the shear process. Material with high G' value shows reversible deformation behaviour therefore G' represents the elastic behaviour of a material. The value of loss (viscous) modulus G'' indicates the deformation energy used by the material during the shear process. The G'' represents the energy dissipated or consumed during frictional process of molecules/particles movement i.e viscous behaviour of a material.^{186,187}

In practical applications, the value of G' and G'' can be used to predict the SMD during fuel atomisation. Fuels that have stronger G' value over G'' tend to produce sprays with high SMDs due to more energy needed to overcome restoring force associated with elastic behaviour before a drop can form as experienced in coal water slurry atomisation.¹⁸⁸ Knowledge about viscoelasticity is also useful to determine type of atomisation. It was suggested that viscoelastic fluid was suitable to be atomized using effervescent atomisation¹⁸⁹ that is a twin-fluid atomisation technique requires bubbling a small amount of gas into the liquid before exiting the nozzle.¹⁹⁰ The loss tangent ($\tan \delta$) is another important viscoelastic parameter^{120,186,191} and it ranges from $0 \leq \tan \delta \leq \infty$ or $0^\circ \leq \delta \leq 90^\circ$, with a case of $\tan \delta = 1^\circ$ indicating the gel point i.e threshold from liquid-like to solid-like behaviour.^{186,192} The phase angle or the loss tangent ($\tan \delta$) can be estimated by taking the ratio of G''/G' . The lower the $\tan \delta$ values are, the more solid-like the material under investigation.^{191,193} The stress dependence of G' and G'' for bioslurry fuels at 25°C and 40°C are presented in Figure 7-8.

For BO-10% and BOR 0.67-10% at 25°C, a decrease of the G' modulus is observed with stress increase whereas the modulus G'' is independent of stress until it reaches ~100 Pa. The linear viscoelastic (LVE) regions for BO-10% in which both G' and G'' are independent of stress is between ~0.1 to 50 Pa whereas for BOR 0.67-10% at ~1-50 Pa. A similar trend is observed at 40°C. Therefore, for BO-10% and BOR 0.67-10%, the modulus $G'' > G'$ indicating that the slurries are dominantly fluid-like materials.¹⁸⁶ However, a different behaviour is exhibited for BO-20% and BOR0.67-

20% that indicate limited LVE regions. A plateau is shown at low stress < 0.02 Pa (see BO-20% at 25°C, 40°C also BOR 0.67-20% at 40°C in Figure 7-8). The LVE region obtained in stress sweep measurement is important as a basis for other dynamic rheological measurement such as frequency sweep whereby a stress value applied has to be chosen within the LVE region. According to the rheometer's specifications,¹⁹⁴ it is also recommended that the stress value picked is at least five times more than the specified minimum torque. Therefore, in case of BO-20% at 25°C and 40°C also BOR 0.67-20% at 40°C, to choose a stress value < 0.02 Pa for other dynamic measurements must be viewed with caution. Beyond 0.02 Pa, the moduli show steep decrease, indicating that the network structures in the material start to break, lose its elasticity and become completely fluid.

Similar with bioslurry fuels at 10 wt% char concentration, the modulus $G'' > G'$ for BO-20% and BOR 0.67-20% suggesting that the slurries behave like fluid in the LVE regions. The viscoelastic behaviour of BO-20% and BOR 0.67-20% also depends on temperature. At 40°C, an additional short plateau are seen for BO-20% and BOR 0.67-20% at ~ 10 -50 Pa however such a trend is not observed at 25°C. In this experiment, all fuels exhibit strong $G'' > G'$ within the range of shear stress measured therefore the viscoelastic behaviour is expected to positively impact the formation of sprays droplet during atomisation which is in agreement with the estimated Ohnesorge number discussed previously.

It is also interesting to note that for all bioslurry fuels in Figure 7-8, a sharp decrease in G' is evidenced at ~ 100 Pa, followed by a steep increase towards 1000 Pa that is accompanied by a slight increase in G'' . The data suggest that at ~ 100 Pa, rearrangement around the bioslurry fuels' network structures do take place although the bioslurry fuels are still dominantly fluid-like. The values of δ for all measurement in stress sweep fall within 0° to 90° which is typical for viscoelastic material.¹⁸⁶

In order to further validate the fuels viscoelastic dependence on frequency, a set of frequency sweep experiment was then conducted for BO-10% and BOR 0.67-10% at stress 4.0 Pa and frequency 0.1-10 Hz, with the results presented in Figure 7-9.

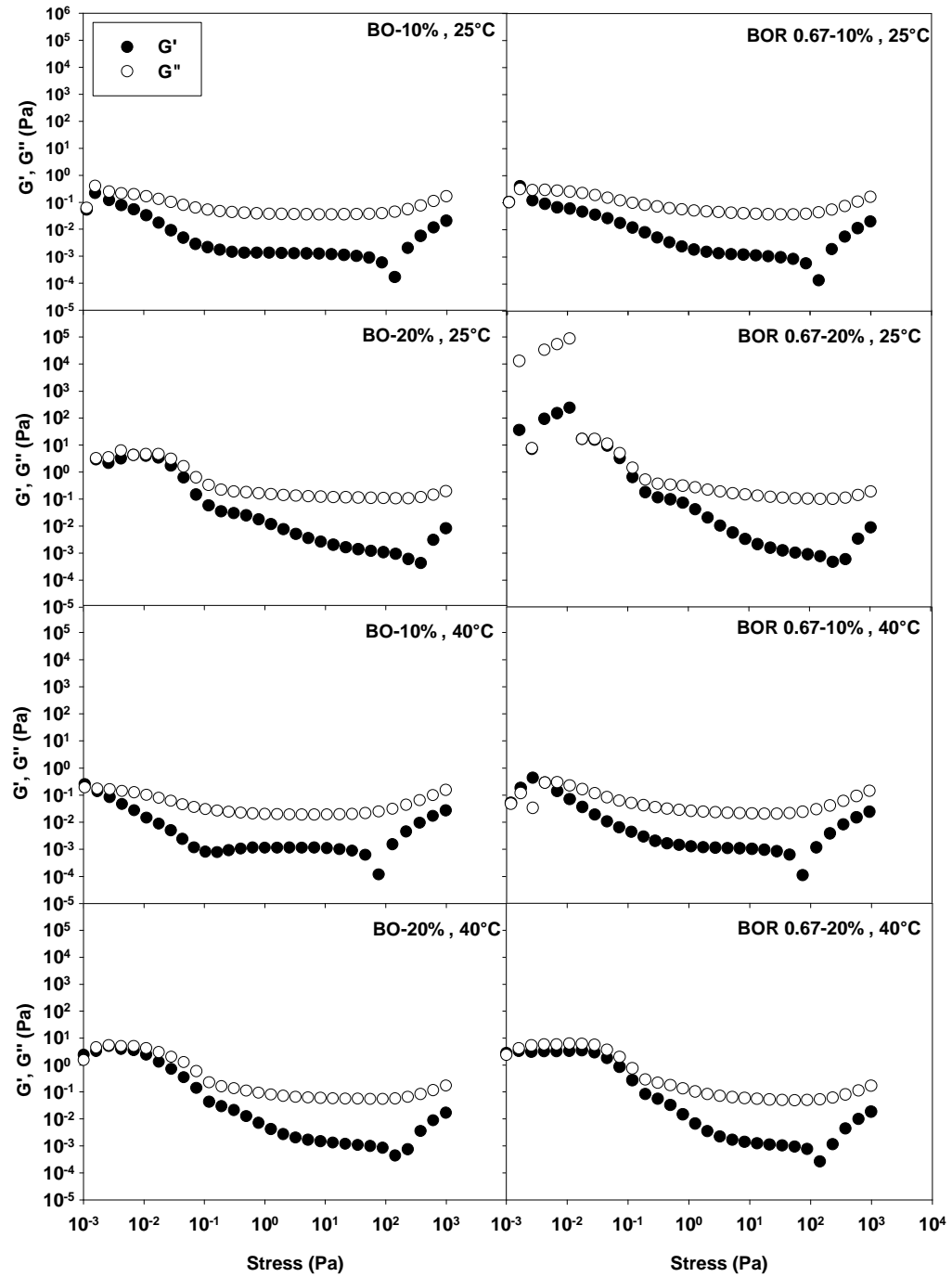


Figure 7-8 Storage (G') and loss (G'') moduli of fuels as a function of stress. BO-10% and BO-20% – bioslurry fuels prepared from the whole bio-oil with 10 wt% and 20 wt% biochar loading, respectively; BOR 0.67-10% and BOR 0.67-20% – bioslurry fuels prepared from bio-oil rich fraction after biodiesel extraction (at a biodiesel to bio-oil ratio of 0.67) with 10 wt% and 20 wt% biochar loading, respectively.

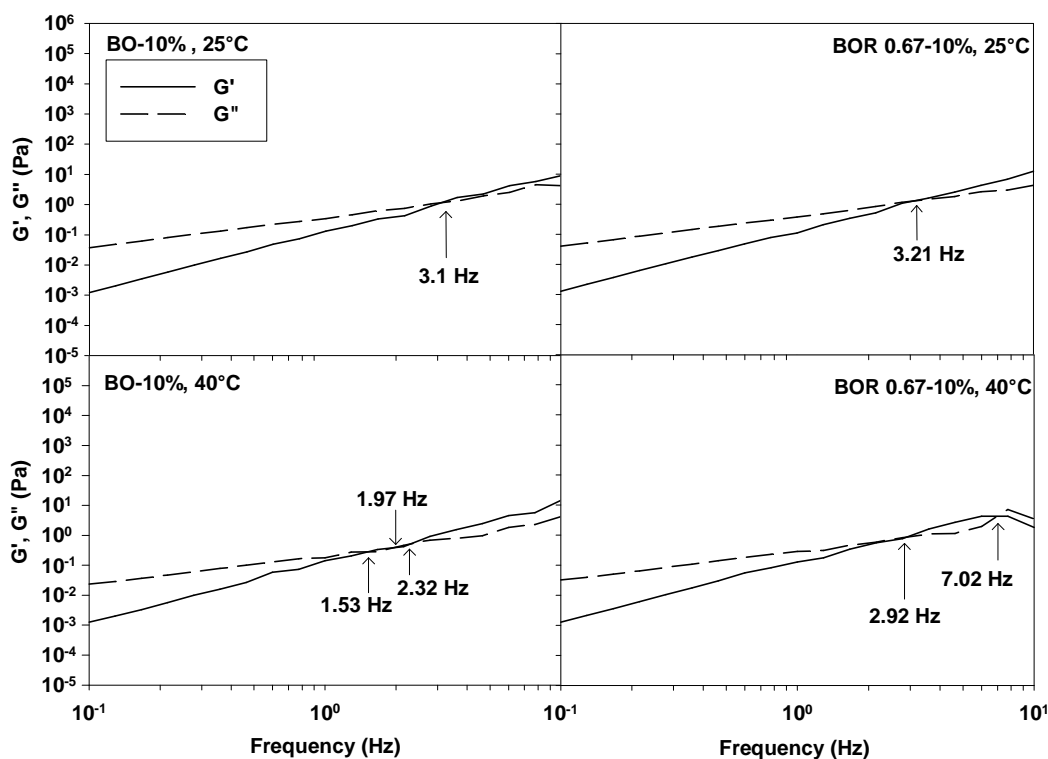


Figure 7-9 Storage (G') and loss (G'') moduli of fuels as a function of frequency. BO-10% and BO-20% – bioslurry fuels prepared from the whole bio-oil with 10 wt% and 20 wt% biochar loading, respectively; BOR 0.67-10% and BOR 0.67-20% – bioslurry fuels prepared from bio-oil rich fraction after biodiesel extraction (at a biodiesel to bio-oil ratio of 0.67) with 10 wt% and 20 wt% biochar loading, respectively.

Initially, $G'' > G'$ and the magnitudes for both moduli are very small. However, for bioslurry fuels, a strong dependence of the moduli on frequency is clearly evidenced. As frequency increases, both moduli increased rapidly whereby G' increased at greater rate than G'' . At 25°C, the crossover frequency (G' is equal to G'') for BO-10% and BOR 0.67-10% is very similar that is 3.1 Hz and 3.21 Hz respectively, suggesting the transition of the network structures from fluid to solid-like materials.¹⁸⁶ Furthermore, at 40°C, for the bioslurry fuel prepared from the whole bio-oil with 10% biochar loading (i.e. BO-10%), the crossovers occur at three frequencies, i.e 1.52 Hz, 1.97 Hz and 2.32 Hz while at frequencies > 2.32 Hz, the bioslurry fuel shows gel-like behaviour. However, at 40°C, for the corresponding bioslurry fuels prepared from the bio-oil rich phases (i.e. BOR 0.67-10%), the first

crossover occurs at a much higher frequency of 2.92 Hz where, the material change to solid-like beyond this value and before the network structure rearranged again to fluid-like behaviour at 7.02 Hz.

As shown in Figure 7-10, the bioslurry fuels prepared at 10% char loading show a typical viscoelastic behaviour in which the $\tan \delta$ value steeply decreases with increasing frequency until it reaches a plateau at frequency $> \sim 2.0$ Hz. The dotted line marks $\tan \delta = 1^\circ$ ($G'' = G'$) in the figure which indicates the gel point, crossover of solid-state and liquid-state. A case of $\tan \delta > 1$ ($G'' > G'$) indicates the behaviour of a viscoelastic liquid while that of $\tan \delta < 1$ ($G' > G''$) shows behaviour of a viscoelastic gel/solid.¹⁸⁶ Obviously, the values of $\tan \delta$ also depend on the temperature, as shown in Figure 7-10 for the BO-10% and BOR 0.67-10% bioslurry fuels. At 40°C, the gel point for BO-10% occurred at lower frequency (but for BOR 0.67 at higher frequency) than those at 25°C, respectively.

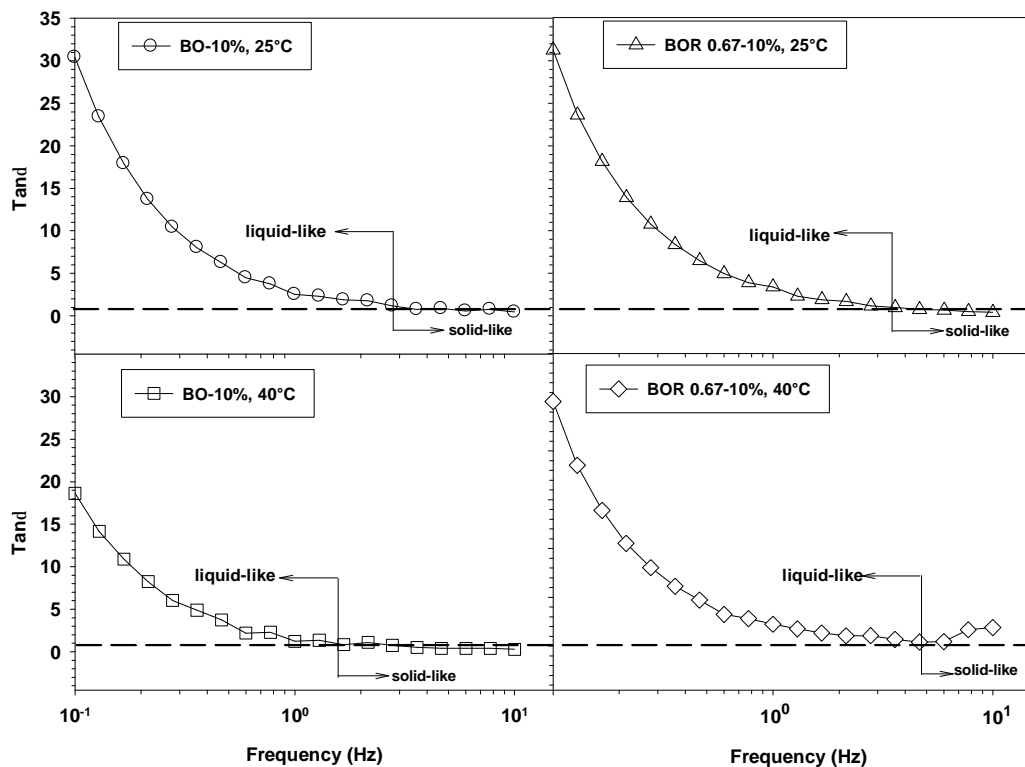


Figure 7-10 Value of fuels $\tan \delta$ as a function of frequency. BO-10% – bioslurry fuels prepared from the whole bio-oil with 10wt% biochar loading; BOR 0.67-10% – bioslurry fuels prepared from bio-oil rich fraction after biodiesel extraction (at a biodiesel to bio-oil ratio of 0.67) with 10 wt% biochar loading

7.4 Implications

Table 7-5 presented a summary of results in this study to compare bioslurry fuels properties prepared using the bio-oil rich fractions (BOR 0.67 as an example), with those prepared from the whole bio-oil. In most of the key fuel properties such as density, volumetric energy density, static stability, viscosity and fluid behaviour, the bioslurry fuel prepared from the bio-oil rich phase have fuel properties that are similar to (if not better than) those prepared from the whole bio-oil. Therefore, the comparisons in Table 7-5 clearly suggest that it is viable and favourable to utilise the bio-oil rich phases after biodiesel extraction for producing bioslurry fuels.

Table 7-5 Summary of bioslurry fuels prepared using bio-oil rich fractions, benchmarking against those prepared using the whole bio-oil

Property	Bioslurry derived from bio-oil rich fraction	Bioslurry derived from the whole bio-oil
density (Tonne/m ³)	1.20-1.25	1.20-1.24
volumetric energy density (GJ/m ³)	~22-24	~22-24
equilibrium surface tension (mN/m)	32.0-35.0	31.5-33.6
viscosity at 100s ⁻¹ (mPa.s)	max ~178	max ~206
viscosity at 1000 s ⁻¹ (mPa.s)	max ~ 69	max ~ 63
static stability, %	~72 %	~72%
fluid behaviour	non-Newtonian pseudoplastic, dominantly fluid-like in LVE region	non-Newtonian pseudoplastic, dominantly fluid-like in LVE region
Ohnesorge number	0.58-1.33	0.60-1.20

The new strategy firstly involves blending of bio-oil with biodiesel in a vessel for extraction. After extraction, due to the immiscible nature, phase separation takes place in the vessel to form a biodiesel rich fraction (top layer) and the residue bio-oil rich fraction (the bottom layer). The biodiesel rich fraction in the top layer contains the desirable fractions (relatively high value and small volume) of bio-oil that have been extracted into biodiesel, and is a good biodiesel/bio-oil blend that has been demonstrated as a suitable liquid transportation fuel.^{106,176} The bio-oil rich fraction

(relatively low value and high volume) in the bottom layer is the fractions of bio-oil and is more suitable to be mixed with biochar (after grinding) for producing bioslurry fuels for combustion and gasification applications.

Therefore, based on the results in this paper, a new strategy is proposed for more effective and better utilisation of bio-oil from biomass fast pyrolysis, as shown in Figure 7-11.

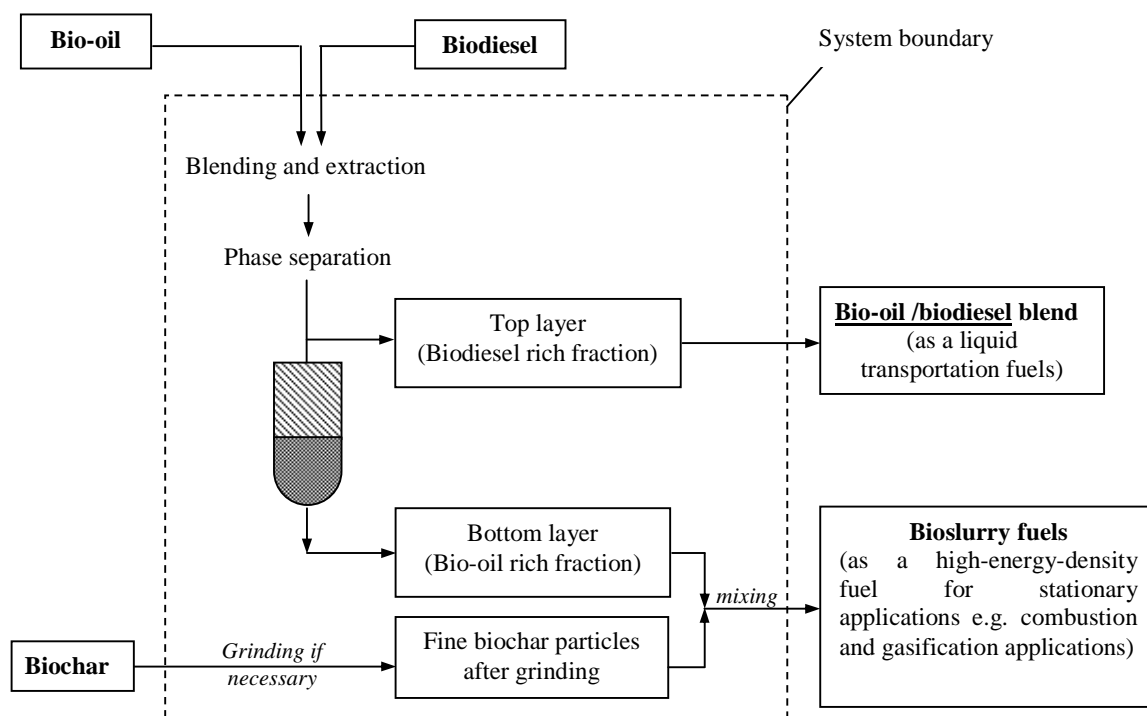


Figure 7-11 A proposed strategy for the coproduction of biodiesel/bio-oil blend (as a liquid transport fuel) and bioslurry fuel (as a high-energy-density fuel for combustion and gasification applications) from bio-oil and biochar products of biomass fast pyrolysis

7.5 Conclusions

This study demonstrates the feasibility of utilising the bio-oil rich fractions from bio-oil/biodiesel extraction for the production of bioslurry fuels. Via bio-oil/biodiesel extraction, the phenolic compounds in bio-oil extracted into biodiesel reduce surface tension of the resulted biodiesel rich fractions (i.e. the biodiesel/bio-oil blends). Bio-oil/biodiesel extractions at low biodiesel to bio-oil mass ratios lead to little changes

in the heating values of the resultant bio-oil rich fractions. Mostly important, this study shows that such bio-oil rich fractions were suitable to be mixed with ground biochar for preparing bioslurry fuels. The bioslurry fuels prepared using the bio-oil rich fraction after biodiesel/bio-oil extraction (biodiesel to bio-oil ratio 0.67) have similar fuel quality in compared to those prepared using the whole bio-oil. Bioslurry fuels derived from both media have good atomisation quality, stability, and pumpability. Based on estimated Ohnesorge number under similar condition, BO-20% and BOR 0.67-20% are estimated to produce droplets with SMDs of ~51% and ~46% smaller than heavy fuel oil respectively. The bioslurry fuels also dominantly behave like fluid in the linear viscoelastic region with $G'' > G'$. Results of steady and dynamic measurement indicate that bioslurry fuels produced in this study have favourable rheological behaviour for fuel handling and atomisation. A new bio-oil utilisation strategy is then proposed via coproduction of a biodiesel/bio-oil blend, which incorporates extractable bio-oil compounds into the blend and can be used as a liquid transportation fuel, and a bioslurry fuel that is prepared by mixing the rest low-quality bio-oil rich fraction with ground biochar and can be used as a high-energy-density fuel for applications e.g. stationary combustion and gasification.

CHAPTER 8

CONCLUSIONS AND RECOMMENDATIONS

8.1 Introduction

In this chapter, the key findings are highlighted to conclude the present study. This research has obtained essential knowledge on mallee biomass pre-treatment via low-temperature pyrolysis to produce high-energy-density fuels. Such a strategy addresses the undesired features of biomass that impose key hurdles in the wide adoption of biomass in the efficient and effective utilisation for power generation. These undesired features of biomass as a direction fuel include its bulky and fibrous nature, low grindability, low volumetric energy density and fuel chemistry mismatch with coal. The versatility of the pyrolysis process within a moderate temperature window successfully produced high-energy-density and high quality solid and/or liquid biofuels which offer clear advantages over green biomass. The excellent grindability of mallee biochar measured with ball milling technique was firstly reported in this field. Such a finding is of great importance to elucidate the transformation of bulky, low energy density mallee green biomass into a more homogenised high volumetric energy biofuel favourable for transport. The significant difference in structural, fuel chemistry and grindability among biochars produced from various mallee components were also revealed. Using bio-oil and the ground biochar to prepare bioslurry fuels also opens an opportunity to achieve drastic fuel energy densification and good fuel matching in biomass/coal co-processing applications. This study also developed an innovative strategy to coproduce a transport liquid fuel and a bioslurry fuel by extracting the high quality bio-oil compounds into biodiesel and employing the residual low-quality bio-oil rich fraction for a bioslurry fuel which is suitable for combustion and gasification applications. This chapter also provides some recommendations for future research in this area.

8.2 Conclusions

8.2.1 Properties and Grindability of Biochar Produced from the Pyrolysis of Mallee Wood Biomass under Slow-heating Conditions

- After pyrolysis, the fuel properties (e.g. fuel chemistry and grindability) of biochar depend strongly on pyrolysis temperature.
- Even at a pyrolysis temperature as low as 320°C, the biochar produced has fuel chemistry similar to Collie coal. At higher temperatures, biochar with even better fuel chemistry thus higher heating value was produced.
- In comparison to that of biomass, the grindability of biochar is drastically improved at pyrolysis temperatures of 300-330°C but only slight further improvement was evidenced at temperature >330°C.
- The excellent grindability of biochar leads to effective size reduction, enabling significant fuel energy densification by a factor of 2 compared to biomass.
- Volumetric energy densities of ground biochars (at pyrolysis temperatures > 330°C) are ~17-23 GJ/m³, comparable to that of Collie coal (~17 GJ/m³).
- Based on our estimation, the excellent grindability of biochar can significantly reduce fuel milling energy consumption by up to 93% in comparison to that of green biomass. The similarities in grindability between biochars and Collie coal indicate that it is possible to co-mill biochar with coal using conventional ball mills infrastructure in coal-based power stations.
- Ground biochar particles have favourable shapes which have a high roundness and a low aspect ratio similar to those of Collie coal, favourable for achieving easy fuel handling, good fluidisation and better conversion during combustion/gasification

8.2.2 Significant Differences in Fuel Quality and Ash Properties of Biochars from Various Biomass Components of Mallee Trees

- Mallee biomass that was harvested from a whole mallee tree consists of three major biomass components, i.e. wood (60 wt% dry base, db), leaf (27 wt% db) and bark (13 wt% db).
- The distribution of the pyrolysis products during the pyrolysis of wood, bark and leaf varies significantly from component to component. The pyrolysis of mallee bark gives the highest biochar yield. The nitrogen and sulphur contents of all biochars were well below guideline limits for combustion applications.
- While bark only makes up ~13% of the whole biomass, its biochars has the highest ash content (~7%, as received). The knowledge on ash-forming species in biochar is also essential to understanding ash-related issues associated with biochar utilisation as a fuel.
- The grindability of biochars obtained from individual components increases with pyrolysis temperature. Bark biochars have the highest grindability. While the grinding bark and wood biochars leads to a more even particle size distribution, that of leaf biochars results in a distinct multiple-peaks particle size distribution.
- The biological structure of the parent biomass plays a key role to determine grindability behaviour of the biochars prepared from leaf, wood and bark. Raw bark and wood appear more homogenous in their biological structure while leaf has a heterogeneous structure with a large number of oil glands widely distributed in leaf. While wood and bark biochars exhibit diminished cell boundary due to pyrolysis, the oil glands in cross sections of leaf biochars are still clearly intact even at a pyrolysis temperature of 800°C.
- The large number of oil glands in leaf is the most likely reason responsible for the poorer grindability of leaf biochars in comparison to wood and bark biochars. This is reflected in less volumetric energy densification for ground

leaf biochars. For example, leaf biochar obtained from pyrolysis at 500°C has a energy density of ~14 GJ/m³ compared to ~22 GJ/m³ for wood biochar obtained under similar conditions.

- Under the conditions (slow heating, large particle size), almost 100% of AAEM species in the biomass are retained in the biochars after pyrolysis at 300-500°C. Bark biochars have the highest ash and calcium content. Leaf biochars have high potassium and sodium contents while wood biochars have low ash and AAEM species. Based on Si/K and Ca/K ratios of biochars, wood biochars have a high slagging propensity, followed by bark biochars and leaf biochars.
- The data indicate that in the utilisation of bulk biochar from the whole mallee biomass, leaf biochar is more likely to impose grinding issue while ash related problems (if any) would be possibly arisen from wood and bark biochars.

8.2.3 Fuel and Rheological Properties of Bioslurry Prepared from the Bio-oil and Biochar of Mallee Biomass Fast Pyrolysis

- This study successfully demonstrated the preparation of bioslurry fuels from a mixture of bio-oil with biochar at various biochar loading (8-20 wt%).
- Due to its excellent grindability, the biochar can easily ground to produce a particle size distribution of 88% < 75µm, meeting the size requirement for combustion/gasification applications. The ground biochar is very porous with ~35% of the pore volume are mesopores so that it has a high bio-oil soakability (~1.4 time of its weight).
- Bioslurry with 20 wt% biochar loading achieves a volumetric energy density of ~23 GJ/m³, considerably higher than ~5 GJ/m³ for green chipped biomass.
- The concentrations of N, S, Ca and K in the prepared bioslurry can be estimated from those of biochar and bio-oil and are well below the guidelines limits for combustion and gasification requirement.

- All bioslurry samples prepared in this study have good stability > 70% as required for combustion/gasification applications. These fuels also have desired rheological properties. The slurry fuels have maximum viscosity < 453 mPa.s when measured at 25°C and 50°C, well below the guideline limits (1000 mPa.s for boilers and 700 mPa.s for gasifiers).
- The dependence of viscosity and shear stress with shear rate indicates that bioslurry fuels have non-Newtonian pseudoplastic or shear thinning behaviour. This is favourable for high pressure accumulator-type injection system. At a higher biochar loading, bioslurry fuels show more deviations from Newtonian behaviour.
- Bioslurry fuels at biochar loadings of 14-20wt% also exhibit thixotropic behaviour that is related to the break-up of spatial structures between char particles and multiphase domain in bio-oil medium. Such a behaviour is consistent with other slurry fuels reported in the literature.

8.2.4 Preparation of Bioslurry Fuels from Biochar and the Bio-oil Rich Fractions after Bio-oil/Biodiesel Extraction

- An innovative strategy has been proposed for alternative approach of bio-oil utilisation and bioslurry fuels preparation. It has demonstrated the feasibility to first extract high quality bio-oil compounds into biodiesel then use the residual bio-oil rich fraction for preparing bioslurry fuels.
- The bio-oil rich fractions is significantly higher than the original bio-oil and biodiesel before extraction, suggesting that water can be produced by either certain reactions during extraction or interference of certain chemicals from bio-oil (e.g. aldehyde, ketones and acetic acid) during Karl Fischer titration.
- During bio-oil/biodiesel extraction, up to ~21 % of bio-oil can be extracted by biodiesel at an extraction ratio of 4.0. After extraction, phase separation leads to two layers. However, practically, it is difficult to achieve complete separation of the biodiesel rich fraction (top) and the bio-oil rich fraction

(bottom) due to the affinity of fine char particles in bio-oil towards the bio-oil/biodiesel interface.

- Bio-oil/biodiesel extraction at low extraction ratios (i.e. 0.25 and 0.67) leads to minimal changes in C, H and O contents and heating values of the bio-oil rich fractions. The bioslurry fuels also have low sulphur and nitrogen contents which are well below the guideline (S <0.1 wt%, N <0.4 wt%).
- GC-MS data demonstrated that mainly bio-oil phenolic compounds are extracted into the biodiesel rich fractions (biodiesel/bio-oil blends). The extracted phenolates appear to play a positive role in lowering surface tension of biodiesel rich fractions.
- The volumetric energy densities of bioslurry fuels prepared using the whole bio-oil or the bio-oil rich fractions are similar, up to $\sim 24 \text{ GJ/m}^3$ significantly higher than that of the green chipped biomass ($\sim 5 \text{ GJ/m}^3$).
- The extraction process has minimal effect on density and stability of the resulted bioslurry fuels prepared from the bio-oil rich fractions. It was estimated that atomisation of BO-20% and BOR 0.67-20% produce much smaller droplets with significant reductions in Sauter Mean Diameters by $\sim 51\%$ and $\sim 46\%$ respectively compared to heavy fuel oil.
- All bioslurry fuels prepared in this study can be pumped safely with viscosity obtained at 100s^{-1} was $\sim 300 \text{ mPa}\cdot\text{s}$ at 25°C and $<200 \text{ mPa}\cdot\text{s}$ at 40°C much less than the guideline number i.e $1000 \text{ mPa}\cdot\text{s}$ and $700 \text{ mPa}\cdot\text{s}$.
- All slurry fuels demonstrated a non Newtonian pseudoplastic behaviour and the bioslurry prepared from bio-oil rich fraction exhibit more deviations from Newtonian behaviour than that from the whole bio-oil.
- A series of stress sweep experiments show that all bioslurry fuels exhibit clear viscoelasticity behaviour with value of $0^\circ < \delta < 90^\circ$ and dominantly fluid-like behaviour with $G'' > G'$ in the linear viscoelastic region. Such a slurry fluid

behaviour is favourable to produce small droplets, in agreement with the estimated results on Sauter Mean Diameter in fuel atomisation

- The bioslurry fuels also show the strong dependence of its fluid behaviour on frequency in frequency sweep experiments. At an increasing frequency, the value of $\tan \delta$ decrease drastically before reaching a plateau at frequency $> \sim 2.0$ Hz that mark $\tan \delta = 1$ or gel point, indicating the transition of fluid-like to gel-like behaviour of viscoelastic material.

8.3 Recommendations

Based on the data collected in this study, various new research gaps have also been identified leading to recommendations for future research as follows:

1. In this study, the grindability experiments were carried out using a small lab-scale ball mill. While the results are sufficient to compare the grindability of various fuels, future experiments at a large-scale is required, particularly for the estimation of grinding energy consumption. Experiments should also be carried out for both the grinding of individual fuels and the co-milling of biochar/coal.
2. For overall fuel supply chain and application of mallee biomass components, other co-production strategy can be considered for better use of the biomass and overcome some of the limitations observed in the present study. For example, apart from using whole mallee leaf biomass directly from the field as feedstock, one approach is to use spent leaf i.e. leaf residue after distillation of eucalyptus oil as a value-added product. Since the extraction of eucalyptus oil involves exudation the oil from leaf oil gland therefore the oil gland are ruptured during the process, it will be interesting to know if spent leaf produces biochar with improved grindability in comparison to those prepared from whole leaf. Since distillation requires either boiling the leaf in water (hydrodistillation) or heating it in hot steam (steam distillation) which is believed to leach out some of the ash forming species, the effect of this ash reduction in subsequent applications of spent biomass-derived biochar especially appears also to be favourable. Future study is recommended on these important aspects.

3. The fuel quality of biochar (Chapter 4 and 5) and bioslurry (Chapter 6 and 7) are below the guideline limits for combustion and gasification applications, However, combustion and/or gasification experiments need to be carried out to collect data for practical evaluations. Atomisation of bioslurry fuels need also be carried out to further validate the slurry atomisation/spray behaviour.
4. The current study highlight the utilisation of bio-oil rich fraction from bio-oil/biodiesel extraction ratio 0.67 to prepare bioslurry as an example of a new co-production strategy for bio-oil application to produce a transportation fuel and a bioslurry fuel. However, further experimental studies are required to evaluate the performance of these fuels in practical applications.

REFERENCES

- (1) ABARE; Australian Bureau of Agricultural and Resource Economics., 2008.
- (2) IPCC; Intergovernmental Panel on Climate Change, <http://www.ipcc.ch>, 2009.
- (3) IEA "World Energy Outlook 2009," OECD/IEA, 2009.
- (4) Van Loo, S.; Koppejan, J. *Biomass Combustion and Co-firing Handbook*; Twente University Press: Enschede, The Netherlands, 2002.
- (5) Yu, Y.; Wu, H. In *CHEMECA*: Newcastle, Australia., 2008.
- (6) Khan, A. A.; de Jong, W.; Jansens, P. J.; Spliethoff, H. *Fuel Processing Technology* **2009**, *90*, 21-50.
- (7) McIlveen-Wright, D. R.; Huang, Y.; Rezvani, S.; Mondol, J. D.; Redpath, D.; Anderson, M.; Hewitt, N. J.; Williams, B. C. *Fuel* **2011**, *90*, 11-18.
- (8) Bartle, J.; Abadi, A. *Energy & Fuels* **2010**, *24*, 2-9.
- (9) Bartle, J.; Olsen, G.; Don, C.; Trevor, H. *Int.J.Global Energy Issues* **2007**, *27*, 115-137.
- (10) Cooper, D. G.; Olsen, G.; J.R., B. *Aust. J. Exp. Agric.* **2005**, *45*, 1369-1388.
- (11) Sochaki, S. J.; Harper, R. J.; Smettem, K. R. J. *Biomass and Bioenergy* **2007**, *31*, 608-613.
- (12) Raison, R. J. *Biomass and Bioenergy* **2006**, *30*, 1021-1024.
- (13) Wu, H.; Qiang, F.; Rick, G.; Bartle, J. *Energy & Fuels* **2008**, *22*, 190-198.
- (14) O'Connell, D.; Batten, D.; O'Connor, M.; May, B.; Raison, J.; Keating, B.; Beer, T.; Braid, A.; Haritos, V.; Begley, C.; Poole, M.; Poulton, P.; Graham, S.; Dunlop, M.; Grant, T.; Campbell, P.; Lamb, D.; CSIRO, Ed.; Rural Industries Research and Development Corporation., 2007.
- (15) Wu, H.; Yu, Y.; Yip, K. *Energy & Fuels* **2010**, *24*, 5652-5659.
- (16) *Coal-Biomass Cofiring Handbook*; Moghtaderi, B.; Ness, J., Eds.; CRC for Coal in Sustainable Development: Kenmore, QLD, Australia 2007.
- (17) Baxter, L. L.; Miles, T. R.; Miles, T. R. J.; Jenkins, B. M.; Milne, T.; Dayton, D.; Bryers, R. W.; Oden, L. L. *Fuel Processing Technology* **1998**, *54*, 47-78.
- (18) Miller, S. F.; Miller, B. G. *Fuel Processing Technology* **2007**, *88*, 1155-1164.
- (19) Maciejewska, A.; Veringa, H.; Sanders, J.; Peteves, S. D. "Co-firing of Biomass with Coal: Constraints and Role of Biomass Pre-treatment," DG JRC Institute for Energy, 2006.
- (20) Yu, Y.; Bartle, J.; Li, C.-Z.; Wu, H. *Energy & Fuels* **2009**, *23*, 3290-3299.
- (21) Allen, J.; Browne, M.; Hunter, A.; Boyd, J.; Palmer, H. *International Journal of Physical Distributions & Logistics Management* **1998**, *28*, 463-477.
- (22) Sami, M.; Annamalai, K.; Wooldridge, M. *Progress in Energy and Combustion Science* **2001**, *27*, 171-214.
- (23) NAFI In *Wood Waste Bioenergy Information Sheet No.9*; The National Association of Forest Industries.
- (24) Fagernäs, L.; Brammer, J.; Wilén, C.; Lauer, M.; Verhoeff, F. *Biomass and Bioenergy* **2010**, *34*, 1267-1277.
- (25) Wang, X.; Chen, H.; Luo, K.; Shao, J.; Yang, H. *Energy & Fuels* **2008**, *22*, 67-74.

- (26) Davidsson, K. O.; Korsgren, J. G.; Pettersson, J. B. C.; Jaglid, U. *Fuel* **2002**, *81*, 137-142.
- (27) Arvelakis, S.; Vourliotis, P.; Kakaras, E.; Koukios, E. G. *Biomass and Bioenergy* **2001**, *20*, 459-470.
- (28) Esteban, L. S.; Carrasco, J. E. *Powder Technology* **2006**, *166*, 139-151.
- (29) Mani, S.; Tabil, L. G.; Sokhansanj, S. *Bioresource Technology* **2006**, *97*, 1420-1426.
- (30) Finney, K. N.; Sharifi, V. N.; Swithenbank, J. *Energy & Fuels* **2009**, *23*, 3195-3202.
- (31) Finney, K. N.; Sharifi, V. N.; Swithenbank, J. *Energy & Fuels* **2009**, *23*, 3203-3210.
- (32) Lehtikangas, P. *Biomass and Bioenergy* **2001**, *20*, 351-360.
- (33) Prins, M. J.; Ptasinski, K. J.; Janssen, F. J. J. G. *Journal of Analytical and Applied Pyrolysis* **2006**, *77*, 35-40.
- (34) Bergman, P. C. A.; Boersma, A. R.; Kiel, J. H. A.; Prins, M. J.; Ptasinski, K. J.; Janssen, F. J. J. G. "Torrefaction for entrained-flow gasification of biomass," Energy Research Centre of the Netherlands 2005.
- (35) Phanphanich, M.; Mani, S. *Bioresource Technology* **2011**, *102*, 1246-1253.
- (36) Bridgeman, T. G.; Jones, J. M.; Shield, I.; Williams, P. T. *Fuel* **2008**, *87*, 844-856.
- (37) Uslu, A.; Faaij, A. P. C.; Bergman, P. C. A. *Energy* **2008**, *33*, 1206-1223.
- (38) Raveendran, K.; Ganesh, A.; Khilar, K. C. *Fuel* **1996**, *75*, 987-998.
- (39) Yaman, S. *Energy Conversion and Management* **2004**, *45*, 651-671.
- (40) Müller-Hagedorn, M.; Bockhorn, H. *Journal of Analytical and Applied Pyrolysis* **2007**, *79*, 136-146.
- (41) Bridgewater, A. V. *Thermal Science* **2004**, *8*, 21-49.
- (42) Balat, M.; Balat, M.; Kirtay, E.; Balat, H. *Energy Conversion and Management* **2009**, *50*, 3147-3157.
- (43) Arias, B.; Pevida, C.; Feroso, J.; Plaza, M. G.; Rubiera, F.; Pis, J. J. *Fuel Processing Technology* **2008**, *89*, 169-175.
- (44) Baxter, L. *Fuel* **2005**, *84*, 1295-1302.
- (45) Baxter, L. L. *Biomass and Bioenergy* **1993**, *4*, 85-102.
- (46) Bridgewater, A. V. *Chemical Engineering Journal* **2003**, *91*, 87-102.
- (47) Chiaramonti, D.; Oasmaa, A.; Solantausta, Y. *Renewable and Sustainable Energy Reviews* **2007**, *11*, 1056-1086.
- (48) Felfli, F. F.; Luengo, A. C.; Suarez, J. A.; Beaton, P. A. *Energy for Sustainable Development* **2005**, *IX*, 19-22.
- (49) Jensen, P. A.; Sander, B.; Dam-Johansen, K. *Biomass and Bioenergy* **2001**, *20*, 431-446.
- (50) Zhang, L.; Xu, C.; Champagne, P. *Energy Conversion and Management* **2010**, *51*, 969-982.
- (51) Svoboda, K.; Pohorelý, M.; Hartman, M.; Martinec, J. *Fuel Processing Technology* **2009**, *90*, 629-635.
- (52) Huber, G. W.; Iborra, S.; Corma, A. *Chem. Rev.* **2006**, *106*, 4044-4098.
- (53) Vassilev, S. V.; Baxter, D.; Andersen, L. K.; Vassileva, C. G. *Fuel* **2009**, *89*, 913-933.
- (54) Fry, S. C. *The Growing Plant Cell Wall*; The Blackburn Press: New Jersey, U.S.A., 1988.
- (55) Mohan, D.; Pittman, C. U.; Steele, P. H. *Energy & Fuels* **2006**, *20*, 846-889.

- (56) ABS; The Australian Bureau of Statistics 2009.
- (57) Stamatov, V.; Honnery, D.; Soria, J. *Renewable Energy* **2006**, *31*, 2108-2121.
- (58) Bernesson, S.; Nilsson, D.; Hansson, P. A. *Biomass and Bioenergy* **2004**, *26*.
- (59) Rustandi, F.; Wu, H. *Ind. Eng. Chem. Res.* **2010**, *49*, 11785-11796.
- (60) Clarke, C. J.; George, R. J.; Bell, R. W.; Hatton, T. J. *Aust. J. Soil Res.* **2002**, *40*, 93-113.
- (61) Shea, S.; University of Notre Dame, representing The Oil Mallee Company of Australia Ltd and CO₂ Australia Limited, 2003.
- (62) Photo Gallery. http://www.oilmallee.org.au/index.php/site/media-centre#photo_gallery (accessed on November 17, 2010).
- (63) Spliethoff, H.; Hein, K. R. G. *Fuel Processing Technology* **1998**, *54*, 189-205.
- (64) Demirbas, A. *Energy Conversion and Management* **2003**, *44*, 1465-1479.
- (65) Jenkins, B. M.; Baxter, L. L.; Miles, T. R. J.; Miles, T. R. *Fuel Processing Technology* **1998**, *54*, 17-46.
- (66) McKendry, P. *Bioresource Technology* **2002**, *83*, 37-46.
- (67) Demirbas, A. *Progress in Energy and Combustion Science* **2004**, *30*, 219-230.
- (68) Nordin, A. *Biomass and Bioenergy* **1994**, *6*, 339-347.
- (69) Arvelakis, S.; Gehrmann, H.; Beckmann, M.; Koukios, E. G. *Biomass and Bioenergy* **2005**, *28*, 331-338.
- (70) Gabra, M.; Pettersson, E.; Backman, R.; Kjellström, B. *Biomass and Bioenergy* **2001**, *21*, 351-369.
- (71) Zulfqar, M. H.; Moghtaderi, B.; Wall, T. F. "Co-milling of coal and biomass in pilot-scale vertical spindle mill," Cooperative Research Centre for Coal in Sustainable Development (CCSD), QCAT, Technology Transfer Centre, Pullenvale, Queensland., 2006.
- (72) Prinzing, D. E.; Hunt, E. F. *Fuel Processing Technology* **1998**, *54*, 143-157.
- (73) Hughes, E. E.; Tillman, D. A. *Fuel Processing Technology* **1998**, *54*, 127-142.
- (74) Boylan, D. M. *Biomass and Bioenergy* **1996**, *10*, 139-147.
- (75) Ryu, C.; Yang, Y. B.; Khor, A.; Yates, N. E.; Sharifi, V. N.; Swithenbank, J. *Fuel* **2006**, *85*, 1039-1046.
- (76) Senelwa, K.; Sims, R. E. H. *Biomass and Bioenergy* **1999**, *17*, 127-140.
- (77) Rothpfeffer, C.; Karlton, E. *Biomass and Bioenergy* **2007**, *31*, 717-725.
- (78) Pérez, S.; Renedo, C. J.; Ortiz, A.; Mañana, M.; Silió, D. *Thermochimica Acta* **2006**, *451*, 57-64.
- (79) Monti, A.; Di Virgilio, N.; Venturi, G. *Biomass and Bioenergy* **2008**, *32*, 216-223.
- (80) Enecon Pty Ltd "Integrated Tree Processing for Mallee Eucalypts. A Report for the RIRDC/Land & Water Australia/FWPRDC Joint Venture Agroforestry Program," RIRDC, 2001.
- (81) Mani, S.; Tabil, L. G.; Sokhansanj, S. *Biomass and Bioenergy* **2006**, *30*, 648-654.
- (82) Kobayashi, N.; Guilin, P.; Kobayashi, J.; Hatano, S.; Itaya, Y.; Mori, S. *Powder Technology* **2008**, *180*, 272-283.
- (83) Jenkins, B. M.; Bakker, R. R.; Wei, J. B. *Biomass and Bioenergy* **1996**, *10*, 177-200.

- (84) Turn, S. Q.; Kinoshita, C. M.; Ishimura, D. M. *Biomass and Bioenergy* **1997**, *12*, 241-252.
- (85) Allica, J. H.; Mitre, A. J.; Bustamante, J. A.; Itoiz, C.; Balnco, F.; Alkorta, I.; Garbisu, C. *Biomass and Bioenergy* **2001**, *21*, 249-258.
- (86) Jensen, P. A.; Sander, B.; Dam-Johansen, K. *Biomass and Bioenergy* **2001**, *20*, 447-457.
- (87) Yaman, S.; Sahan, M.; Haykiri-açma, H.; Sesen, K.; Küçükbayrak, S. *Fuel Processing Technology* **2000**, *68*, 23-31.
- (88) Yaman, S. *Fuel Processing Technology* **2001**, *72*, 1-8.
- (89) Kaliyan, N.; Morey, R. V. *Fuel Processing Technology*, *91*, 559-565.
- (90) Demirbas, A. *Energy* **1999**, *24*, 141-150.
- (91) Larsson, S. H.; Thyrel, M.; Geladi, P.; Lestander, T. A. *Bioresource Technology* **2008**, *99*, 7176-7182.
- (92) Kaliyan, N.; Vance Morey, R. *Biomass and Bioenergy* **2009**, *33*, 337-359.
- (93) Bridgeman, T. G.; Jones, J. M.; Williams, A.; Waldron, D. J. *Fuel* **2010**, *89*, 3911-3918.
- (94) Couhert, C.; Salvador, S.; Commandré, J. M. *Fuel* **2009**, *88*, 2286-2290.
- (95) A World Leader in Straw Bale Education. <http://www.strawbale.com/two-string-vs-three-string>(accessed on October 16, 2010).
- (96) Pellets and briquettes. <http://www.btgworld.com/index.php?id=115&rid=36&r=consultancy> (accessed on October 16, 2010).
- (97) What is Torrefication. <http://ecofuelsinc.net/technology/>(accessed on October 16, 2010).
- (98) Sinha, S.; Jhalani, A.; Ravi, M. R.; Ray, A. *J. Solar Energy Society of India* **2000**, *10*, 41-62.
- (99) Garcia-Perez, M.; Wang, X. S.; Shen, J.; Rhodes, M. J.; Tian, F.; Lee, W.; Wu, H.; Li, C. *Ind. Eng. Chem. Res.* **2008**, *47*, 1846-1854.
- (100) Garcia-Perez, M.; Wang, S.; Shen, J.; Rhodes, M.; Lee, W. J.; Li, C.-Z. *Energy & Fuels* **2008**, *22*, 2022-2032.
- (101) Boucher, M. E.; Chaala, A.; Roy, C. *Biomass and Bioenergy* **2000**, *19*, 337-350.
- (102) Luo, Z.; Wang, S.; Liao, Y.; Zhou, J.; Gu, Y.; Cen, K. *Biomass and Bioenergy* **2004**, *26*, 455-462.
- (103) Bridgewater, A. V.; Carson, P.; Coulson, M. *Int.J.Global Energy Issues* **2007**, *27*, 204-216.
- (104) Garcia-Perez, M.; Chaala, A.; Pakdel, H.; Kretschmer, D.; Rodrigue, D.; Roy, C. *J.Anal.Appl.Pyrolysis* **2007**, *78*, 104-116.
- (105) Agblevor, F. A.; Besler, S. *Energy & Fuels* **1996**, *10*, 293-298.
- (106) Garcia-Perez, M.; Adams, T. T.; Goodrum, J. W.; Geller, D. P. a. D., K.C. *Energy & Fuels* **2007**, *21*, 1827-2774.
- (107) Vivarelli, S.; Tondi, G. In *International Workshop Bioenergy for A Sustainable Development: Casino Vina del Mar-Chile*, 2004.
- (108) Yu, Y.; Wu, H. *Energy & Fuels* **2010**, *24*, 5660-5668.
- (109) Veal, C. J.; Wall, D. R. *Fuel* **1981**, *60*, 873-876.
- (110) Bienstock, D.; Jamgochian, E. M. *Fuel* **1981**, *60*, 851-864.
- (111) Cui, L.; An, L.; Jiang, H. *Fuel* **2008**, *87*, 2296-2303.
- (112) Umar, D. F.; Usui, H.; Komoda, Y.; Muta'alim *Fuel Processing Technology* **2009**, *90*, 611-615.

- (113) Shukla, S. C.; Kukade, S.; Mandal, S. K.; Kundu, G. *Fuel* **2008**, *87*, 3428-3432.
- (114) Atesok, G.; Boylu, F.; Sirkeci, A. A.; Dincer, H. *Fuel* **2002**, *81*, 1855-1858.
- (115) Boylu, F.; Dincer, H.; Atesok, G. *Fuel Processing Technology* **2004**, *85*, 241-250.
- (116) Liu, J.; Zhao, W.; Zhou, J.; Cheng, J.; Zhang, G.; Feng, Y.; Cen, K. *Fuel Processing Technology* **2009**, *90*, 91-98.
- (117) Oren, M. J.; MacKay, G. D. M. *Fuel* **1990**, *69*, 1326-1327.
- (118) Diebold, J. P.; Czernik, S. *Energy & Fuels* **1997**, *11*, 1081-1091.
- (119) Shaddix, C. R.; Hardesty, D. R. "Combustion Properties of Biomass Flash Pyrolysis Oils: Final Project Report, SAND99-8238" Sandia National Laboratories: Livermore, CA., 1999.
- (120) Garcia-Perez, M.; Chaala, A.; Pakdel, H.; Kretschmer, D.; Rodrigue, D.; Roy, C. *Energy & Fuels* **2006**, *20*.
- (121) Czernik, S.; Bridgewater, A. V. *Energy & Fuels* **2004**, *18*, 590-598.
- (122) Calabria, R.; Chiariello, F.; Massoli, P. *Experimental Thermal and Fluid Science* **2007**, *31*, 413-420.
- (123) Ikura, M.; Stanculescu, M.; Hogan, E. *Biomass and Bioenergy* **2003**, *24*, 221-232.
- (124) Blowes, E. I. J. H. "Evaluation of Complementary Technologies to Reduce Bio Engine Emissions. ETSU B/T1/00761/00/REP URN 02/1437," DTI New and Renewable Energy Programme, UK., 2003.
- (125) Henrich, E.; Weirich, F. *Env. Eng. Science* **2004**, *21*, 53-64.
- (126) Dynamotive BioOil Plus.
http://www.dynamotive.com/industrialfuels/biooil_plus/ (accessed on June 19, 2010).
- (127) Benter, M. M.; Gilmour, I. A.; Arnoux, L. *Biomass and Bioenergy* **1997**, *12*, 253-261.
- (128) Oasmaa, A.; Peacocke, C.; VTT Technical Research Centre of Finland ESPOO 2001, 2001.
- (129) Qi, Z.; Jie, C.; Tiejun, W.; Ying, X. *Energy Conversion and Management* **2007**, *48*, 87-92.
- (130) Chaala, A.; Ba, T.; Garcia-Perez, M.; Roy, C. *Energy & Fuels* **2004**, *18*, 1535-1542.
- (131) Oasmaa, A.; Czernik, S. *Energy & Fuels* **1999**, *13*, 914-921.
- (132) Oasmaa, A.; Kuoppala, E.; Selin, J.-F.; Gust, S.; Solantausta, Y. *Energy & Fuels* **2004**, *18*, 1578-1583.
- (133) Falcon, J.; Carbonell, J. *Energy & Fuels* **2003**, *17*, 302-307.
- (134) Jiang, X.; Ellis, N. *Energy & Fuels* **2010**, *24*, 1358-1364.
- (135) Jiang, X.; Ellis, N. *Energy & Fuels* **2010**, *24*, 2699-2706.
- (136) Yip, K.; Wu, H.; Zhang, D.-k. *Energy & Fuels* **2007**, *21*, 2883-2891.
- (137) Yip, K.; Wu, H.; Zhang, D.-k. *Energy & Fuels* **2007**, *21*, 419-425.
- (138) Emrich, W. *Handbook of Charcoal Making: The Traditional and Industrial Methods*; Springer, 1985.
- (139) Wu, H.; Wall, T.; Liu, G.; Bryant, G. *Energy & Fuels* **1999**, *13*, 1197-1202.
- (140) Wu, H.; Bryant, G.; Benfell, K.; Wall, T. *Energy & Fuels* **2000**, *14*, 282-290.
- (141) Wu, H.; Bryant, G.; Wall, T. *Energy & Fuels* **2000**, *14*, 745-750.
- (142) Yu, J.; Harris, D.; Lucas, J.; Roberts, D.; Wu, H.; Wall, T. *Energy & Fuels* **2004**, *18*, 1346-1353.

- (143) Wee, H. L.; Wu, H.; Zhang, D.-k. *Energy & Fuels* **2007**, *21*, 441-450.
- (144) Ngu, L.-n.; Wu, H.; Zhang, D.-k. *Energy & Fuels* **2007**, *21*, 3437-3445.
- (145) Yip, K.; Tian, F.; Hayashi, J.-i.; Wu, H. *Energy & Fuels* **2010**, *24*, 173-181.
- (146) Lievens, C.; Yperman, J.; Vangronsveld, J.; Carleer, R. *Fuel* **2008**, *87*, 1894-1905.
- (147) Apaydin-Varol, E.; Pütün, E.; Pütün, A. E. *Fuel* **2007**, *86*, 892-1899.
- (148) Onay, O. *Fuel Processing Technology* **2007**, *88*, 523-531.
- (149) Sensöz, S.; AngIn, D. *Bioresource Technology* **2008**, *99*, 5492-5497.
- (150) Zulfiqar, M., Moghtaderi, B., Wall, T.F. *Fuel Processing Technology* **2006**, *87*, 281-288.
- (151) Coppen, J.J.W. (Ed) *Eucalyptus: the genus Eucalyptus*; Taylor & Francis, 2002.
- (152) Obernberger, I.; Brunner, T.; Bärnthaler, G. *Biomass and Bioenergy* **2006**, *30*, 973-982.
- (153) King, D. J.; Gleadow, R. M.; Woodrow, I. E. *New Phytologist* **2006**, *172*, 440-451.
- (154) Blomberg, T. E. In *7th International Conference on Heat Exchanger Fouling and Cleaning-Challenges and Opportunities*; Engineering Conferences International Tomar, Portugal 2007.
- (155) Okuno, T.; Sonoyama, N.; Hayashi, J.-i.; Li, C.-Z.; C., S.; Chiba, T. *Energy & Fuels* **2005**, *19*, 2164-2171.
- (156) Öhman, M.; Nordin, A.; Hedman, H.; Jirjis, R. *Biomass and Bioenergy* **2004**, *27*, 597-605.
- (157) Al-Amrousi, F. A.; Al-Sabagh, A. M.; Magda, M. O. *Fuel* **1996**, *75*, 1193-1198.
- (158) Natarajan, V. P.; Suppes, G. J. *Fuel* **1997**, *76*, 1527-1535.
- (159) Raju, A. S. K.; Park, C. S.; Norbeck, J. M. *Fuel Processing Technology* **2009**, *90*, 330-336.
- (160) He, W.; Park, C. S.; Norbeck, J. M. *Energy & Fuels* **2009**, *23*, 4763-4767.
- (161) Li, W.; Li, W.; Liu, H. *Fuel* **2010**, *89*, 965-970.
- (162) Li, W.; Li, W.; Liu, H.; Yu, Z. *Fuel* **2009**, *88*, 2241-2246.
- (163) Carmi, S.; Ghassemzadeh, M. R. *Fuel* **1981**, *60*, 529-533.
- (164) Gan, H.; Nandi, S. P.; Walker Jr, P. L. *Fuel* **1972**, *51*, 272-277.
- (165) Elliott, D. C. *Biomass and Bioenergy* **1994**, *7*, 179-185.
- (166) Adiga, K. C.; Shah, D. O. *Colloids and Surfaces* **1982**, *4*, 271-284.
- (167) Tzanetakis, T.; Ashgriz, N.; James, D. F.; Thomson, M. J. *Energy & Fuels* **2008**, *22*, 2725-2733.
- (168) Guo, D.-h.; Li, X.-c.; Yuan, J.-s.; Jiang, L. *Fuel* **1998**, *77*, 209-210.
- (169) Barnes, H. A. *Journal of Non-Newtonian Fluid Mechanics* **1997**, *70*, 1-33.
- (170) Oren, M. J.; MacKay, G. D. M. *Fuel* **1986**, *65*, 644-646.
- (171) Calabria, R.; Chiariello, F.; De Bellis, V.; Massoli, P. In *4th Mediterranean Combustion Symposium*: Lisbon, Portugal, 2005.
- (172) Wang, J.-J.; Chang, J.; Fan, J. *Energy & Fuels* **2010**, *24*, 3251-3255.
- (173) Hilten, R. N.; Bibens, B. P.; Kastner, J. R.; Das, K. C. *Energy & Fuels* **2010**, *24*, 673-682.
- (174) Elliott, D. C. *Energy & Fuels* **2007**, *21*, 1792-1815.
- (175) Oasmaa, A.; Kuoppala, E.; Ardiyanti, A.; Venderbosch, R. H.; Heeres, H. J. *Energy & Fuels* **2010**, *24*, 5264-5272.

- (176) García-Perez, M.; Shen, J.; Shan Wang, X.; Li, C.-Z. *Fuel Processing Technology* **2010**, *91*, 296-305.
- (177) Bruttel, P.; Schlink, R. *Water Determination by Karl Fischer Titration*; Metrohm Ltd.: Herisau, Switzerland, 2003-09; Vol. 8.026.5003.
- (178) Oasmaa, A.; Kuoppala, E. *Energy & Fuels* **2003**, *17*, 1075-1084.
- (179) Ba, T.; Chaala, A.; Garcia-Perez, M.; Roy, C. *Energy & Fuels* **2004**, *18*, 188-201.
- (180) Lefebvre, A. H. *Progress in Energy and Combustion Science* **1980**, *6*, 233-261.
- (181) Lefebvre, A. H. *Atomisation and Sprays*; Hemisphere Publishing Corporation, 1989.
- (182) Shaddix, C. R.; Tennison, P. J. In *Twenty-Seventh Symposium (International) on Combustion/The Combustion Institute*, 1998.
- (183) Hernandez, J. F.; Morla, J. C. *Energy & Fuels* **2003**, *17*, 302-307.
- (184) Allen, C. A. W.; Watts, K. C.; Ackman, R. G. *JAOCs* **1999**, *76*, 317-323.
- (185) Tsai, S. C.; Vu, T. *Fuel* **1987**, *66*, 1596-1602.
- (186) Mezger, T. C. *The Rheology Handbook*; Vincentz Network: Hannover, 2006.
- (187) Takanohashi, T.; Kudo, T.; Iino, M. *Energy & Fuels* **1998**, *12*, 470-475.
- (188) Ohene, F. "Rheological Properties Essential for the Atomisation of Coal Water Slurries (CWS)," U.S. Department of Energy, 1995.
- (189) Geckler, S. C.; Sojka, P. E. *Journal of Fluids Engineering* **2008**, *130*, 061303-11.
- (190) Sovani, S. D.; Sojka, P. E.; Lefebvre, A. H. *Progress in Energy and Combustion Science* **2001**, *27*, 483-521.
- (191) Niraula, B.; King, T. C.; Misran, M. *Colloids and Surfaces A: Physicochemical and Engineering Aspects* **2003**, *231*, 159-172.
- (192) Koopman, D. C. "Development of Alternative Rheological Measurements For DWPF Slurry Samples (U)," U.S. Department of Energy, 2005.
- (193) Zhang, M.; Chen, Y.; Li, G.; Du, Z. *Korea-Australia Rheology Journal* **2010**, *22*, 119-127.
- (194) Thermo, E. C. *HAAKE MARS Modular Advanced Rheometer System (Brochure)* Thermo Electron Corporation, 2006.

Every reasonable effort has been made to acknowledge the owners of copyright material. I would be pleased to hear from any copyright owner who has been omitted or incorrectly acknowledged.